Preparing Nanotubes via Polymerization of Diacetylene Functionality Containing Carbon-based Macrocycles

by

Jiaqi Xu

A thesis

presented to the University of Waterloo

in fulfillment of the

thesis requirement for the degree of

Master of Science

in

Chemistry

Waterloo, Ontario, Canada, 2013

Author’s Declaration

I hereby declare that I am the sole author of this thesis. This is a true copy of the thesis, including any required final revisions, as accepted by my examiners.

I understand that my thesis may be made electronically available to the public.

Abstract

Nanofibers and nanotubes have been extensively studied in materials science due to their extraordinary thermal conductivity, excellent mechanical and electrical properties, and their potential capability for gas storage. Their potential applications at the forefront of technology areas have attracted people's attention.

Diacetylene functionality containing macrocycles with different frameworks have been designed and synthesized. (*S*)-BINOL-based building block macrocyclic ether **2.4,** macrocyclic ester **2.9a** and amide **2.9b** have been synthesized. A single crystal was obtained for **2.9b** from a THF-hexanes solvent system and X-ray data was collected while the other macrocycle **2.9a** furnished gels. X-ray crystallography demonstrated that macrocycle **2.9b** does not stack face-to-face, due to steric hindrance.

Planar macrocycles with carbazole and dibenzofuran as flat backbone to minimize steric hindrance have also been designed, which may increase the possibility to obtain a state of supramolecular stacking, and synthesis of some of the proposed structures was attempted. Carbazole-based tetramer building block macrocycles **3.6** (side chain free) and **3.16** (alkylated) have been successfully synthesized and characterized.

Acknowledgements

I would like to start off by thanking my supervisor Professor Eric Fillion for providing me this valuable opportunity to study in Canada and particularly work in his group. Studying overseas has been one of the most important decisions in my life. Professor Eric Fillion is one of the most knowledgeable and helpful supervisors I have ever met. His great guidance, support and patience have truly encouraged me to continue my research. When I first came to Canada, I had lots of problems in both English and Chemistry. Without ever giving up on me, Professor Eric Fillion was using his warm heart and patience to guide me, for example, by welcoming me to his home and answering my questions in group meetings. I am especially appreciative for all of his help in making me strive harder, think deeper, and to go further as a scientist and as a person in general.

My gratitude also goes out to my committee members, Professor Scott Taylor and Professor Gary Dmitrienko. Their positive criticism, suggestions, and discussions during my research project have been indispensable, and motivated me to think deeper.

Secondly, I also owe my true gratitude to the past and present labmates in the Fillion group, who welcomed me to this big “family” with open arms and warm heart: Siawash Ahmar, Azadeh Kavoosi, Ganna Bondarenko, Eric Beaton, Mengxiu Zheng. Especially Ganna Bondarenko and Siawash Ahmar, they are like older sister and brother taking care of me during these past few years, helping me adjust to the foreign life and study styles. Eric Beaton brings tones of happiness to our whole group, and makes the lab more like a team. They not only give me suggestions to aid my chemistry, but also make my overseas

study life more colorful. For all the friends in the lab, they shared my happiness, celebrations, and even sadness and disappointments during these years.

Moreover, I would like to thank the staff of the chemistry department for great help, particularly Ms. Jan Venne for NMR assitance, Dr. Jalil Assourd for X-Ray data collection, and the friendly graduate secretary Ms. Cathy van Esch.

Last but not least, I would like to express my deepest appreciation to my dear parents for their unconditional love and support over the years that encouraged me to overcome all the obstacles in my way, without which I could not have achieved what I already have. Thank you, dad and mom.

All the friends here at Waterloo make my study and life very bright and enjoyable, while other friends that I made elsewhere in Canada and China are also a big part of my life and I appreciate our friendship very much.

Table of Contents

List of Figures

List of Schemes

List of Tables

List of Abbreviations

AcOH	acetic acid
BINOL	1,1′-binaphthyl-2,2′-diol
C	carbon
DICD	diisopropylcarbodiimide
DMF	dimethylformamide
DPTS	4-(dimethy1amino)pyridinium 4-toluenesulfonate
equiv	equivalent
Et_2O	diethyl ether
Et_3N	triethylamine
EtOAc	ethyl acetate
h	hour
HBC	hexa-peri- hexabenzocoronene
M	molar (mole per litre)
mp	melting point
MeI	methyl iodide
MeO	methoxyl
min	minute
MOFs	metal-containing organic frameworks
o-	*ortho*
OH	hydroxyl
OTf	triflate
p-	*para*
Py	pyridine
rt	room temperature
TBAF	tetra-*n*-butylammonium fluoride
THF	tetrahydrofuran
TIPS	triisopropylsilyl
TIPSA	triisopropylsilylacetylene
TLC	thin-layer chromatography
TMEDA	tetramethylethylenediamine
TMS	trimethylsilyl
TMSA	trimethylsilylacetylene

Chapter 1 Introduction

1.1 Background

Nanofibers and nanotubes have been extensively studied in materials science due to their extraordinary thermal conductivity, excellent mechanical and electrical properties, and their potential capability for gas storage. Their potential applications at the forefront of several areas of technology have attracted people's attention.

Highly conjugated polymers are important building blocks for nanostructures, such as all carbon-based nanostructures, metal-containing nanostructures and heteroatom-containing nanostructures. Nanostructures based on highly conjugated polymers are potential candidates to be used as sensors, actuators, electronic devices, drug carriers, organic solar cells and engineering materials.[1] For example, using metal-containing organic frameworks (MOFs) as the backbone, the resulting microporous materials and zeolites can be used for gas storage, separation, and catalysis.[2] Transition metal ions and organic monomeric units are linked through covalent bonds to afford varied porous materials that possess high surface area and excellent thermal stabilities. [3]

In recent years, research on the synthesis and application of novel highly conjugated polymers has attracted broad interest. Noticeable strides have been made over the last 40 years. Different cyclic monomeric units have been studied, such as phenylacetylene macrocycles, amide-containing macrocycles and urea-containing structures. Stacking via H-bonding and π-π interactions is the most common strategy for

building up the tubular structure for such types of macrocycles. [4]

For certain materials (e.g. metal and silica), physical treatments such as melting (floating zone growth), sublimation (vapor transport), and magnetic force[4,5] are frequently used to prepare the desired nanoarchitectures. However, the physical methods can only provide limited nanostructures from the known materials, and in many cases the size and shape of the formed nanostructures cannot be controlled. On the other hand, organic synthesis could provide numerous new materials capable of forming such nanoarchitectures either chemically or upon further physical treatment. Organic synthetic strategies that give rise to nanoarchitectures provide a bright future for nano-science applications.

1.2 Basic Design Rules

A common strategy to make nano-scale porous materials with a large surface area is to assemble the molecular units by non-covalent interactions such as hydrogen bonding, π-π stacking or van der Waals interactions. Columnar conjugated building blocks provide a route to the synthesis of porous materials by means of self-assembly or face-to-face stacking. The face-to-face stacking of highly conjugated macrocycle is an efficient and convenient strategy for building pre-organized supramolecular architectures (Scheme 1).

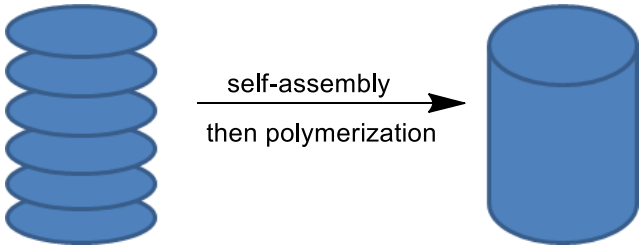

Scheme 1. Synthesis of tubular structure via face-to-face stacking of macrocycles

Macrocyclic compounds possessing a covalent backbone with suitable linkers allow self-assembly to form a nanotube. The internal cavity of the nanotube has a dimension similar to that in the monomeric macrocycle, which is dictated by the monomer's property.

1.3 Diacetylene-Containing Macrocycles

Diacetylenes have been used to construct supramolecular interaction networks for the past few decades. It has been shown by X-ray diffraction studies that polymerization of diacetylene systems to form the corresponding conjugated polydiacetylenes requires a precise prealignment of the reacting units in the crystalline and gel phases (Scheme 2).[6-9] The ideal monomer repeat distance should be approximately 4.9 Å, and a neighboring C(1)–C(4) distance should be approximately 3.4 Å, which is close to the van der Waals contact distance and the orientation angle should be around 45°. Similarly, the ideal alignment for the reacting units of the triacetylene system has also been examined (Scheme 2).[6]

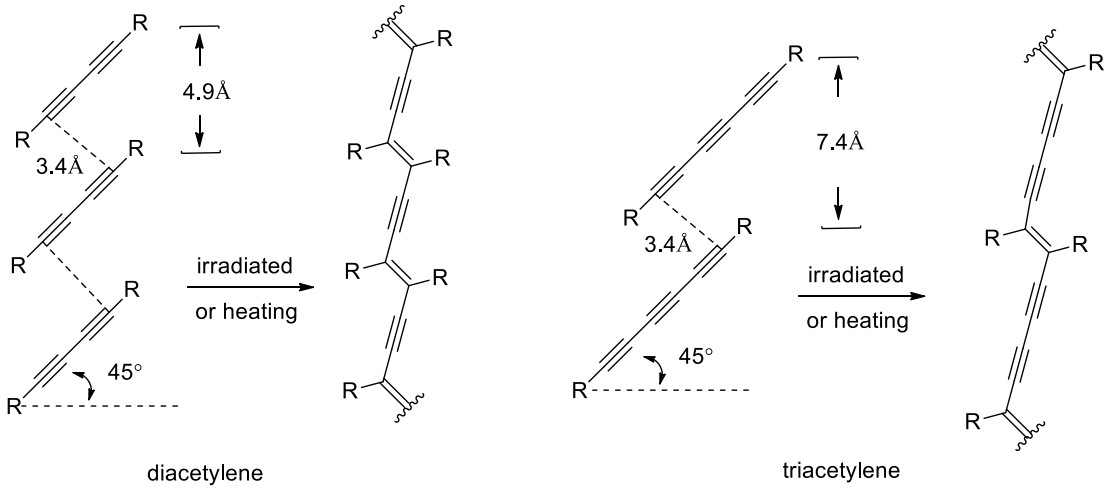

Scheme 2. Polymerization of diacetylene and triacetylene systems

The synthesis of the diacetylene macrocycle system is rather simple. Triangular acetylene compounds containing an aryl framework as the backbone are the most common building blocks to construct the desired macrocycle (Scheme 3), since such macrocycles can bear large loads without deformation. Coupling of terminal acetylenes of such triangular building blocks then form the diacetylene macrocycles. The building blocks of the macrocycle are rigid and their connection is in such a way that the final structure cannot collapse, in contrast to flexible macrocycle structures like crown ethers or cycloalkanes.[10] As a result of the rigid sp or sp^2 hybridized carbon atoms in the structure, this macrocycle possesses minimal conformational freedom and a high degree of shape-persistency.

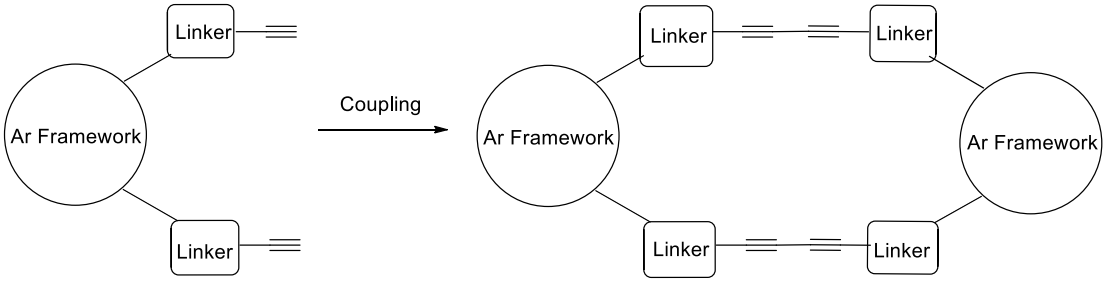

Scheme 3. Synthesis of macrocycles from terminal alkyne precursors

Coupling is the essential method to build such macrocycles as discussed above. The most important reactions are Sonogashira coupling and Hay coupling (Scheme 4). The former occurs between an aryl halide and a terminal acetylene, while the Hay reaction is an oxidative coupling that allows ring closure to provide rapid access to large macrocycles.

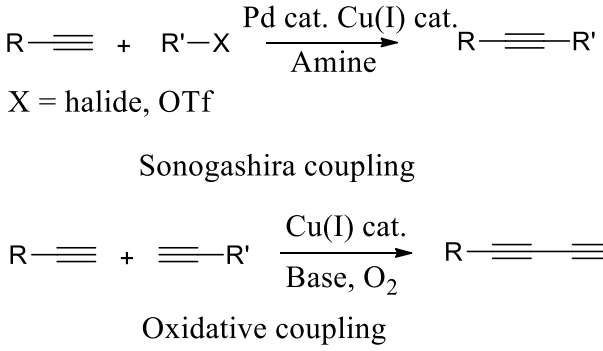

Scheme 4. General Sonogashira and oxidative coupling

In 1974 Baughman and Yee first reported that solid state polymerization of a cyclic diacetylene afforded large polymeric single crystals of ring-bridged polymer (Scheme 5).[11] The diacetylene macrocycle crystal was colorless, while the obtained polymer crystal was deeply colored and possessed an asbestos-like shape with a metallic appearance under the microscope. The polymer crystals were found to have high thermal stability,

and were infusible and insoluble after exposure of diffuse light or annealing (i.e., slowly heating below the melting point). The corresponding X-ray study of the polymer crystal was reported a few years later.[12]

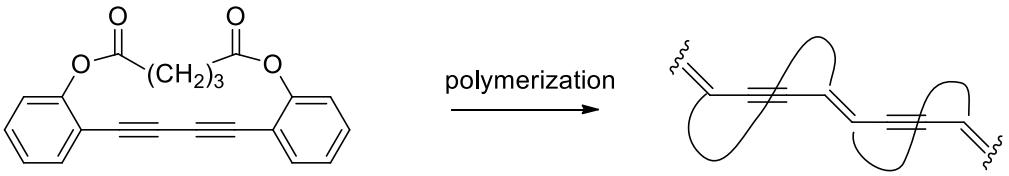

Scheme 5. Ring bridged *o*,*o*′-diacetylenyldiphenyl glutarate

Swager and co-workers reported a family of macrocycles prepared from 1,2-diethynylbenzenes (Figure 1), which can be polymerized in both crystalline and liquid crystalline phase to afford novel conjugated polymers.[13] However, these polymers were difficult to characterize.

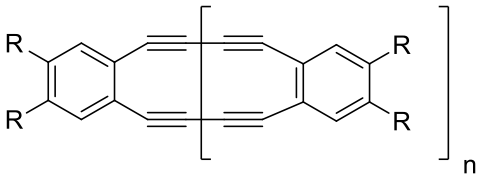

n= 1, 2, 3
R= H, C_4H_9, C_6H_{13}, $C_{10}H_{21}$, $C_{12}H_{25}$, $OC_{10}H_{21}$

Figure 1. 1,2-Diethynylbenzene derivatived macrocycles

Young reported the synthesis and polymerization of a strained tribenzodehydro annulene, which was extremely light sensitive and thermally unstable (Figure 2).[14] The polymer was formed via polymerization. Unfortunately, an X-ray structure of the polymer could not be obtained.

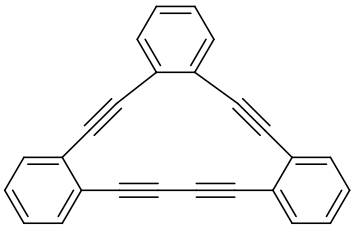

Figure 2. Tribenzodehydro annulene macrocycle

In 2011, Tamaoki and coworkers studied the synthesis and photo polymerizability of macrocyclic diacetylene dicarboxamide derivatives (Figure 3).[15] Only one of the derivatives formed as a single crystal; all the other derivatives gave gels. Furthermore, the diacetylene did not undergo polymerization in the solid phase. It was also shown that gels that have a relatively short spacer length (n = 3) do not undergo photo polymerization. On the other hand, compounds with a large ring size and a longer spacer (n ≥ 4) can adopt a conformation suitable for polymerization due to less rigid diacetylene moieties.

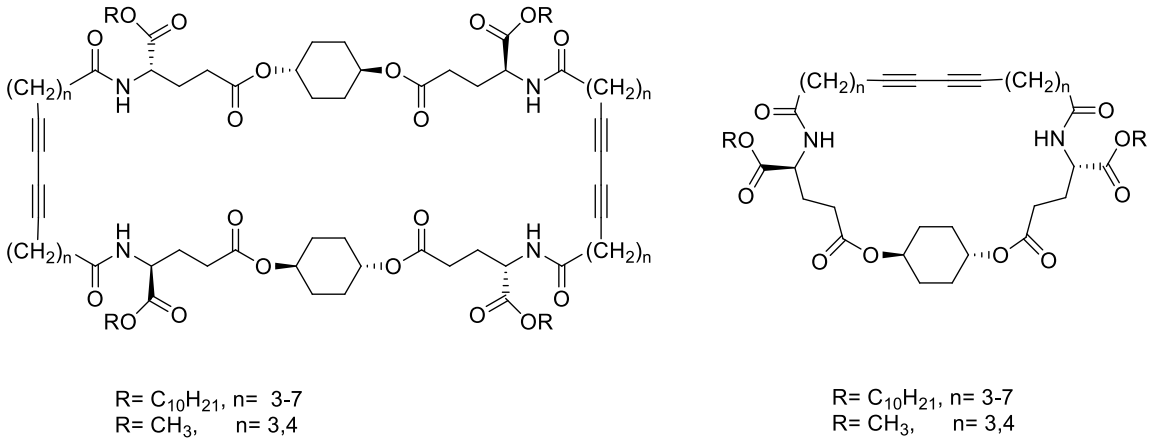

Figure 3. Monomer and dimer of macrocyclic diacetylene dicarboxamide derivatives

1.4 Mechanisms of Polymerization of Diacetylene Functionality

Several methods could trigger the polymerization of the diacetylene systems, including irradiation with UV light, heating below the melting point, and exposure to high energy radiation.[7-9] 1,4-Addition is a generally accepted mechanism for the polymerization of the diacetylene systems, but the detailed polymerization pathways under the photochemical and thermal conditions are different and two corresponding mechanisms have been proposed. Irradiation provides a change in bond structure of the linear diacetylene monomer to afford a bent di-carbene intermediate (Scheme 6).[9] The reactive di-carbene species can then react with an adjacent parallel di-carbene to form a double bond between the two neighboring monomer units, which could lead to further polymerization propagating through the monomeric stack. It is also possible that all di-carbenes add together at once.

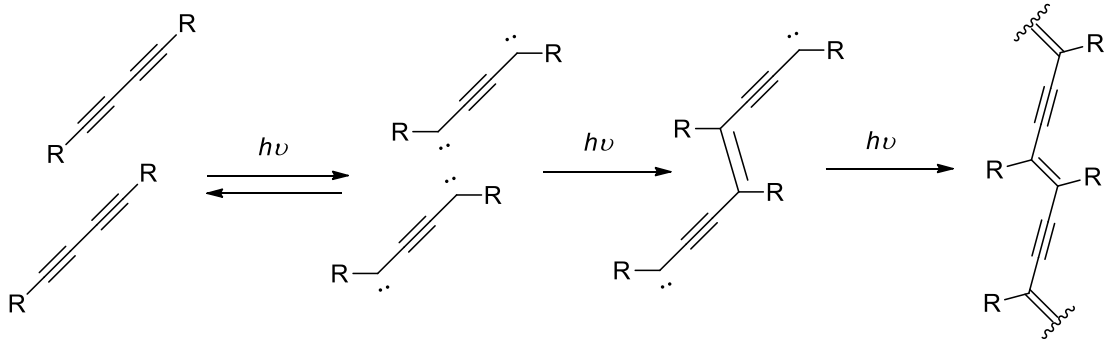

Scheme 6. Mechanism of polymerization of diacetylene via irradiation

The mechanism for polymerization of the diacetylene system under thermal condition consists of two different types.[6] For a diacetylene system adopting the slip stacking state, it is more likely to undergo a "turnstile" type of mechanism (Scheme 7),

which commonly applies to symmetric diacetylene systems.[6] The monomers have the same pivot in the middle of the diacetylene, each C(1) and C(4) shift approximately 1Å toward each other and the terminal R groups should be bent around 30 °, which allow new bonds to form between the neighboring diacetylenes. On the other hand, the strait face-to-face stacking system undergoes the "swinging gate" mechanism that is common for aryl-substituted diacetylenes and terminal diacetylenes (Scheme 7). In this case, the molecules pivot is at C(4) position and the rest of C(1–3) move about 3Å. The R group that is attached to C(4) keeps the original angle, meanwhile the R attaches to C(1) undergoes the most movement.[6]

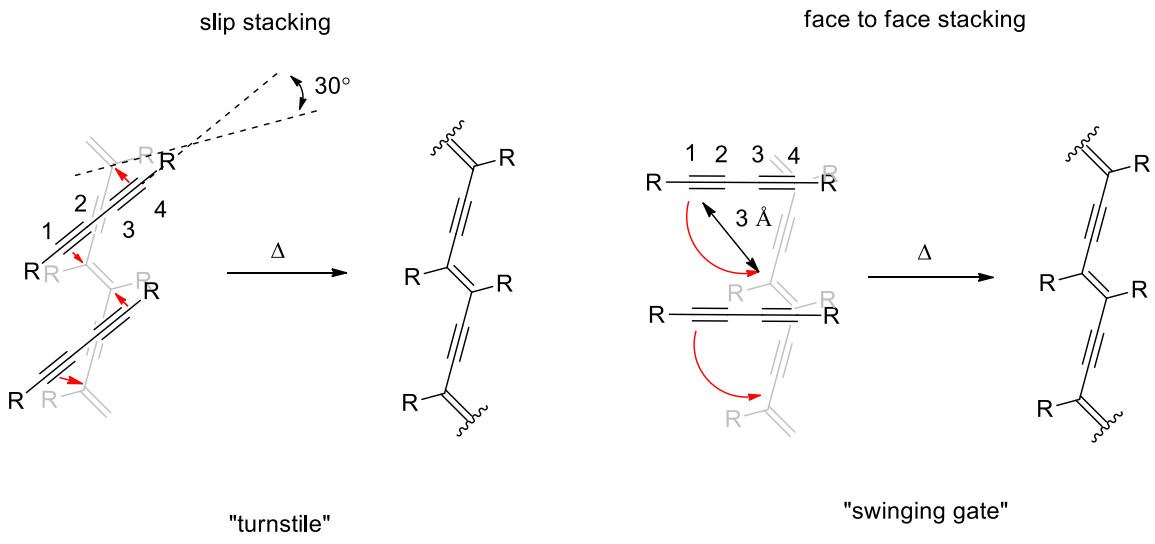

Scheme 7. Two types of mechanisms of polymerization for diacetylenes under thermal conditions

1.5 Characterization of Diacetylene Polymers

Polymerization of the diacetylene systems usually affords polydiacetylene compounds that typically possess various reddish and blue hues. Single crystals of polyacetylenes often demonstrate a metallic appearance under the microscope. To characterize the diacetylene polymers, Raman spectroscopy is commonly employed. Strong Raman peaks corresponding to triple-bond stretching usually can be observed in the range of 2050–2150 cm^{-1}, and 1350–1450 cm^{-1} for double bond stretching.[6] Moreover, solid-state ^{13}C NMR spectra and X-ray diffraction are also common characterization methods. [6]

Chapter 2 Macrocycles Possessing A BINOL Backbone

2.1.1 Introduction

The synthesis of macrocycles with diacetylene functionalities within the cavity has attracted the interest of many research groups, including the Fillion lab at the University of Waterloo. The main task of this project is to design and synthesize macrocycles that can stack into a tubular structure and then polymerize into a nanotube (Scheme 8). The advantage of forming polymers from a tubular structure is that the nanotube will carry on the property of the macrocycle, such as being robust while keeping the same cavity as the macrocycles.

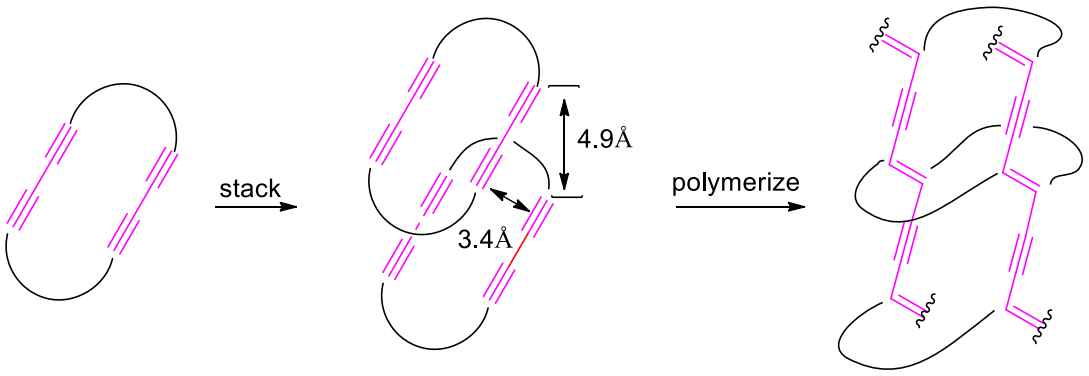

Scheme 8. Route to a tubular polymer via polymerization

Upon introducing aromatic backbones into the diacetylene systems, the possible aromatic π-π stacking might align such macrocyles in a parallel manner and thus stack perpendicularly. The distance between the stacked and parallel diacetylene system might be close to the ideal distance of about 3.4 Å required for the polymerization of

diacetylenes (Scheme 8). A recent example of the diacetylene system having a tubular architecture was reported by Lauher and co-workers (Scheme 9).[16] Sonogashira coupling of 1,3-diiodobenzene with propargyl alcohol followed by ether formation led to the macrocycle precursor. Copper catalyzed oxidative coupling in highly diluted solution offered a mixture of macrocyles, where the desired dimer was the major product (46%) and the monomer and trimer were minor products (10% and trace respectively).

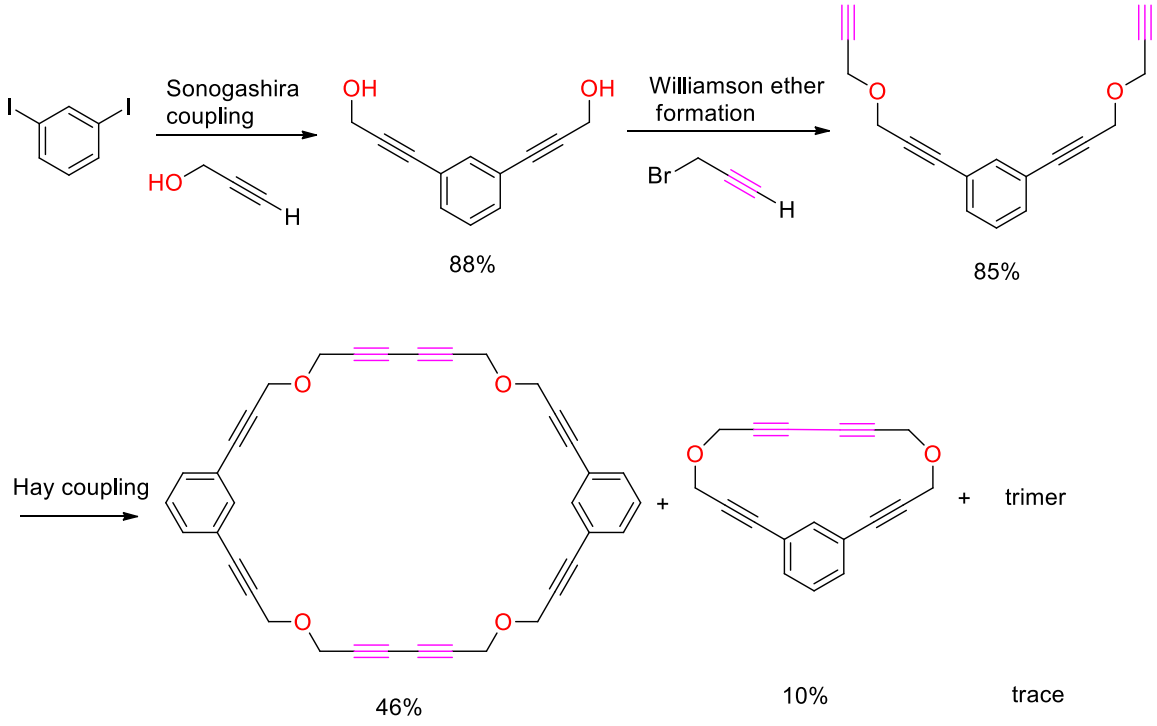

Scheme 9. Synthesis of macrocycle from 1,3-diiodobenzene

The single crystal of the dimer was investigated by X-ray diffraction, which showed that the repeat distance of neighboring diacetylene C(1)−C(4) carbon atoms (5.09 Å) was longer than the ideal one (4.9Å). Moreover, the crystal was thermally unstable. The crystalline form was converted rapidly to an amorphous state at 50 ℃, or slowly at room temperature after one month. Polymerization occurred when the dimer crystal was

annealed carefully at 40 ℃ for 35 days. Furthermore, the obtained polymer was completely insoluble in a wide range of solvents and its structure could not be determined.

For this project, a suitable aromatic framework/backbone capable of π-π stacking for diacetylene systems was needed. Among the many available aromatic structure candidates, BINOL (1,1′-binaphthyl-2,2′-diol) drew our attention. BINOL has been widely used in asymmetric synthesis as a chiral catalyst or ligand, and BINOL-based synthons are becoming more attractive in materials and nano-science recently because of their ability to transfer chiral information.[17, 18] The basic BINOL moiety can be functionalized easily at various positions, the most common one being the 3,3′ position, although modification at 4,4′ and 6,6′ positions are also well documented (Figure 4).[19, 27]

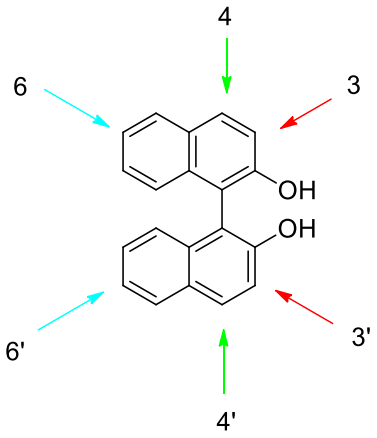

(±) BINOL

Figure 4. Possible functionalized positions of (±) BINOL

Macrocycles that incorporate two or more BINOL units have been studied. In 2010, Pasini and coworkers reported a one-pot etherification to make rigid and chiral BINOL-based macrocycles (Scheme 10).[17] Single crystals of these BINOL-based

macrocycles were obtained, which showed that dimers with linker **b** and **c** (Scheme 10) have non-helical packing tubular arrangements.

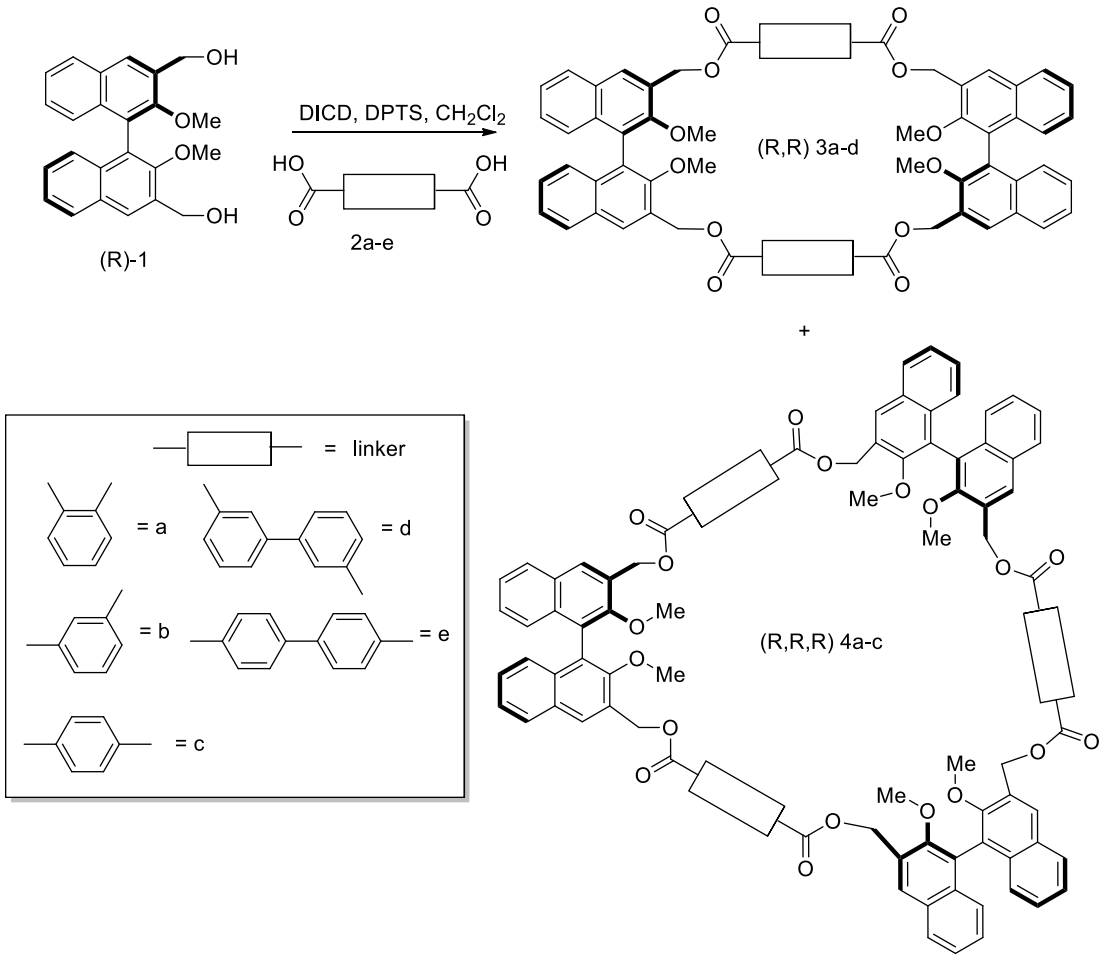

Scheme 10. Synthesis of dimers and trimers of BINOL backbone macrocycles with different linkers

Subsequently, Pasini's group reported some related macrocycles in which the ester functionalities was replaced by an amide, a moiety capable of participating in H-bonding.[17] A novel and rigid tetra-amidic macrocycle (Scheme 11) was designed, synthesized and characterized, which performed as a carrier substrate to host a semiconductor C_{60} into its cavity.

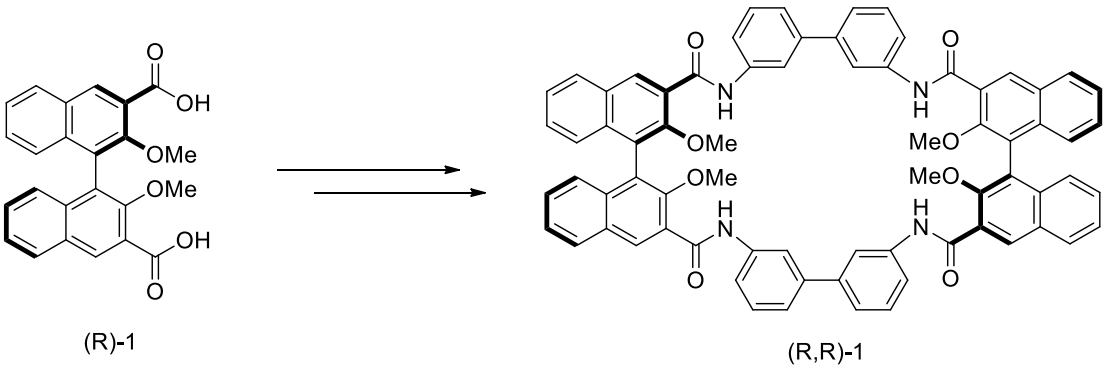

Scheme 11. Amide-containing (*R*)-BINOL backbone macrocycle

More recently, Pasini's group developed some shape-persistent, optically active new arylamide macrocycles (Scheme 12), possessing different functionalities such as methoxy and acetoxy groups at 2,2′ positions and different conformation of linkers Y.[18] The crystal structures were obtained and showed that the macrocycle bearing the sterically less demanding methoxy substituents was a good supramolecular receptor for dicarboxylate anions.

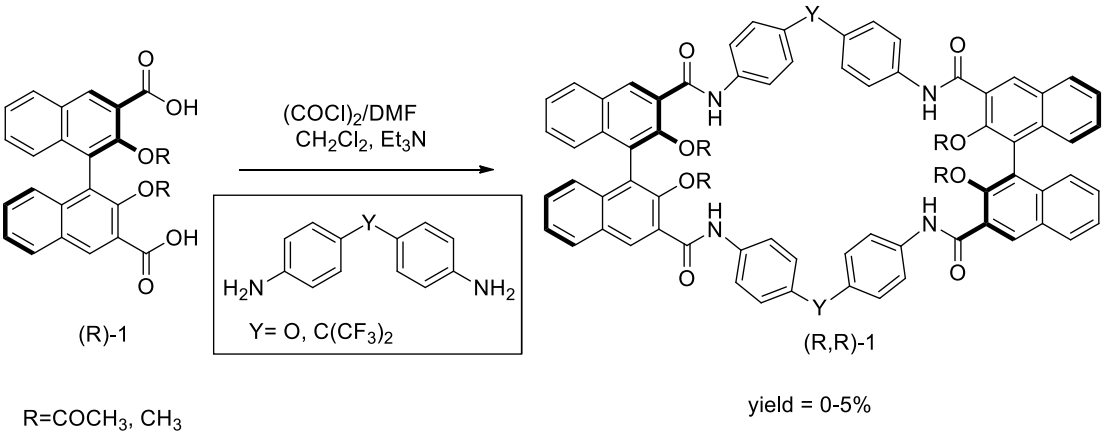

Scheme 12. Macrocycles with different functionalities

2.1.2 Proposal

Inspired by Lauher's and Pasini's work, our group aimed to broaden the scope of aromatic frameworks in the diacetylene systems that may help to form the desired nanotubes, among which the binaphthyl structure seems to be of certain value to our goal.

In our proposed structure, BINOL is used as a framework in combination with a rigid and linear spacer. In general, the number of sp^3 carbon atoms in the spacer should be minimized due to their conformational flexibility that may lead to twisting of the system. sp and sp^2 hybridized carbon atoms would contribute to stabilize the whole macrocycle structure. However, introduction of a few sp^3 carbons is still necessary in many cases to balance the conformational flexibility caused by the rotation of the C-C bond at 1,1′ position of the BINOL backbone.

Based on the previous literature results, (*S*)-1,1′-binaphthyl-2,2′-diol was chosen as a chiral scaffold for new shape-persistent macrocycles, and the proposed macrocyclic structure is shown below (Figure 5). The possible π-π stacking between the two adjacent molecules of such structures would contribute to the formation of pre-organized supramolecular tubular assemblies.

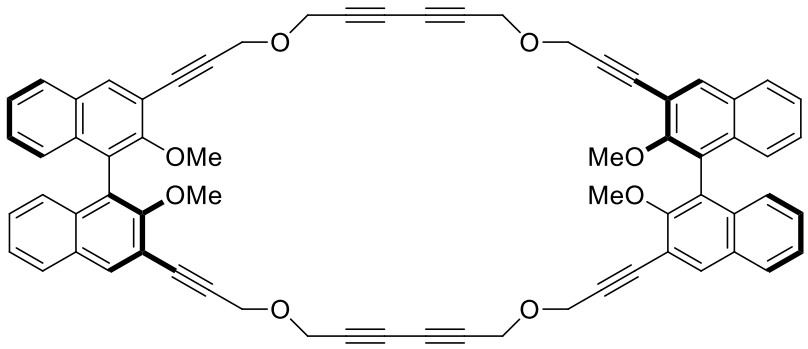

Figure 5. (*S*,*S*)-BINOL backbone marocycle

2.1.3 Results and Discussion

Synthesis of The Ether Macrocycle

The synthesis started by converting the two free -OH of BINOL to the corresponding methoxy ether (Scheme 13), which is a suitable protecting group as it is stable under most reaction conditions. Moreover, replacement of the free hydroxyl group by the methoxy moiety eliminates the H-bonding interaction in the final structure, and π-π stacking should be the major factor controlling the three-dimensional arrangement. The aromatic positions α to both methoxy groups in **2.0** was deprotonated by *n*-BuLi in the presence of TMEDA, and the resulting di-anion was trapped with I_2 to produce compound **2.1** in good yields.[20]

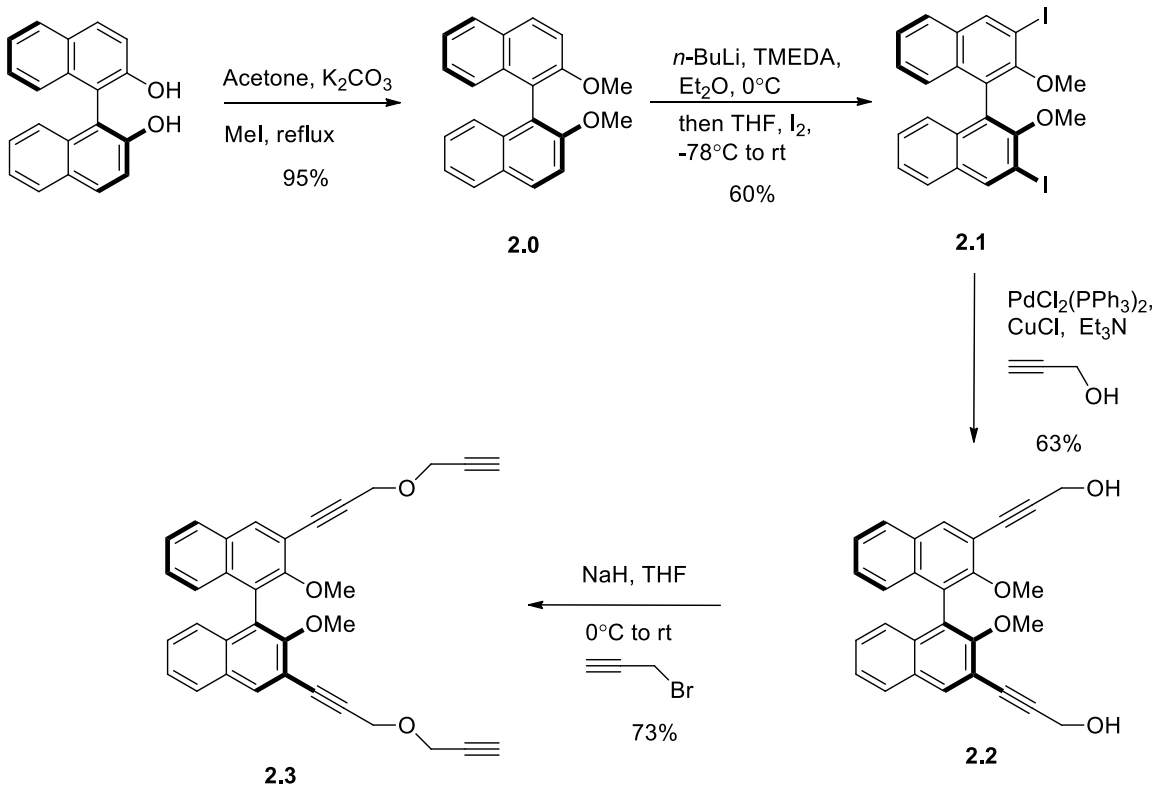

Scheme 13. Synthesis of precursor **2.3**

Sonogashira coupling of the di-iodide **2.1** with propargyl alcohol furnished the diol **2.2** in quantitative yield under solvent-free conditions (Scheme 13). Deprotonation of the alcohol **2.2** with NaH followed by treatment of the resulting alkoxide with propargyl bromide led to acetylene monomer **2.3**. Mono-etherification occurred when the reaction was carried out at 0 ℃, while using propargyl bromide in slight excess and warming up the reaction to room temperature pushed the reaction to completion.

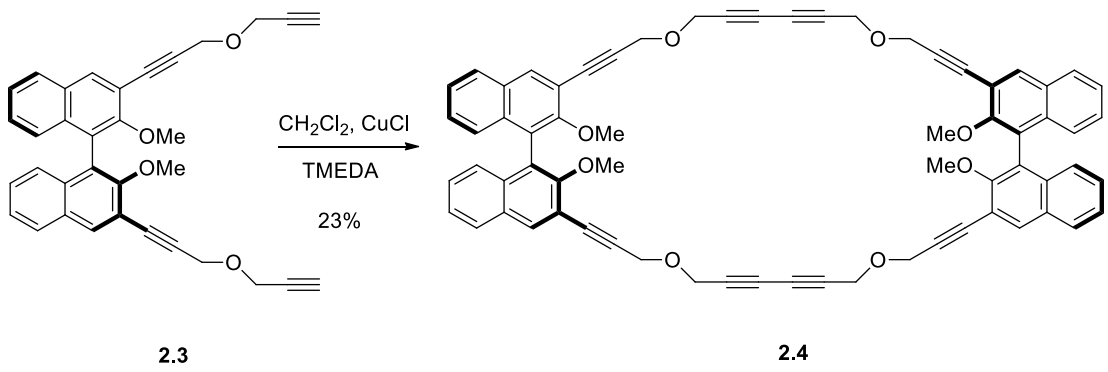

2.3 **2.4**

Scheme 14. Synthesis of macrocycle **2.4**

The last macrocyclization step was quite challenging (Scheme 14). Firstly, to avoid polymerization, macrocyclization had to be carried out under highly diluted conditions. In addition, to further minimize polymerization, extremely slow addition of the starting material to the reaction mixture (i.e. adding the substrate dropwise to catalyst and a large amount of solvent by syringe pump over 12 h) was also essential. Reaction was carried in the absence of light (foil-covered) to avoid decomposition of the formed macrocycle. In principle, the reaction should be carried out under air to regenerate the copper catalyst. However, in this case the copper catalyst was used in large excess (7.4 equiv) according to a literature procedure,[16] so an air atmosphere was not necessary. Despite all these efforts, unwanted compounds, which were presumed to be the linear polymers, were still the major component in the obtained product and the desired macrocycle was prepared in 23% yield.

After obtaining the desired macrocycle, it was necessary to grow a single crystal to first determine the three dimensional structure and then to attempt polymerization. Different solvents were used in attempts to grow the single crystal. Simple solvent evaporation was attempted first, which is the most common method for growing single

crystals. Solvents such as EtOAc, acetone, CH_2Cl_2, MeOH, THF, and $CHCl_3$ did not furnish single crystals but produced gels.

Even if solvent evaporation may succeed, in many cases it produces crystals with poor quality and it is hard to control the crystal growth speed. Therefore, liquid-liquid diffusion was then attempted (Table 1). In this case, two different but miscible solvents are involved. A higher density solvent dissolving the compound to be crystallized is placed in a small vial, then a lower density pure solvent is simply laid on top of the higher density one to form two layers initially, and in principle single crystals would slowly form at the bottom of the vial after the two solvents start to diffuse.

Table 1. Different liquid-liquid diffusion combinations for single crystal growing

Top / Bottom	EtOAc	acetone	CH_2Cl_2	MeOH	THF	$CHCl_3$
Hexane	Gel	Gel	Gel	Gel	Gel	Gel
Pentane	Gel	Gel	Gel	Gel	Gel	Gel
Et_2O	Gel	Gel	Gel	Gel	Gel	Gel

Combinations of various solvents as summarized in Table 1 were attempted. Unfortunately, only gels and no single crystals were obtained. In addition, another significant issue was the stability of the macrocycle **2.4**, which decomposed at room temperature during a few weeks even in the absence of light.

2.1.4 Summary

In summary, (*S*)-BINOL based building block macrocyclic ether **2.4** with two potentially polymerizable diacetylene functionalities was synthesized and characterized by NMR successfully. However, since no single crystal could be generated, the stacking mode could not be determined. The stability of the macrocycle at room temperature and in the absence of light was modest.

These problems forced us to rethink and redesign the structure of the macrocycle. First, to improve the chance of getting crystalline macrocycle instead of gels, H-bonding could be introduced in the system. H-bonding and π-π stacking interactions working together might lead to good quality single crystals.

Second, the problem of stability may be caused by the flexibility and the strain of the cyclic structure. The bond between the 1,1′ position offers flexibility to the entire structure, as the two parts of the BINOL might rotate around the 1,1′ C-C bond. Moreover, the “arms” at the 3,3′ position can also rotate, which may twist the ring and lead to ring collapse. The solution to this challenge is that some intramolecular interactions would be introduced to fix the backbone and stabilize the entire cyclic unit.

2.2.1 Amide-containing Macrocycle

Supramolecular stacking of macrocycle upon self-assembly is crucial for preparing the nanotubes. Certain functional groups capable of forming H-bonding interactions, such as the amide, might be useful in the design of our targeted molecules. The amide moiety's intrinsic ability to act as both H-bond donor and acceptor plays an important role in some nanostructures, by stabilizing the conformation.[10]

In 1993, Ghadiri and co-workers published the first example of a hollow tubular structure containing amide functionality (Scheme 15).[21] The hollow shape tubes were formed by cyclic peptides stacking flatly via backbone-backbone hydrogen bonds.

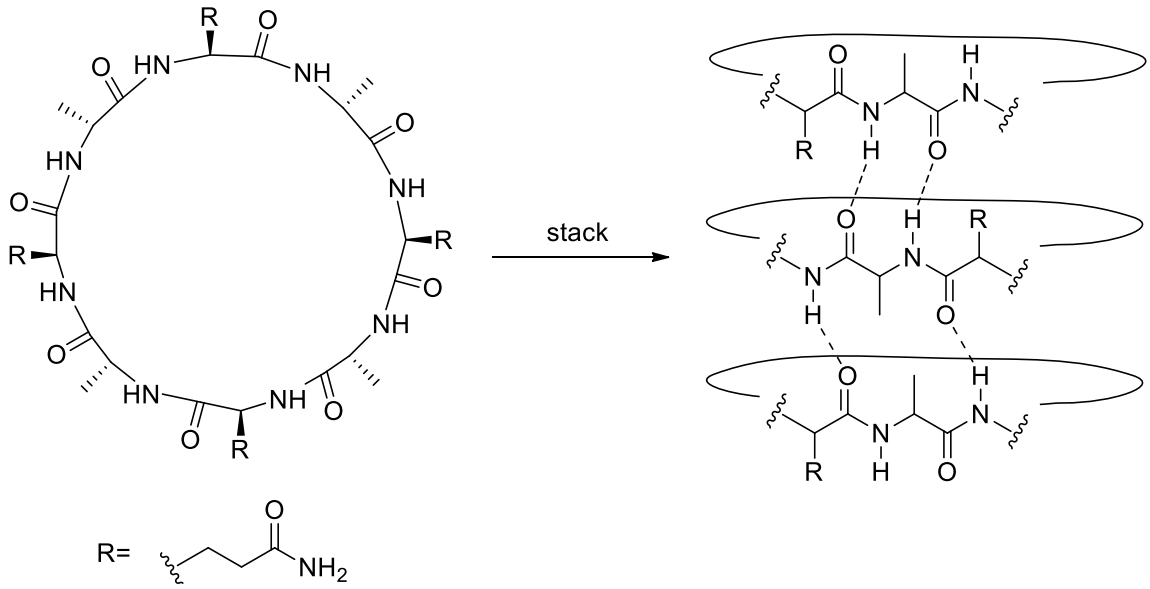

Scheme 15. Hollow tubular structure containing amide functionality

In 2010, Shimizu and co-workers synthesized a diacetylene macrocycle with benzamide functionalities that assembled into columnar structures (Figure 6).[22] The

macrocycles assemble via amide-amide hydrogen bonds and stack face-to-face. The corresponding X-ray study showed that the monomer repeat distance was 4.98 Å and the neighboring C(1)-C(4) distance was about 3.58 Å, close to the ideal distance required for stacking the diacetylene systems to form the nanotube. Insoluble polymer formed under thermal conditions (180 ℃, 12 h), which was found to be capable of adsorbing CO_2 at 0 ℃ and releasing the gas upon heating. This indicated that the obtained polymer retains accessible tubular channels, and is thus potentially useful for gas storage. [22]

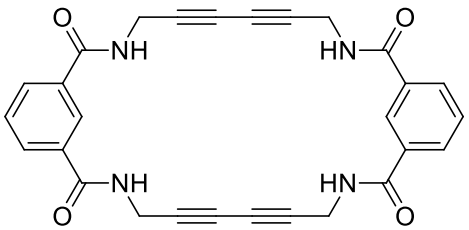

Figure 6. Macrocycle with benzamide functionalities

In 2011, Morin and coworkers synthesized an amide-containing phenyl acetylene macrocycle, which formed organogels at low concentration in many common solvents (Figure 7).[23] H-bonding between amide NH and carbonyl oxygen contributed to the increased intermolecular interactions between the macrocycles. The functional groups introduced on the side chain that contributed aryl π-π interactions and helped the macrocycle to stack face-to-face. In addition, a long alkyl side chain was added to enhance the solubility of the macrocycle (macrocycle A in Figure 7). A highly diluted solution was used for macrocyclization but the yield was still low. Polymerization of the macrocycle afforded only short polymers in low yields.

In 2012, Morin's group developed a strategy to overcome this problem.[24] They proposed that two diacetylene functionalities in the ring of macrocycle A were too rigid to undergo polymerization. Therefore, they introduced a cross-linkable diacetylene unit with a four-carbon alkyl fragment in between the benzamide and the dodecane moiety (macrocycle B in Figure 7) to make the macrocycle more reactive toward polymerization. Interestingly and unexpectedly, not only the newly introduced diacetylene moieties underwent polymerization as expected, but so too did the original rigid and unreactive diacetylenes within the macrocycle skeleton. This was the first report of a conversion that successfully activated unreactive diacetylene for polymerization. [24]

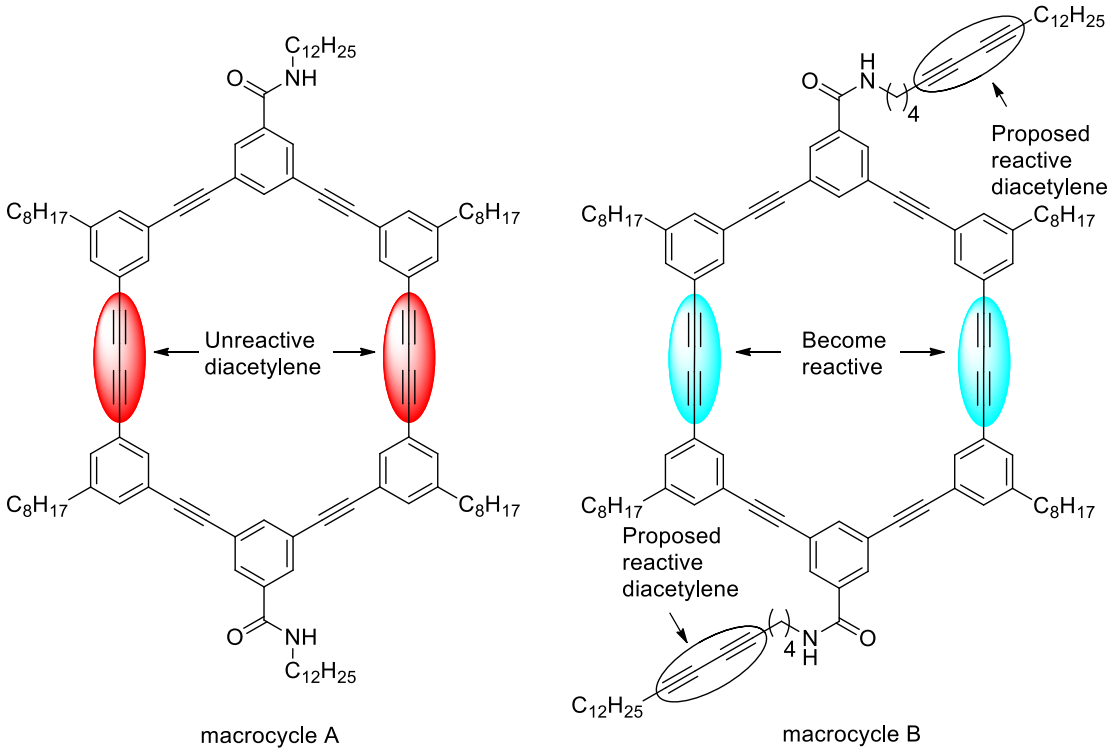

Figure 7. Phenylacetylene macrocycles A and B

2.2.2 Proposal

Base on literature precedence, it was proposed that benzamide functionality should be introduced to the BINOL system (Figure 8, left). The intramolecular H-bonding interaction between the existing BINOL methoxy groups and the newly introduced benzamide functionalities could provide some internal rigidity and minimize the free rotation at the BINOL's 3,3′ positions, which may enhance the thermal stability of the final product and increase the yield of macrocyclization. It is still necessary to mask the BINOL's free –OHs, whose co-existence with a nearby carbonyl moiety, in this case the amide group, may form additional but unwanted H-bonding interaction (Figure 8, right) that could hamper the desired macrocyclization. Another advantage of having a methoxy group is that the amide groups at 3,3′ positions are the only functionalities capable of acting as hydrogen-bond donors, which could minimize the number of possible alignments when two molecules stack together.

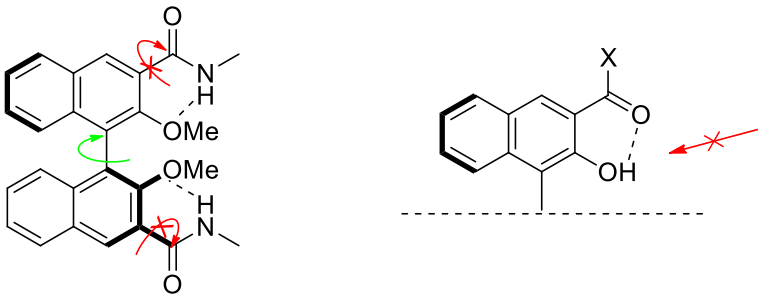

Figure 8. Intramolecular H-bonding interaction fixes the conformation

Therefore, the new macrocycle **2.9b** as shown in Figure 9 was proposed based on the assumption that intramolecular H-bonding interactions could increase the stability of the macrocycle, and the chance to form a solid product. Moreover, an analogous structure **2.9a** (Figure 9) was also proposed, which possesses the same core skeleton as **2.9a** but the H-bonding capable amide moiety was replaced by a H-bonding incapable ester functionality.

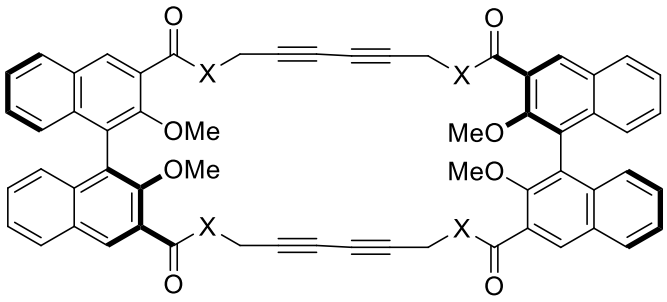

X= O **2.9a**
X= NH **2.9b**

Figure 9. New benzamide and ester macrocycles

2.2.3 Results and Discussion

Deprotonation at the 3,3′ positions of (*S*)-2,2′-dimethoxy-1,1′-binaphthalene by *n*-BuLi in the presence of TMEDA followed by reaction with carbon dioxide led to the formation of the corresponding dicarboxylic acid (Scheme 16). To make the amide and ester containing precursors **2.7** and **2.8**, the first attempt was to use the carboxylate as a nucleophile to react with propargyl bromide. Unfortunately, a low yield was obtained. Then the carboxylic acid was converted to much more reactive acid chloride. Compound **2.6** was obtained quantitatively without purification as it decomposes on silica gel. Using

propargyl alcohol and amine as nucleophiles to react with **2.6** offered the corresponding terminal alkyne precursors in good yields (77% and 79% respectively).

Macrocyclization was attempted by following Shimizu's procedure[22] using $Cu(OAc)_2$ H_2O as catalyst, but no desired macrocycle was obtained under this condition and a complex mixture was isolated. Fortunately, switching to CuCl as the catalyst in the presence of TMEDA led to a successful macrocyclization. The amide containing macrocycle **2.9b** was isolated in relatively high yield (40%) when compared to macrocycle **2.9a** (10% yield).

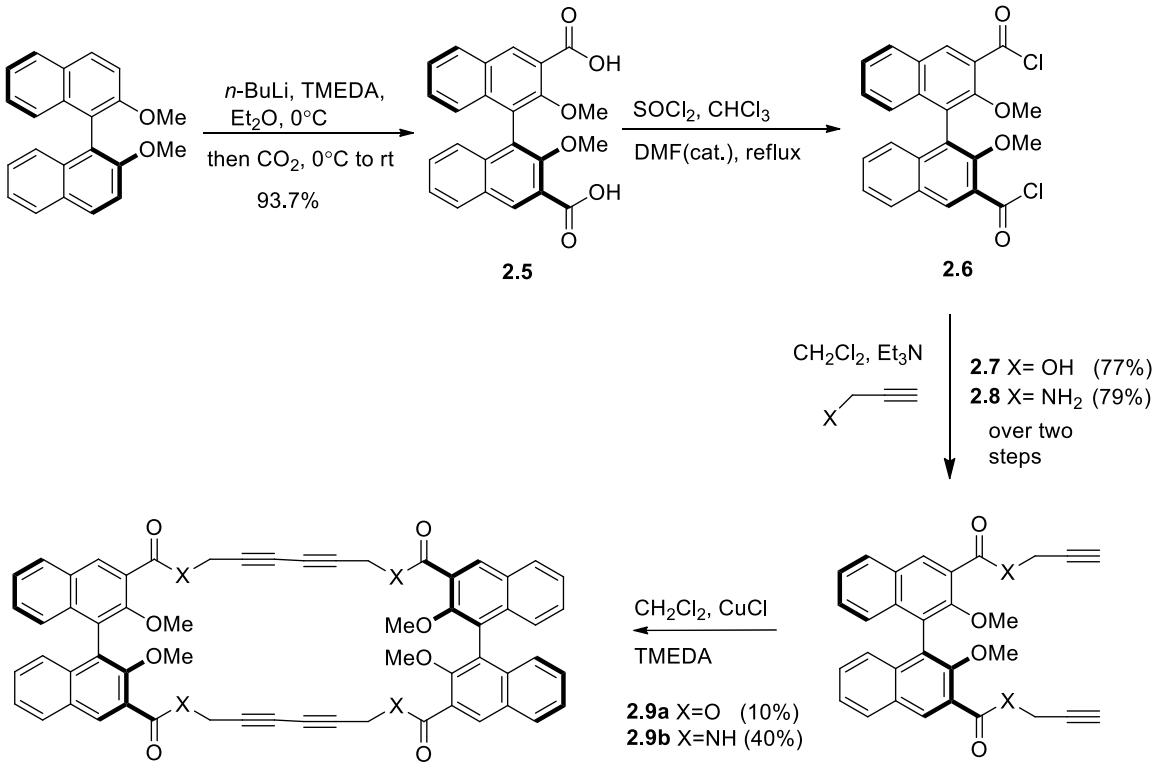

Scheme 16. Synthesis of macrocycles **2.9a** and **2.9b**

Interestingly, dimer **2.9b** was only obtained in the case of the amide macrocycle, while for the ester macrocycle, dimer **2.9a** was obtained in low yield and a trace amount of monomer and/or trimer was also isolated. This finding suggested that the intramolecular H-bonding reduces the conformational flexibility of the amide precursor **2.8**, thus favoring the macrocyclization reaction. Higher flexibility in the case of the ester containing precursor **2.7** led to much lower yield and the formation of trimer and/or monomer byproduct. It is possible that after one pair of terminal alkynes couple to each other, the free rotation of the other two alkyne "arms" reduces the chance of intramolecular coupling and leads to intermolecular polymerization instead (Figure 10). This result was consistent with the initial hypothesis and the amide macrocycle was obtained in high yield as a stable solid.

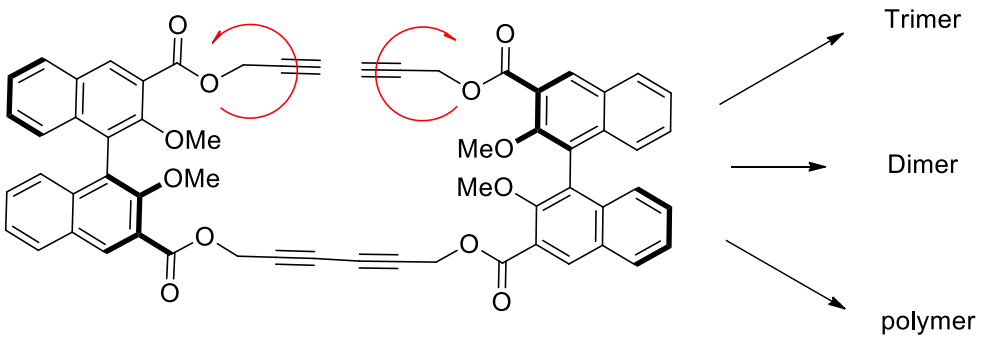

Figure 10. Flexibility of two "arms" causes possible different products

A range of methods was attempted to grow single crystals of **2.9a** and **2.9b** (Table 2). For the ester macrocycle **2.9a** only gels were obtained. In the case of the amide macrocycle **2.9b**, although no good quality crystal formed, it did produce solids, which encouraged us to further improve the method for crystal growth.

Table 2. Liquid-liquid diffusion for macrocycles **2.9a** and **2.9b**

Top / Bottom	EtOAc	acetone	CH_2Cl_2	MeOH	THF	$CHCl_3$
Hexane	G/S	G/S	G/S	G/S	G/S	G/S
Pentane	G/S	G/S	G/S	G/S	G/S	G/S
Et_2O	G/S	G/S	G/S	G/S	G/S	G/S

2.9a/2.9b S= solid G= gel

Vapor diffusion had been tried to crystallize the macrocycles (Table 3). In the vapor diffusion attempts, hexanes were chosen as the volatile/poor solvent to bring about the crystals from a good solvent dissolving the macrocycles, while other commonly used solvents such as pentanes and Et_2O was found to be too volatile to form good quality single crystals in this case.

Table 3. Vapor diffusion for new macrocycls **2.9a** and **2.9b**

	EtOAc	acetone	CH_2Cl_2	MeOH	THF	$CHCl_3$
Hexane	G/C	G/C	G/C	G/C	G/C	G/C

2.9a/2.9b C= crystal G= gel

For the ester macrocycle **2.9a**, no crystal formed from the vapor diffusion experiments. Meanwhile, for the amide macrocycle **2.9b**, some low quality crystals formed from EtOAc, acetone, MeOH and $CHCl_3$. It was quite satisfying to find that, however, good quality crystals formed in CH_2Cl_2 and THF. Crystals from CH_2Cl_2 were

colorless with a diamond shape; and those obtained from THF were colorless, thin, plate-shaped crystals. Crystals from CH_2Cl_2 produced poor X-ray data but crystals from THF gave good X-ray results for the macrocycle, which will be discussed in the following section.

The X-ray data shows that the macrocycle **2.9b** has a "boat" shape conformation and the two diacetylene units cross to each other (Figure 12). The molecule is symmetrical and among its four naphthol backbones, two sit nearly flat and two are perpendicular. The steric interaction between the two rear flat naphthol backbones from one molecule and the two vertical naphthol backbones from another adjacent molecule prevent the two stacking face-to-face (Figure 11). Instead, the molecules stack in a helical manner.

It can be seen that each amide group within the molecule forms one intramolecular H-bond between the amide NH and the methoxyl oxygen. It also forms an intermolecular H-bond between the amide NH and amide oxygen as initially proposed (Figure 12). The unit cell also demonstrated the lack of π-π interaction between two adjacent molecules and that only one H-bond (2.856Å) between amide-amide groups contributes to the helical stacking (Figure 13).

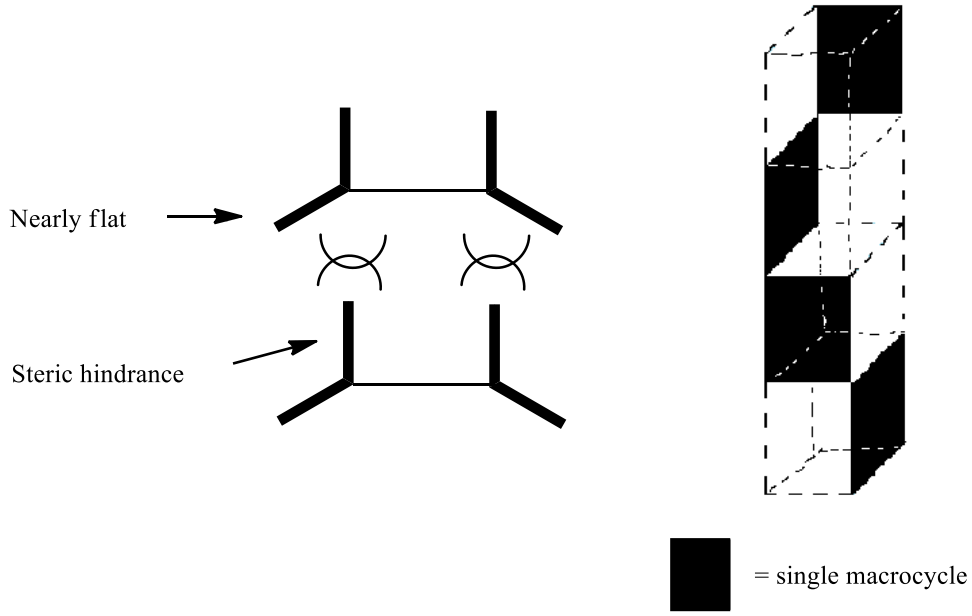

Figure 11. Steric hindrances between two molecules leading to a helical stacking state

In addition, H-bonding interactions between the amide NH and the methoxyl oxygen fix the conformation of the diacetylene units (Figure 12). The length of the H-bond is 2.736 Å, which falls into the range of the typical moderate H-bonding interactions[25]. This result confirms the previous hypothesis that reducing the flexibility of the macrocycle would increase the stability of the macrocycle. Moreover, less flexibility of the "arms" favors macrocyclization.

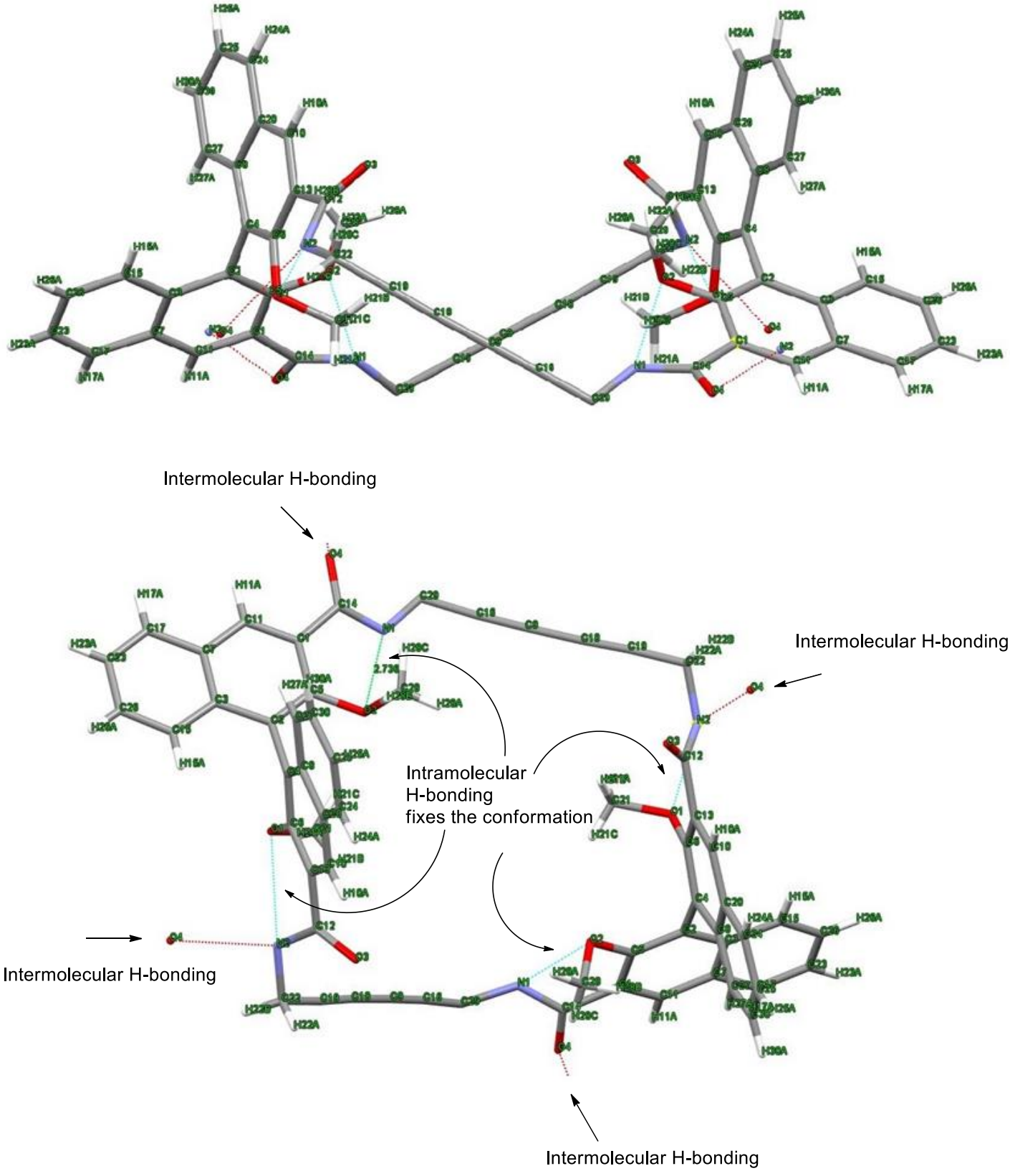

Figure 12. Two different orientations of macrocycle **2.9b**

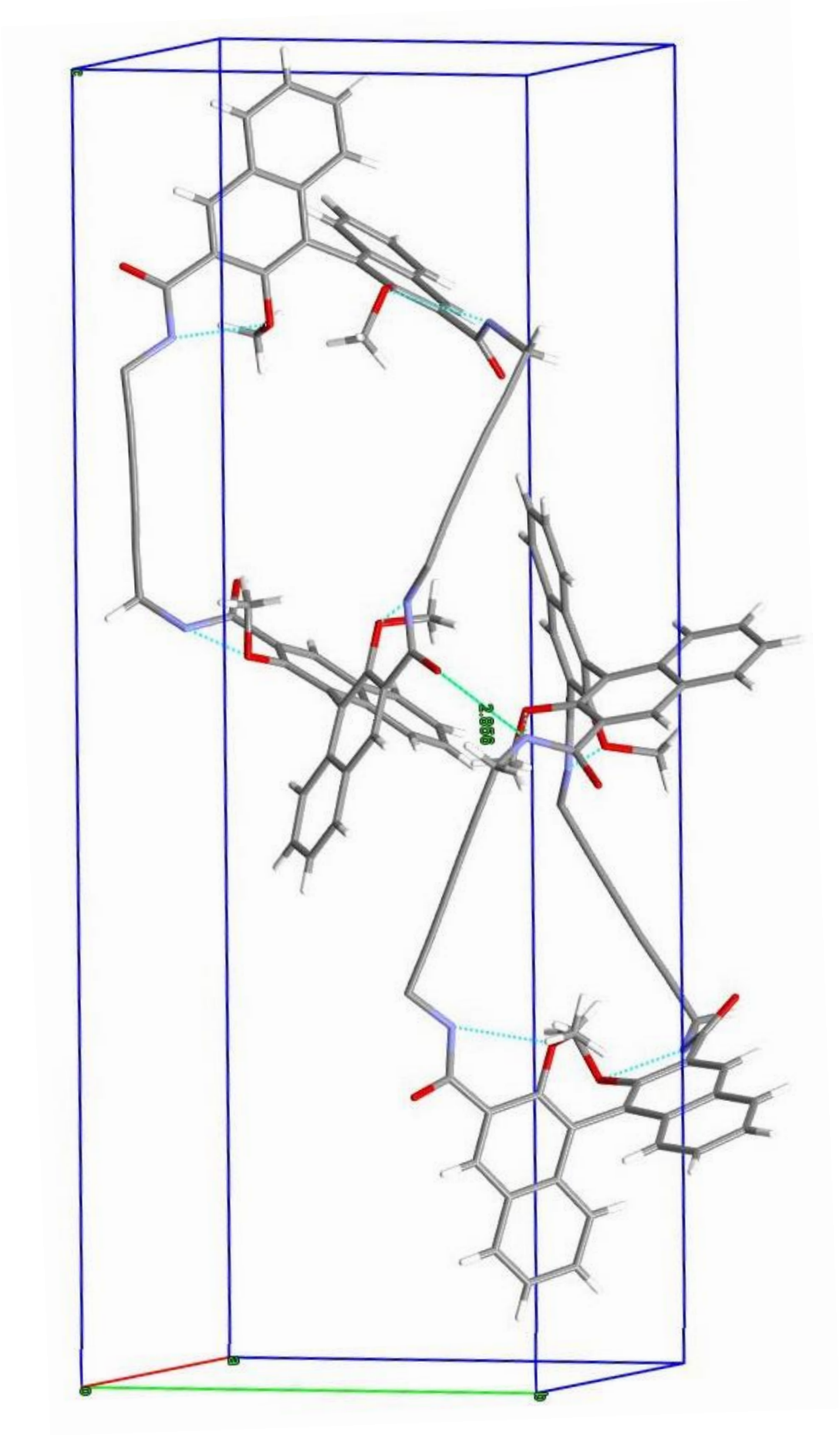

Figure 13. Helical stacking state of macrocycle **2.9b**

2.2.4 Summary

(*S*)-BINOL based building block macrocyclic amide **2.9a** and ester **2.9b** with two potentially polymerizable diacetylene functionalities have been successfully synthesized and characterized. The yield and stability of the macrocycles were modest to excellent. H-bonding-free macrocycle **2.9a** was obtained in low yield and furnished a gel upon crystallization, while the amide-containing macrocycle **2.9b** was obtained in high yield as a solid.

Single crystals were obtained for **2.9b** from THF-hexanes system. The corresponding X-ray data showed that two molecules of **2.9b** do not stack face-to-face due to steric hindrance from the BINOL units, which suggests that it is not an ideal backbone. Therefore, a search for some totally flat aryl-backbones and synthesis of flat macrocycles became the next task for this project.

2.3 Experimental

General Reactions

All reactions were carried out under a dry nitrogen atmosphere except the macrocyclization, which was open to air. All the glassware and stir bars were oven- or flame-dried. All the glassware, stir bars and needles used were washed with aqueous 1 M HCl and rinsed with deionized water and then acetone. Dry THF and Et_2O were distilled over Na, dry CH_2Cl_2 was distilled over CaH_2. TMEDA was distilled over CaH_2 into a Schlenk flask and stored under N_2. Et_3N was distilled with CaH_2 into a sealed flask under

N_2. NaH was washed with pentanes under a nitrogen atmosphere before use to remove mineral oil and freed of residual pentane under N_2. CuCl was recrystallized by a known procedure and stored in the glove box under N_2 atmosphere in the dark in a flask covered with foil.[26]

Reactions were monitored using commercial thin-layer chromatography (TLC) plates. Developed TLC plates were examined under a UV lamp (254 nm) or exposed to iodine stain. Flash chromatography was performed using 230–400 mesh silica gel.

Characterization

^{1}H and ^{13}C NMR spectra were obtained in $CDCl_3$ at 300 MHz and 75 MHz, respectively. Chemical shifts are reported in parts per million (ppm, δ). The residual chloroform peak at 7.24 ppm was used to calibrate proton NMR spectra and carbon spectra were calibrated to $^{13}CDCl_3$ at 77.0 ppm for the middle peak. DEPT 90/135 experiments were carried out to determine CH, CH_2 and CH_3 signals. Melting points were measured with a Melt-Temp apparatus and were not corrected.

Synthesis of terminal alkyne precursor

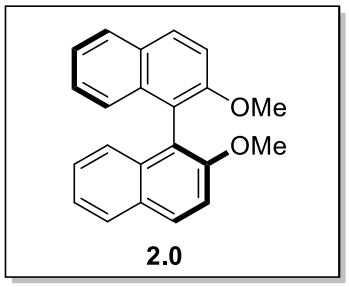

2.0

(*S*)-2,2'-dimethoxy-1,1'-binaphthalene

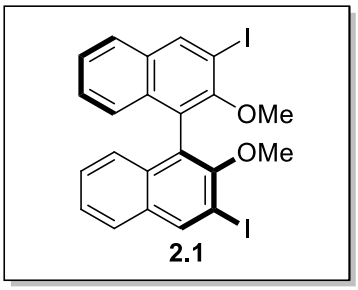

2.1

(*S*)-3,3'-diiodo-2,2'-dimethoxy-1,1'-binaphthalene

The compound **2.0** and **2.1** are prepared following literature procedures. [19, 20]

(*S*)-3,3′-(2,2′-Dimethoxy-[1,1′-binaphthalene]-3,3′-diyl)bisprop-2-yn-1-ol) (2.2)

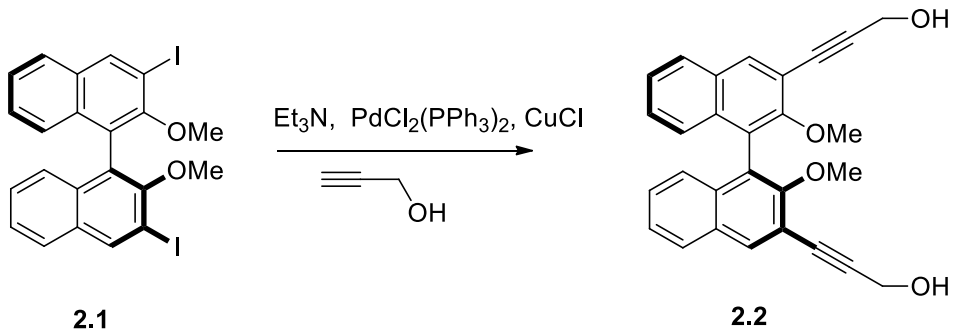

2.1 **2.2**

A 50 mL round-bottom flask equipped with a stir bar, was charged with diiodo **2.1** (0.5 g, 0.88 mmol, 1.0 equiv), $PdCl_2(PPh_3)_2$ (68 mg, 11 mol %) and CuCl (2.8 mg, 3.2 mol %). Et_3N (6.8 mL, 0.13 M) was added dropwise by syringe followed by propargyl alcohol (0.35 mL, 6.84 equiv). The reaction was stirred for 8 h at room temperature under a nitrogen atmosphere. The solvent was removed in vacuo using a rotavapor. The residue was dissolved in EtOAc (20 mL) and washed with 1M HCl (20 mL), sat. $NaHCO_3$ and brine, dried over $MgSO_4$, filtered and concentrated. The residue was purified by flash chromatography on silica gel (2:1 hexane-ethyl acetate and then 1:1 hexane-ethyl acetate) to give product **2.2** (240 mg) as a white gel in 63% yield. mp = 95-99 ℃; ^{1}H NMR ($CDCl_3$, 300 MHz) 8.07 (s, 2H), 7.78 (d, *J* = 8.1 Hz, 2H), 7.36 (dt, *J* = 7.0, 0.8 Hz, 2H), 7.25-7.20 (m, 2H), 7.06 (d, *J* = 8.4Hz, 2H), 4.54 (s, 4H), 3.59 (s, 6H), 2.21 (br s, 2H); ^{13}C NMR ($CDCl_3$, 75 MHz) 155.4, 134.4 (CH), 133.7, 130.1, 127.8 (CH), 127.3 (CH), 125.5 (CH), 125.3 (CH), 124.7, 116.6, 91.9, 82.2, 61.1 (CH_3), 51.6 (CH_2).

(*S*)-2,2′-Dimethoxy-3,3′-bis(3-(prop-2-yn-1-yloxy)prop-1-yn-1-yl)-1,1′-bin aphthalene (2.3)

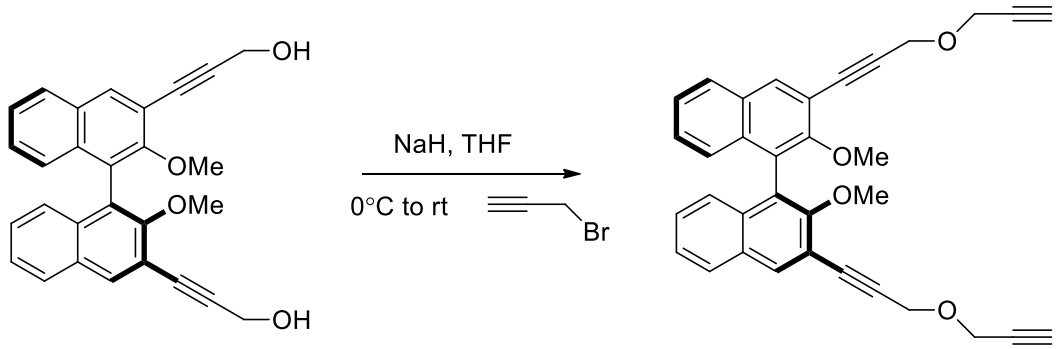

2.2 **2.3**

A 50 mL round-bottom flask was charged with the diol **2.2** (100 mg, 0.24 mmol, 1.0 equiv) and 1 mL THF. A 50 mL flask equipped with stirred bar was charge with NaH (54.9 mg, 9.66 equiv washed with pentane) and 1.5 mL of THF, cooled to 0 ℃. The solution of diol **2.2** was transferred via canula to the NaH dropwise. The reaction was kept at 0 ℃ and stirred for 30 min, then propargyl bromide was added (0.11 mL, 1.42 mmol, 6 equiv) dropwise over 30 min at 0 ℃. Then the reaction mixture was warmed to rt. and stirred for 8 h. The reaction was quenched slowly by the addition of cold water and was extracted by EtOAc (3 ×20 mL) .The combined organic layers were washed with sat. $NaHCO_3$ and brine, dried over $MgSO_4$, filtered and concentrated. The residue was purified by flash chromatography on silica gel (4:1 hexane-ethyl acetate and then 2:1 hexane-ethyl acetate) to give product **2.3** (86 mg) as a colorless oil in 73% yield. ^{1}H NMR ($CDCl_3$, 300 MHz) 8.13 (s, 2H), 7.82 (d, *J* = 8.1Hz, 2H), 7.38 (dt, *J* = 8.2, 0.8Hz, 2H), 7.24 (dt, *J* = 8.0, 1.1 Hz, 2H), 7.06 (d, *J* = 8.4Hz, 2H), 4.57 (s, 4H), 4.37 (d, *J* = 2.4Hz, 4H), 3.60 (s, 6H), 2.45 (t, 2.4Hz, 2H); ^{13}C NMR ($CDCl_3$, 75 MHz) 155.7, 134.7 (CH), 133.9, 130.1, 127.8 (CH), 127.4 (CH), 125.6 (CH), 125.4 (CH), 124.8, 116.5, 88.5, 83.8,

78.9, 75.0, 61.2 (CH_3), 57.4 (CH_2), 56.5 (CH_2).

Preparation of ether macrocycle 2.4

General procedure A

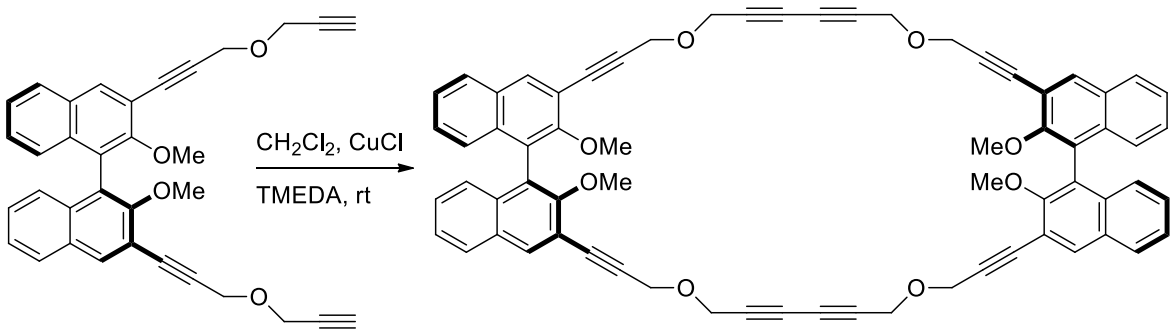

2.3 **2.4**

A 100 mL round-bottom flask equipped with a stir bar was charged with CuCl (149 mg, 1.48 mmol, 7.4 equiv), TMEDA (0.32 mL, 3.68 mmol, 18.4 equiv) and CH_2Cl_2 (50 mL). Compound **2.3** (0.1 g, 0.2 mmol, 1.0 equiv) was dissolved in 10 mL CH_2Cl_2 and transferred to the previous flask via syringe pump over 12 h. The reaction was stirred at rt with exposure to an air atmosphere in the dark (covered with aluminum foil) for 24 h. The reaction was monitored by TLC until there was no starting material left. When the reaction was completed, the solvent was removed and the residue was dissolved in EtOAc (150 mL). The organic layer was washed with approximately 500 mL of H_2O until the blue color (Cu catalyst) of aqueous layer disappears, then dried over $MgSO_4$, filtered and concentrated. The residue was purified by flash chromatography on silica gel (1:1 hexane-ethyl acetate and then 1:2 hexane-ethyl acetate) to give product **2.4** (34 mg) as a white solid in 23% yield. ^{1}H NMR ($CDCl_3$, 300 MHz) 8.11 (s, 4H), 7.82 (d, J = 8.2Hz, 4H), 7.38 (t, J = 7.7Hz, 4H), 7.24 (dt, J = 6.3, 1.0 Hz, 4H), 7.06 (d, J = 8.3Hz, 4H), 4.55 (s, 8H), 4.44 (s, 8H), 3.60 (s, 12H). ^{13}C NMR ($CDCl_3$, 125 MHz) 155.7, 134.6 (CH),

133.9, 130.1, 127.9 (CH), 127.4 (CH), 125.6 (CH), 125.4 (CH), 124.8, 116.4, 88.1, 84.2, 74.8, 70.9, 61.2 (CH_3), 57.5 (CH_2), 56.7 (CH_2)

(*S*)-2,2′-dimethoxy-[1,1′-binaphthalene]-3,3′-dicarboxylic acid (2.5)

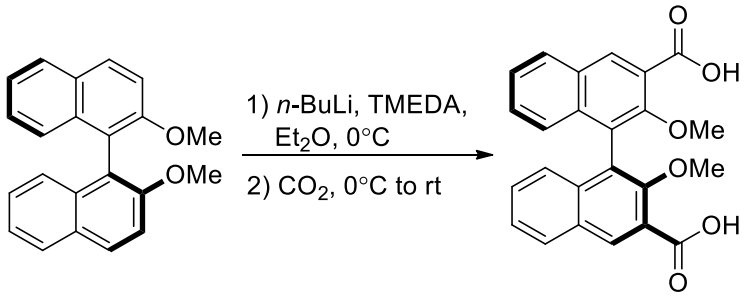

2.5

A 50 mL round-bottom flask equipped with a stir bar was charged with (S)-2, 2′-dimethoxy-1, 1′-binaphthalene (500 mg, 1.59 mmol, 1.0 equiv), Et_2O (0.2 M, 8 mL), and TMEDA (4.77 mmol, 0.71 mL, 3 equiv) and the mixture was cooled to 0 ℃. *n*-BuLi (2 M, 2.4 mL, 3 equiv) was introduced to the flask dropwise and the reaction was stirred for 30 min under a nitrogen atmosphere. Then, the reaction mixture was warmed to rt and stirred for 3 h. The reaction was cooled back to 0 ℃ and then CO_2 gas was introduced. The CO_2 gas was prepared from dry ice and bubbled into the solution for 2 h. The reaction was quenched slowly by the addition of cold water and was extracted with EtOAc (3 × 20 mL) .The combined organic layers were washed with 1M HCl (20 mL), sat. $NaHCO_3$ and brine, dried over $MgSO_4$, filtered and concentrated. The residue was purified by flash chromatography on silica gel (9:1 hexane-ethyl acetate and then 4:1 hexane-ethyl acetate) to give product **2.5** (60 mg) as a white solid in 94% yield. mp 118-120 ℃; ^{1}H NMR ($CDCl_3$, 300 MHz) 11.0 (br s, 2H), 8.09 (s, 2H), 8.06 (d, *J* = 8.1 Hz, 2H), 7.52 (t, *J* = 7.5 Hz, 2H), 7.42 (t, *J* = 7.4 Hz, 2H), 7.19 (d, *J* = 8.4 Hz, 2H), 3.46 (s, 6H); ^{13}C NMR ($CDCl_3$, 75 MHz) 167.9, 153.9, 136.0 (CH), 135.8, 129.7 (CH), 129.5

(CH), 126.2 (CH), 125.2 (CH), 124.8, 121.7, 62.3 (CH_3).

(*S*)-2,2′-Dimethoxy-[1,1′-binaphthalene]-3,3′-dicarbonyldichloride (2.6)

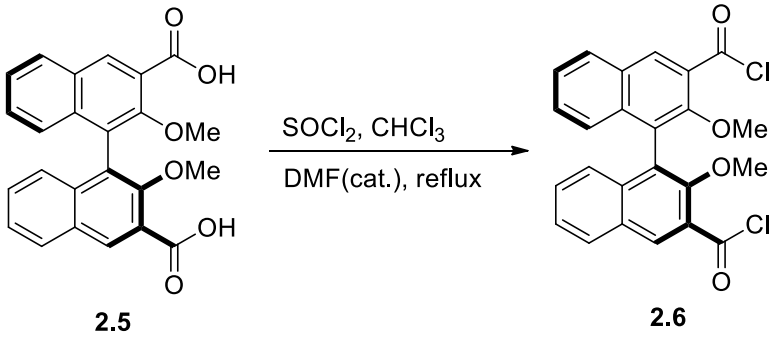

2.5 **2.6**

A 250 mL round-bottom flask equipped with a stir bar, was charged with **2.5** (4.5 g, 11.18 mmol 1.0 equiv), chloroform (75 mL) and DMF (0.1 mL, 10 mol %). The reaction was carried out under a nitrogen atmosphere. $SOCl_2$ (4.9 mL, 67.08 mmol, 6.0 equiv) was added dropwise using a syringe and the reaction was refluxed for 16 h. The solvent was removed in vacuo using a rotavapor. The crude compound **2.6** (6.2g) was used in the next step without purification.

Synthesis of Terminal Alkynes 2.7 and 2.8

General procedure B

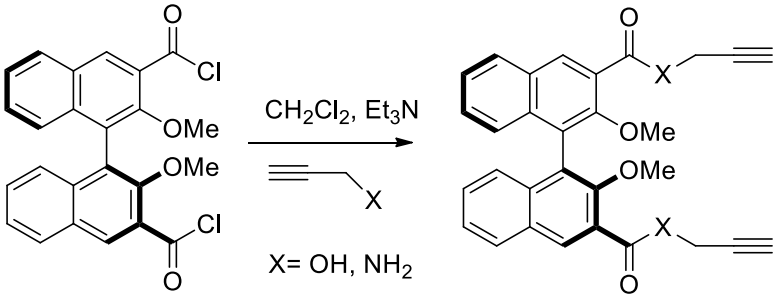

A 50 mL round-bottom flask equipped with a stir bar, was charged with compound **2.6** (1.0 equiv), DCM (0.5 M) and Et_3N (2.4 equiv) at 0 ℃ under a nitrogen atmosphere.

Propargyl alcohol or amine (2.2 equiv) was added to the mixture dropwise over 30 min at 0 ℃. Then the reaction mixture was warmed to rt and stirred for 12 h. The reaction was quenched slowly by the addition 1 M HCl and extracted by EtOAc (3 × 20 mL). The combined organic layers were washed with sat. $NaHCO_3$ and brine, dried over $MgSO_4$, filtered and concentrated. The residue was purified by flash chromatography on silica gel.

(*S*)-2,2′-Dimethoxy-N3,N3′-di(prop-2-yn-1-yl)-[1,1′-binaphthalene]-3,3′-dicarboxamide (2.8)

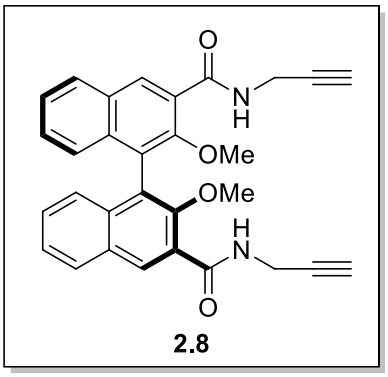

2.8

Compound **2.8** was prepared according to the General procedure B (flash chromatography eluent = 4:1 hexane-ethyl acetate and then 1:1 hexane-ethyl acetate) to give product **2.8** as a light yellow solid in 79% yield. mp 80-84 ℃; ^{1}H NMR ($CDCl_3$, 300 MHz) 8.86 (s, 2H), 8.13 (br t, *J* = 5.1 Hz, 2H), 8.03 (d, *J* = 8.1 Hz, 2H), 7.46 (t, *J* = 7.3 Hz, 2H), 7.33 (t, *J* = 8.2 Hz, 2H), 7.05 (d, *J* = 8.4 Hz, 2H), 4.46-4.19 (m, 4H), 3.36 (s, 6H), 2.23 (t, *J* = 2.5 Hz, 2H); ^{13}C NMR ($CDCl_3$, 75 MHz) 164.8, 153.1, 135.2, 133.9 (CH), 130.0, 129.4 (CH), 128.5 (CH), 125.7 (CH), 125.2, 125.1 (CH), 125.0, 79.4, 71.4, 61.8 (CH_3), 29.3 (CH_2).

(*S*)-Di(prop-2-yn-1-yl)2,2′dimethoxy-[1,1′-binaphthalene]-3,3′-dicarboxylate (2.7)

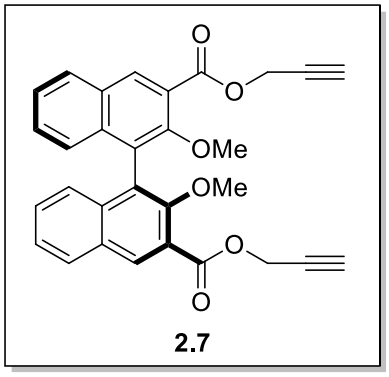

2.7

Prepared according General to procedure B (flash chromatography eluent = 9:1 hexane-ethyl acetate and then 4:1 hexane-ethyl acetate) to give product **2.7** as a white gel in 77% yield. ^{1}H NMR ($CDCl_3$, 300 MHz) 8.58

(s, 2H), 7.97 (d, *J* = 8.1 Hz, 2H), 7.44 (t, *J* = 8.0 Hz, 2H), 7.33 (t, *J* = 8.4 Hz, 2H), 7.12 (d, *J* = 8.4 Hz, 2H), 4.98 (d, *J* = 2.4 Hz, 4H), 3.47 (s, 6H), 2.52 (t, *J* = 2.4 Hz, 2H); ^{13}C NMR ($CDCl_3$, 75 MHz) 165.4, 154.4, 135.9, 133.9 (CH), 129.5, 129.2 (CH), 128.8 (CH), 126.3, 125.7 (CH), 125.5 (CH), 124.0, 77.6 75.2, 62.2 (CH_3), 52.7 (CH_2).

Synthesis of Macrocycle 2.9a and 2.9b

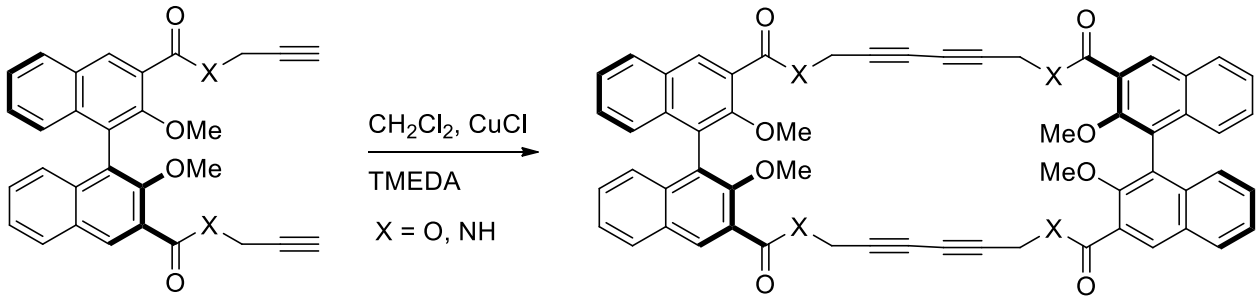

Ester containing (*S*,*S*) macrocycle (2.9a)

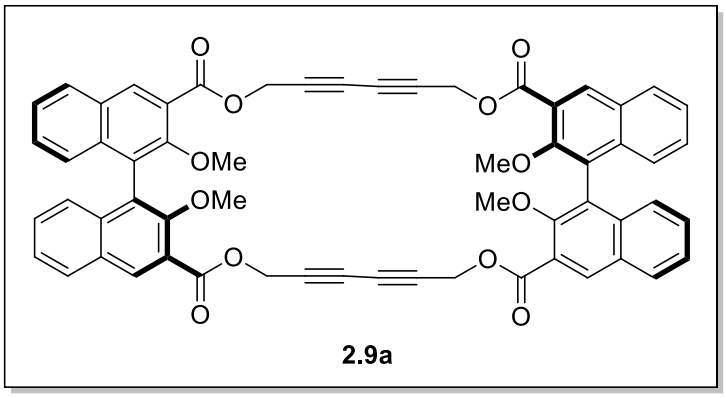

Compound **2.9a** was prepared according to General procedure A (flash chromatography eluent = 4:1 hexane-ethyl acetate and then 1:1 hexane-ethyl acetate) to give product **2.9a** as a white solid in 10% yield. ^{1}H NMR ($CDCl_3$, 300 MHz) 8.53 (s, 4H), 7.94 (d, *J* = 8.0 Hz, 4H), 7.42 (t, *J* = 7.1 Hz, 4H), 7.32 (t, *J* = 8.3 Hz, 4H), 7.10 (d, *J* = 8.4 Hz, 4H), 5.08 (d, *J* = 15.9 Hz, 4H), 4.96 (d, *J* = 15.9 Hz, 4H), 3.44 (s, 12H); ^{13}C NMR ($CDCl_3$, 75 MHz)

165.8, 154.3, 135.9, 134.1 (CH), 129.5, 129.3 (CH), 128.8 (CH), 126.3, 125.7 (CH), 125.5 (CH), 123.9, 73.5, 70.6, 62.3 (CH_3), 53.0 (CH_2)

Amide-containing (*S*,*S*) macrocycle (2.9b)

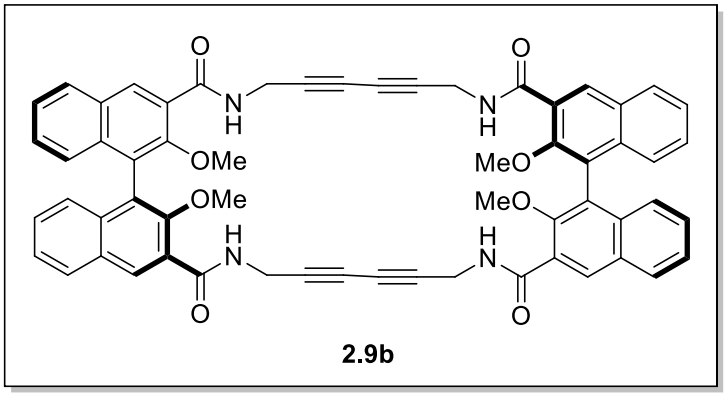

2.9b

Compound **2.9b** was prepared according General procedure A (flash chromatography eluent = 4:1 hexane-ethyl acetate and then 1:1 hexane-ethyl acetate) to give the final product **2.9b** as a light yellow solid in 40% yield. mp 296-298 ℃; ^{1}H NMR ($CDCl_3$, 300 MHz) 8.82 (s, 4H), 8.08 (br t, *J* = 4.8 Hz, 4H), 8.00 (d, *J* = 7.7 Hz, 4H), 7.46 (t, *J* = 7.2 Hz, 4H), 7.33 (t, *J* = 7.3 Hz, 4H), 7.02 (d, *J* = 8.4 Hz, 4H), 4.53 (dd, *J* = 18.3 Hz, 5.4 Hz, 4H), 4.27 (dd, *J* = 18.3 Hz, 4.7 Hz, 4H), 3.33 (s,12H); ^{13}C NMR ($CDCl_3$, 75 MHz) 164.8, 153.2, 135.5, 134.4 (CH), 130.2, 129.7 (CH), 128.9 (CH), 126.1 (CH), 125.3 (CH), 125.2, 124.9, 74.1, 67.8, 62.1 (CH_3), 30.2 (CH_2)

Chapter 3 Planar Macrocycles

3.1.1 Introduction

The synthesis of a planar macrocycle was the next task of this project, since the planarity might minimize steric hindrance and increase the possibility to obtain supramolecular stacking. Carbazole and dibenzofuran drew interest in the context of present project based on their planar skeleton. In addition, different aromatic carbon positions on the carbazole and dibenzofuran (*o* and *p* positions to the heteroatom X) can be chemically modified (Figure 14). To the best of our knowledge, macrocycles containing carbazole or dibenzofuran as building blocks and with diacetylene for polymerization has not been reported in the literature to date. Carbazole and dibenzofuran are tricyclic aromatic heterocyclic molecules, which have two benzene rings fused on both sides of a five membered heteroatom-containing ring. Carbazole and similar heterocyclic molecules have demonstrated wide usage in various fields, such as pharmaceuticals, agrochemicals, dyes, pigments, photosensitizer and display devices.[28-31]

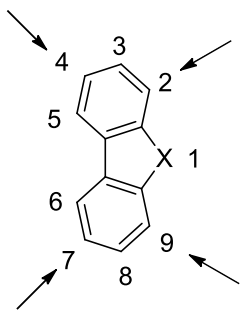

X = O, NH

Figure 14. Chemically modified positions of carbazole and dibenzofuran

Macrocycles containing carbazole and dibenzofuran have also been studied for several decades. In 2009, Mullen and co-workers synthesized a fully π-conjugated carbazole-based macrocycle (Figure 15). A hexa-peri-hexabenzocoronene (HBC) molecule, which acts as an organic semiconductor, is deposited inside the cavity of the carbazole-based macrocycle to form a 1:1 host-guest complex. In the bulk phase, π-stacking interactions between the rigid aromatic circle and the flexible alkyl side chains contributes to the conjugated macrocycles self-assembling into columnar structures.[32]

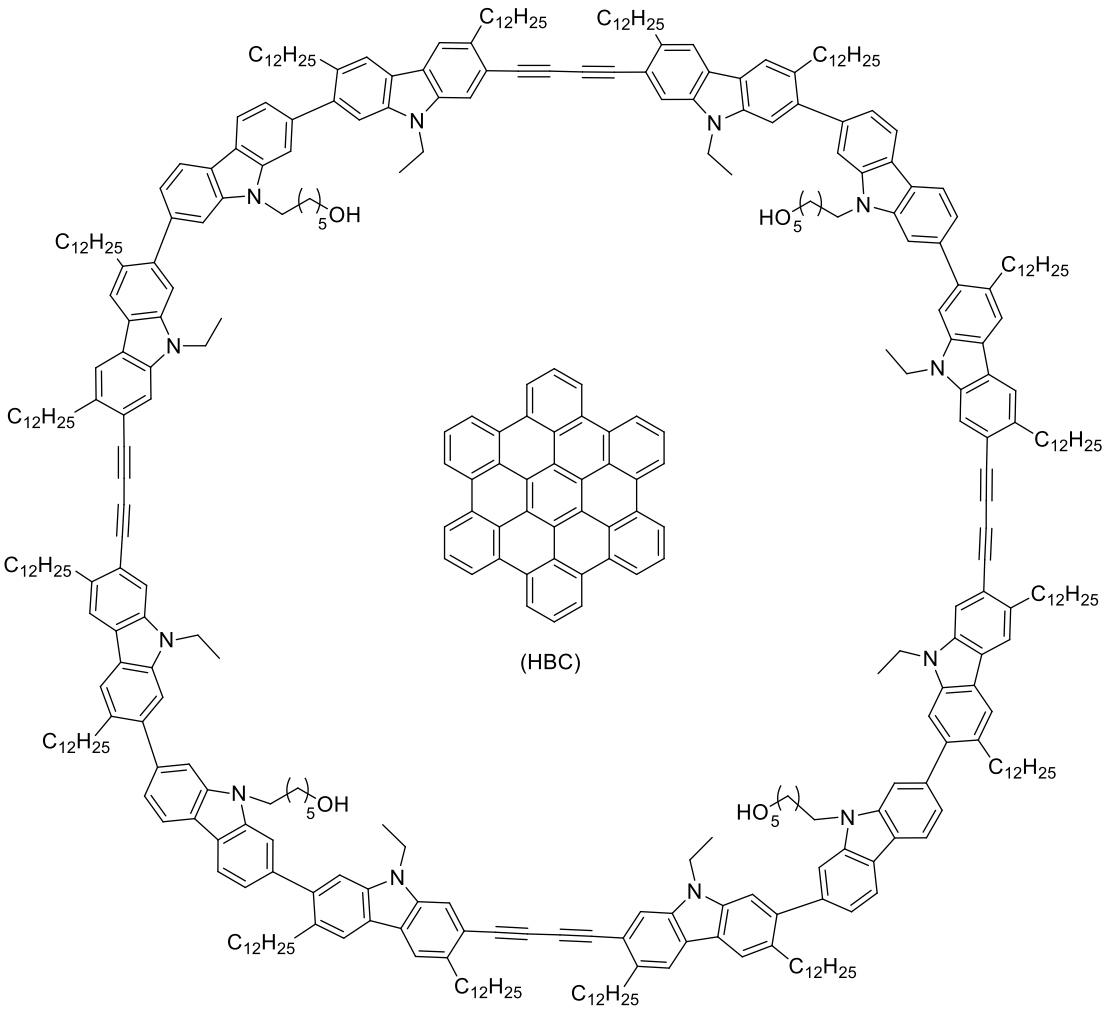

Figure 15. Carbazole-based macrocycle with organic semiconductor

In 2010, Felix and co-workers designed and synthesized two different macrocycles that contain dibenzofuran units as backbone and amine functionalities within the macrocycle (Figure 16).[33] The macrocycles were examined as receptors with several substrates such as imidazole, some carboxylates and even metal salts based on the host-guest strategy. X-ray data indicated that the dibenzofuran units are planar as expected.

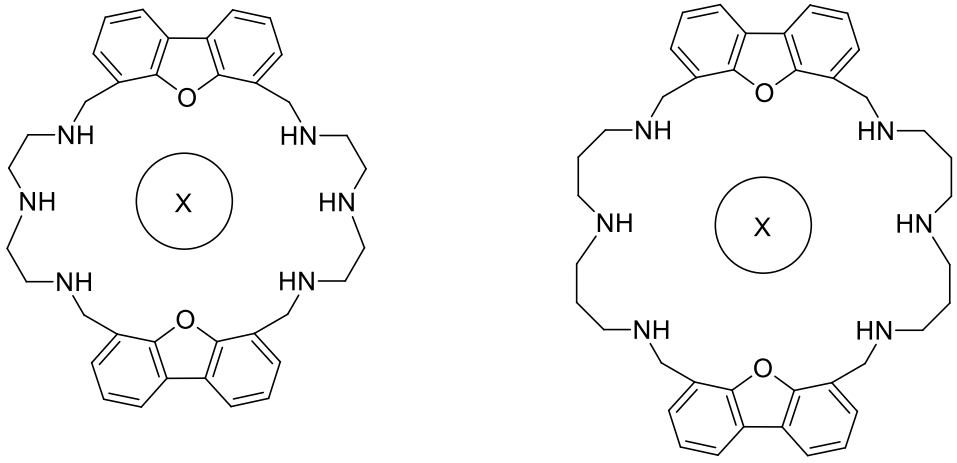

X = imidazole, carboxylates, metal salts

Figure 16. Dibenzofuran-based macrocycles

In 2012, Machida's group reported the synthesis, structure and electronic state of a macrocycle composed of a carbazole and a diacetylene unit (Scheme 17).[34] Mixtures of intramolecular and intermolecular coupling compounds were obtained. The structure of a strained mono-macrocycle and its unstrained dimer were revealed by X-ray analysis. It showed that there are two conformations for the strained monomer, with either a bent diacetylene unit or carbazole unit.

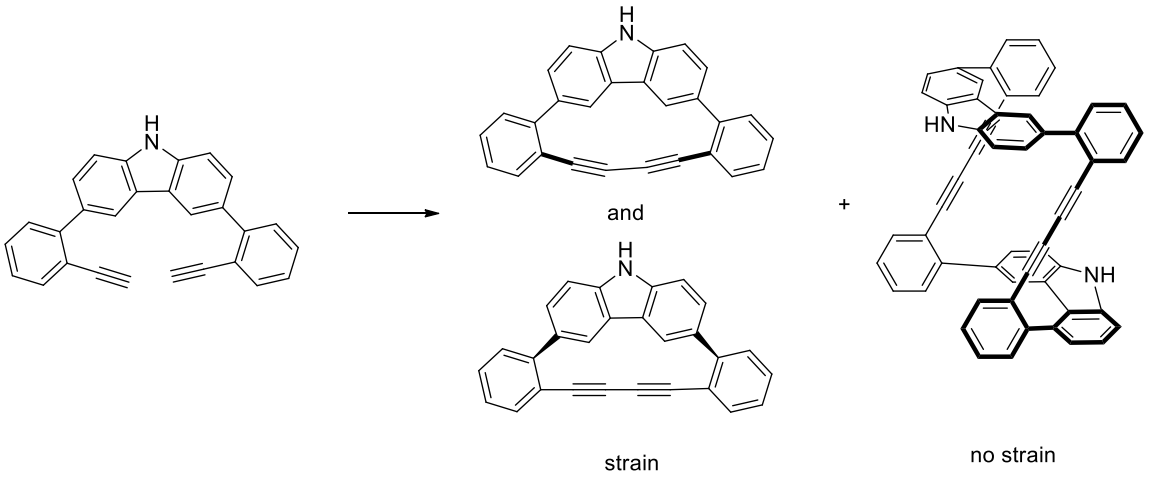

Scheme 17. Intramolecular and intermolecular macrocycles containing diacetylene functionality

3.1.2 Proposal

Carbazole and dibenzofuran were chosen as new backbones because of their planar shape. Benzamide functionality will be used as a stabilizing linker, and dibenzofuran will be the framework for this macrocycle. The oxygen atom of the dibenzofuran will be the H-bonding acceptor that can undergo intramolecular H-bonding with two nearby benzamide NHs (Figure 17). As a consequence of these favorable H-bonding interactions, the two "arms" shall be fixed to avoid free rotations, which may enhance the thermal stability of the final product and increase the yield of macrocyclization.

Alternatively the carbazole backbone could allow for modification at the C(3), C(6) positions, leaving the N atom outside of the cavity for further modification (Figure 17). For example, *N*-alkylation would provide an easy way to reduce the polarity of the entire molecule. Otherwise, the carbazole's –NH could form additional H-bonding with other acceptors such as oxygen atoms, if not alkylated, which may hamper the desired

face-to-face stacking.

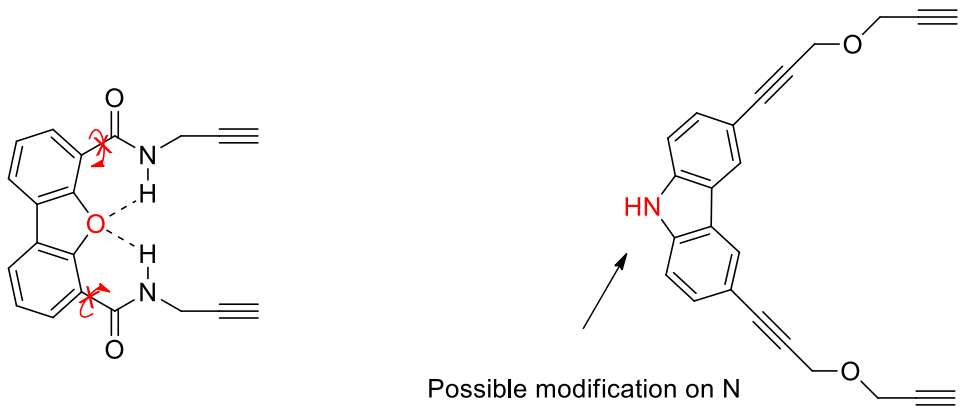

Figure 17. Strategy for designing carbazole-based and dibenzofuran-based macrocycles

Therefore, two new macrocycles as shown below were proposed (Figure 18). The first one is an amide-functionalized dibenzofuran macrocycle that possesses intramolecular H-bonding interactions. Interactions of π-π stacking and H-bonding between two such molecules might work together to form a tubular structure. Secondly, H-bonding-free carbazole macrocycle was also proposed. It contains an N atom on either side of the ring pointing outside of the cycle, which allows further modification. The π-π stacking interaction would be the main force to form a face-to-face stacking.

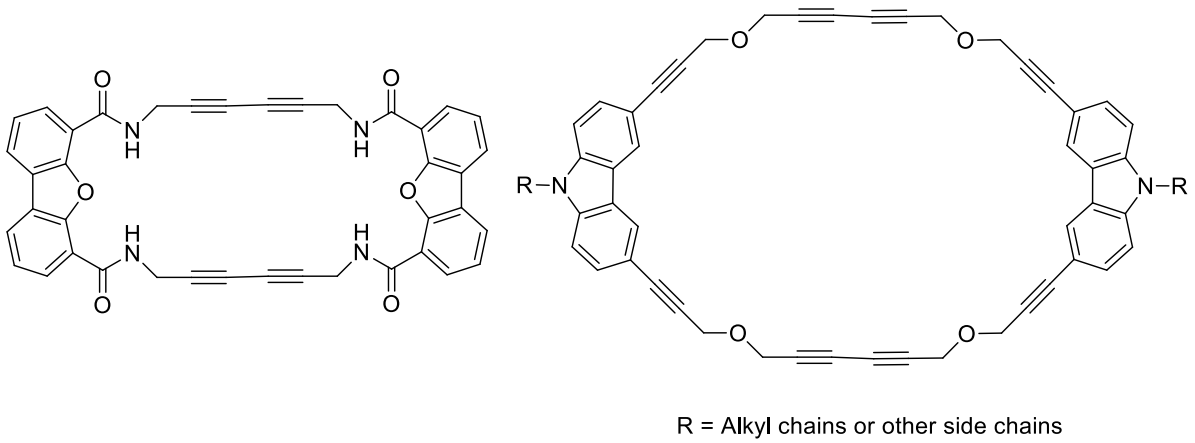

Figure 18. Two proposed macrocycles

3.1.3 Results and Discussion

Lithiation at the *ortho* positions to the oxygen atom of the dibenzofuran and then reaction with CO_2 provided the corresponding dicarboxylic acid (Scheme 18). Early attempts using *n*-BuLi and TMEDA did not work. The more basic *s*-BuLi was used to deprotonate the α-protons and the reaction proceeded smoothly to give a high yield of the dicarboxylic acid. The dicarboxylic acid was then converted to the corresponding acid chloride via a known procedure.[35] Propargyl amine reacted with the acid chloride to form the corresponding terminal alkyne precursor. The first attempt for this key coupling step was performed by using CuCl with TMEDA in CH_2Cl_2. However, even after 2 days, there was no macrocycle formed.

After examining different literature conditions on macrocyclization, various solvents were tried at ambient temperature. In a polar solvent such as DMF, acetone and MeOH, the macrocyclization reactions were even worse than in CH_2Cl_2, as no macrocycle was observed and many byproducts formed as indicated by TLC. Then the reaction

temperature was raised to 40 ℃ to promote the macrocyclization. Unfortunately, no macrocycle was formed despite the increased reaction temperature.

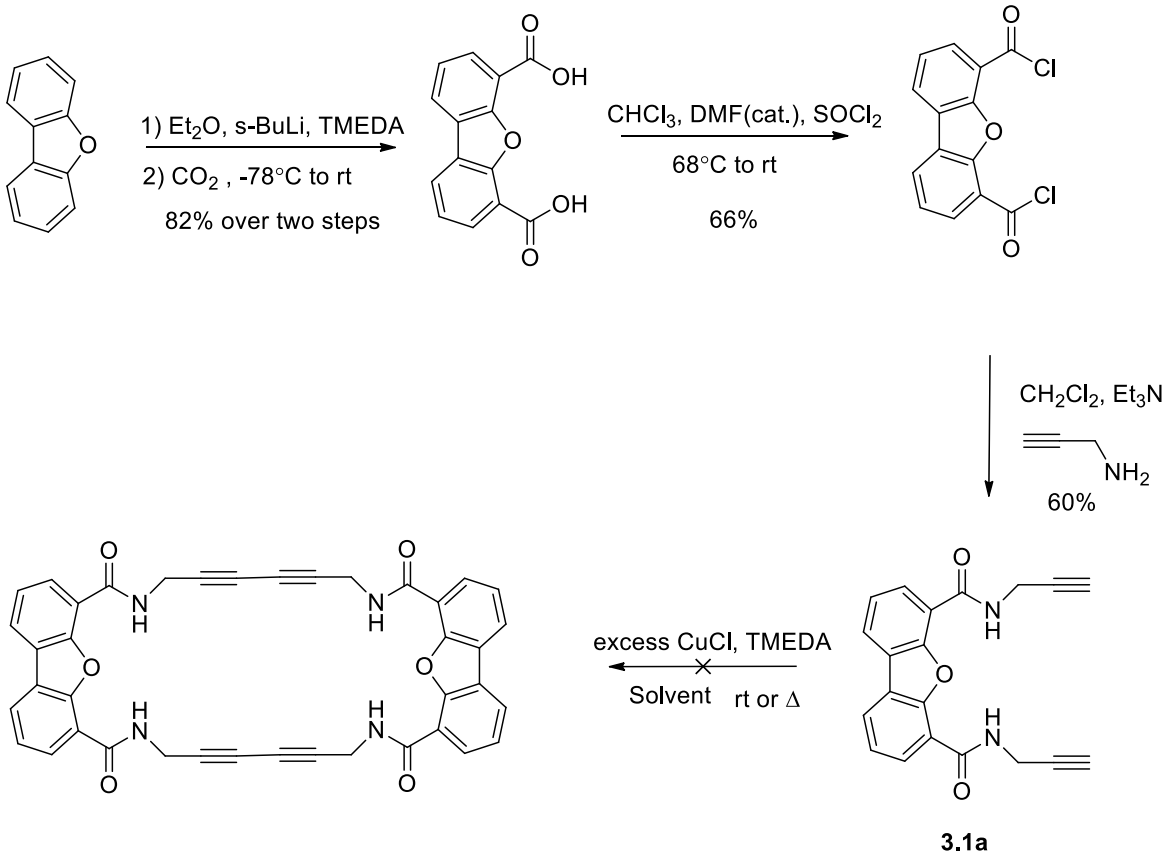

Scheme 18. Synthesis of dibenzofuran-based macrocycle

In parallel, the synthesis of a carbazole-based ether-containing macrocycle was performed as depicted in Scheme 19. 3,6-Diiodocarbazole was prepared based on a known procedure,[35] followed by alkylation of the carbazole with MeI. N-alkylation by alkyl chains with different lengths can be attempted in the future. Further building of the architecture involved the Sonogashira reaction followed by etherification. However, in THF, the etherification did not occur. More polar solvent DMF was used instead, and a

quantitative yield was obtained. However, no product was obtained in the attempted macrocyclization and only starting material and polymeric side-products were observed.

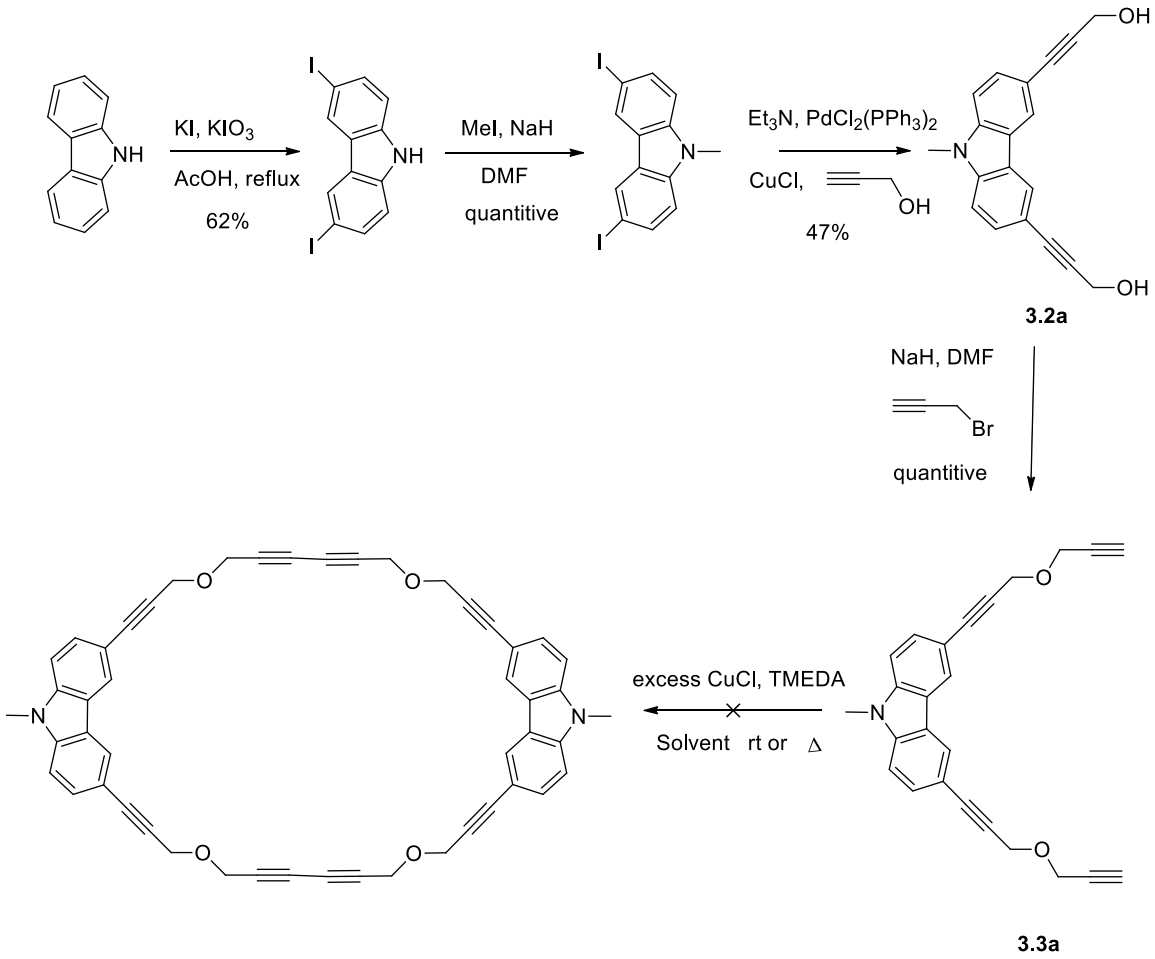

Scheme 19. Synthesis of carbazole-based macrocycle

3.1.4 Summary

Synthetic effort to make macrocycles with new frameworks failed. The failure forces a reconsideration of the proposed structures, in which the problem might be the angle between the two "arms" involved. For the successful examples in the literature, the angle between the two "arms" is about 120°, whereas the corresponding angles in the newly

designed systems are around 30 ° and 90 ° (Figure 19), as the five-membered heterocyclic ring in the middle of the backbone positions the two benzene rings at a small angle to each other. In other words, the two benzene rings are not parallel to each other. Thus, using the same linker will lead the two terminal alkynes to not be parallel to each other on the planer face. Steric hindrance of terminal alkynes makes it hard to couple intermolecularly. Moreover, to bend the bond to form a strained macrocycle may disturb the planar conformation, and cause the macrocycle to fail to stack face-to-face.

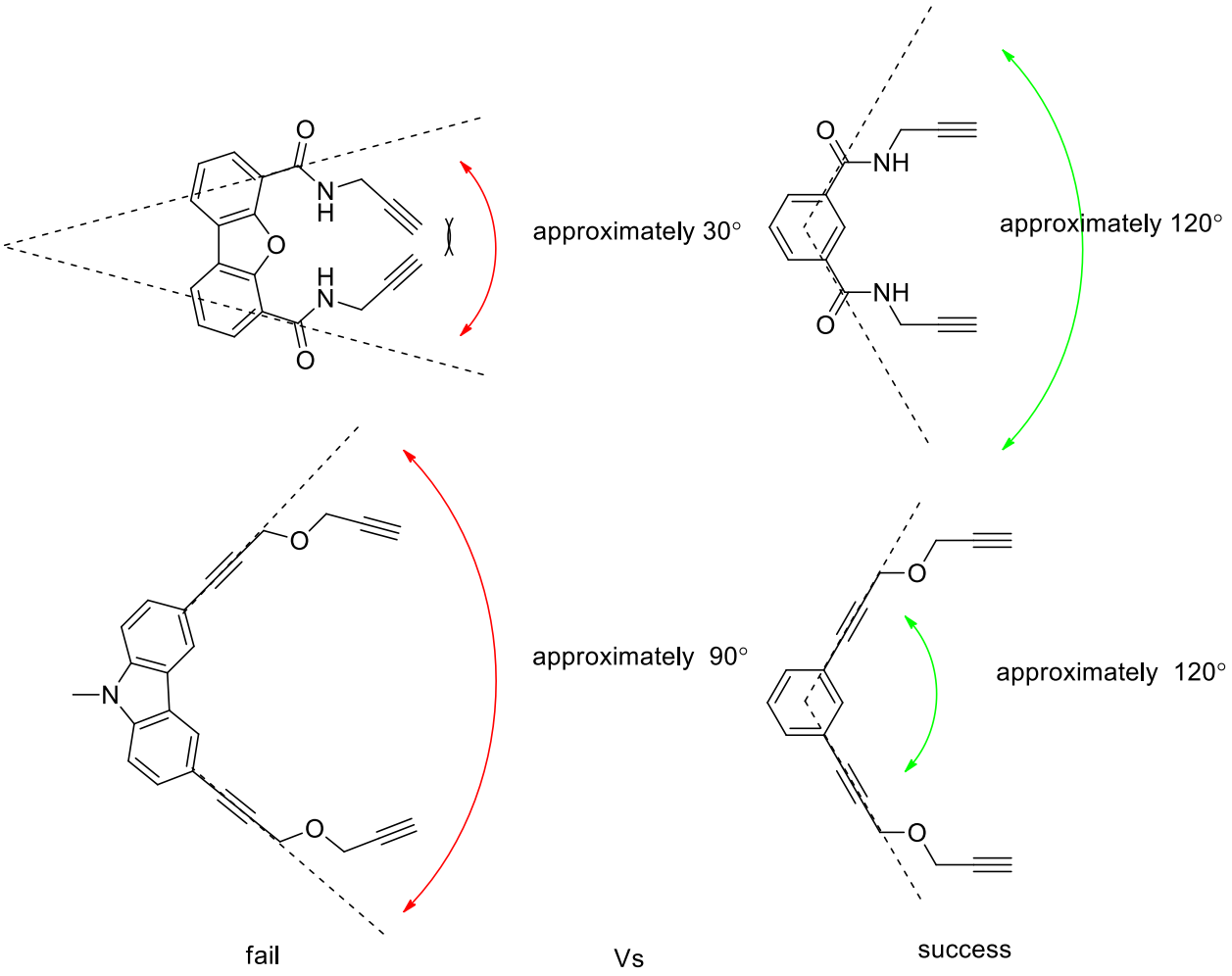

Figure 19. Angle issue for designing macrocycles

Therefore, it seems that proposed macrocycles precursors were not suitable dimerization substrates. The 3,6-diiodocarbazole was still viewed as a promising building block. Because the two substitutes adopt an angle near 90°, the might be able to form tetrameric macrocycles with linear linkers.

3.2.1 Carbazole Backbone Tetramer Macrocycles

Based on our previous results, the shape of the macrocycles was redesigned. It was postulated that a planar system with a tetramer building block could favor the formation of nanotubes.

In 2006, Zhu's group developed a shape-persistent macrocycle based on a carbazole backbone, which has tetramer building blocks and simple diacetylene as linker (Scheme 20).[36] The tetramer macrocycle was prepared from either the monomer or dimer precursors, but the dimer pathway gave significantly higher yield when compared with the monomer pathway (35% and 6% respectively). The macrocycle's electronic properties were also studied, which might be used for organic solar cells. Unfortunately, no X-ray data was obtained and polymerization of the macrocycle into the tubular structure had not been studied.

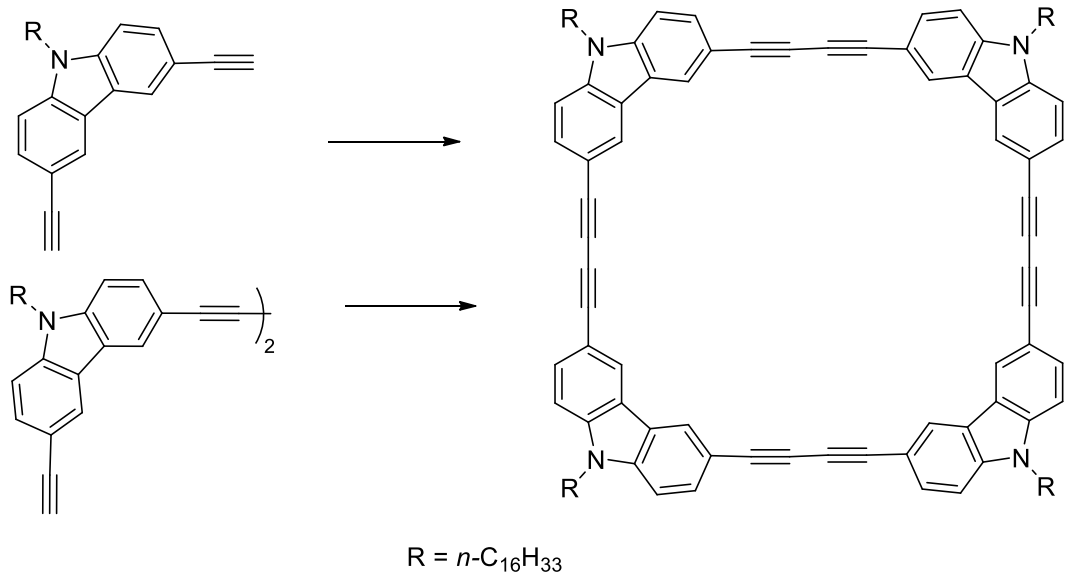

Scheme 20. Alkylated carbazole-based macrocycle

In 2011, Mukherjee and co-workers designed and synthesized a new Pt-based organometallic building block with a 90 °geometry, possessing a carbazole backbone with an ethynyl functionality macrocycle (Scheme 21).[37] Mukherjee found that the flexible ditopic donors (L_a and L_b) prefer to form a closed macrocycle instead of open-chain polymers when reacting with the Pt-containing carbazole unit. However, only the X-ray of the macrocycle with L_a was obtained, which showed that it has a near square-planer geometry and the C-N-Pt angle is nearly liner. Fluorescence studies were also carried out and demonstrated that these macrocycles were weakly luminescent in the solution, due to the presence of Pt-ethynyl functionality and the conjugated backbone.

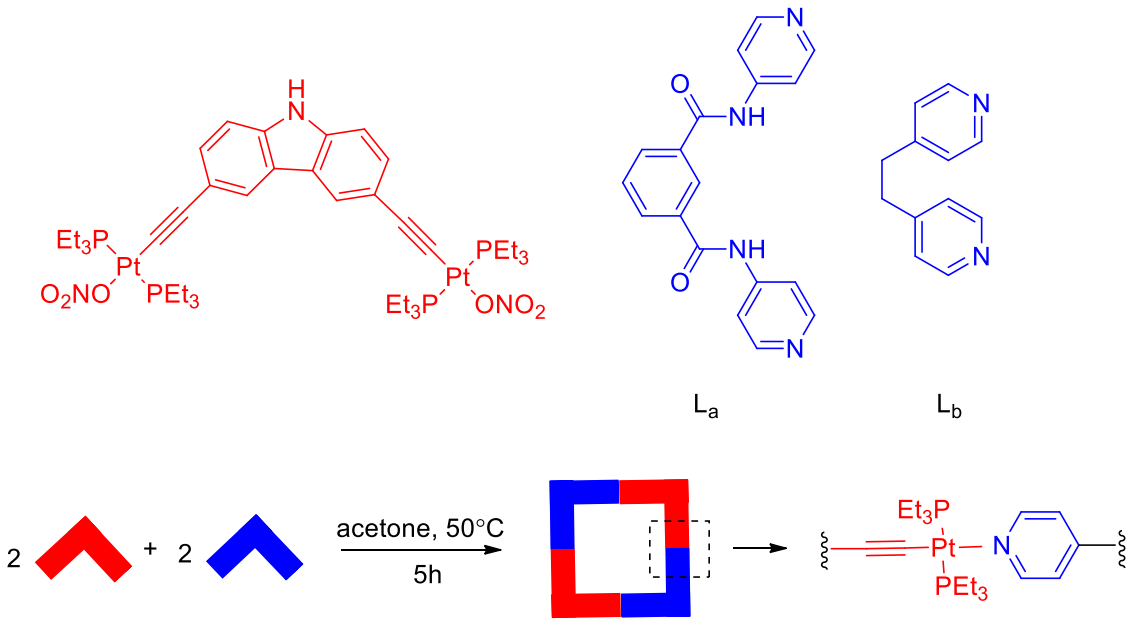

Scheme 21. Macrocycle with Pt-based organometallic building block with 90 °geometry

In 2011, Moore's group reported the synthesis of some carbazole-based macrocycles with different side chains (Scheme 22).[38] Macrocyclic depolymerization of carbazolyl-ethynylene homopolymers with highly active molybdenum alkylidyne catalyst offered macrocycles. Simple starting materials (terminal alkynes and aryl halides) were used to prepare the homopolymers. X-ray analysis of the crystal for the macrocycle with long *N*-alkyl chain indicated that it adopts a non-coplanar shape. When an ester functional group was inserted between the carbazole nitrogen and the long alkyl chain, the carbonyl linkage promotes coplanar arrangement of the side chains and the core skeleton of the macrocycle that enhances the π-π stacking.

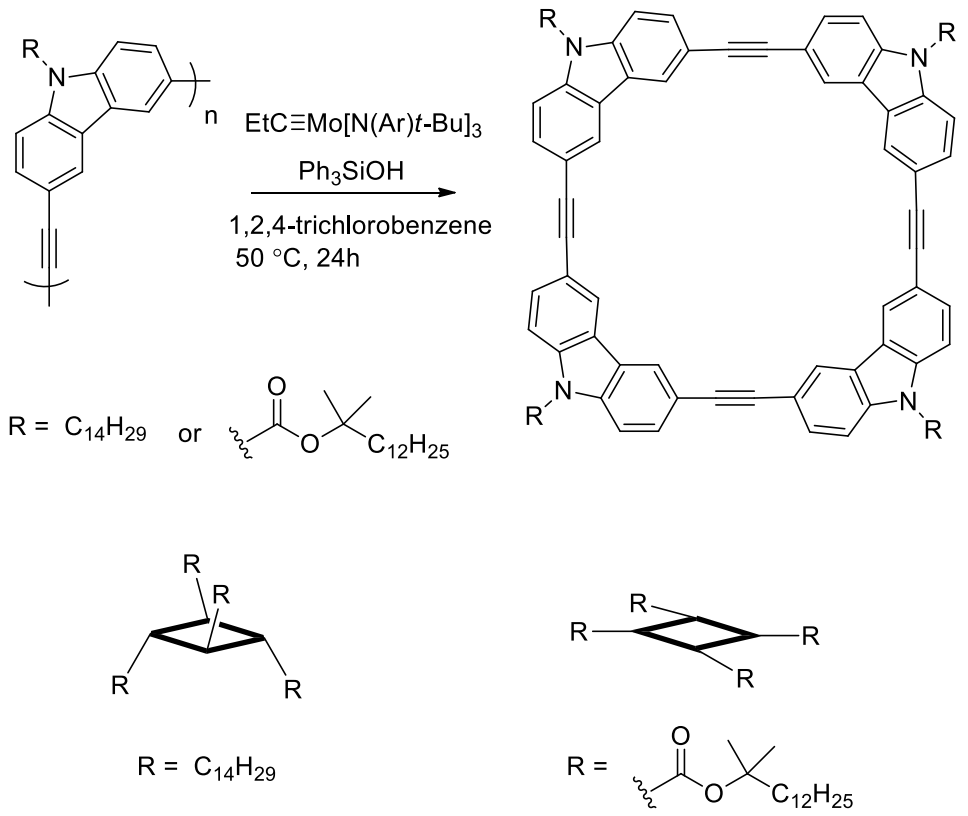

Scheme 22. Non-coplanar and coplanar carbazole-based macrocycles

Different H-bonding-capable functionalities to be introduced into the side chain have been considered for the backbone. Urea functionality has been used in the design of tubular structures as a locating group due to its bi-directional H-bonding interactions.

In 2001, Shimizu and co-workers presented the bis-urea macrocycle C that self-assembled into columnar nanotubes primarily via H-bonding (Scheme 23).[39] The macrocycle bears a rigid *m*-phenylene linker and assembles to form tubular structures. Single crystal X-ray crystallographic analysis showed that the intermolecular H-bonding interactions and π-π stacking interaction hold the macrocycle together. However, transannular H-bonding also exists between the urea groups. The two urea functionalities within the macrocycles adopt an antiparallel fashion when stacking, which could

minimize the overall dipole moment. A few years later, macrocycle D was designed and synthesized by the Shimizu group as well.[40] The larger space between the two urea groups within macrocycle D than that of macrocycle C avoids the formation of intramolecular H-bonding. Similar to macrocycle C, carbonyl moieties of macrocycle D in the crystal were also aligned in parallel but in opposite orientations.

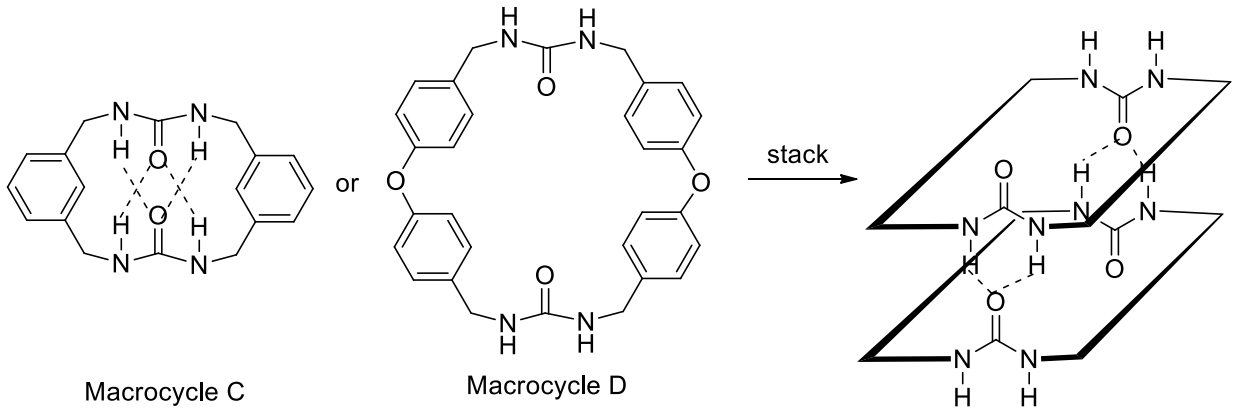

Scheme 23. Bis-urea macrocycles C and D

The urea functionality was also used by Guichard and co-workers in designing tubular structures (Scheme 24)[41] made up of cyclic tetrameric urea macrocycle possessing an overall symmetry of C_4. X-ray crystallographic analysis of this macrocycle revealed a planar conformation with all urea carbonyl groups pointing in the same direction, and all the NH urea groups pointing in the opposite direction. The carbonyl of one urea functionality forms H-bonds with two hydrogen atoms from the neighboring NH urea fragment, which helps the formation of the tubular structure. [41]

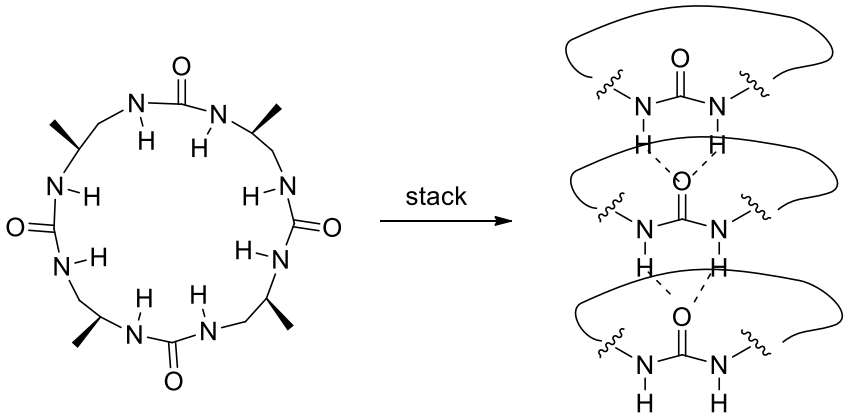

Scheme 24. Tetrameric urea macrocycle with an overall symmetry of C_4

3.2.2 Proposal

After the search of new framework and side chains, new tetrameric carbazole-based macrocycles were proposed (Figure 20). The idea is to build the architectures at C(3), C(6) positions and form a 90 °building block with further modification outside of the cavity.

To the best of our knowledge, similar macrocycles in previous literature examples always had the side chain attached to the nitrogen atom, and the side chain-free macrocycle had not been synthesized previously. Moreover, a macrocycle with a long side chain containing a urea group was also designed and synthesized. Reduction of the polarity and introducing H-bonding donors and acceptors are the two main reasons for this new proposed macrocycle. In addition, alkylation with extra flexible diacetylene-containing long side chains will help the polymerization to occur, if the diacetylene in the ring are too rigid to undergo the polymerization.[24]

Therefore, three variants with respect to substitution at nitrogen were initially considered: a side chain-free macrocycle, alkylaminoacyl functionality H-bonding

interaction containing macrocycle, and flexible diacetylene-containing alkyl chain.

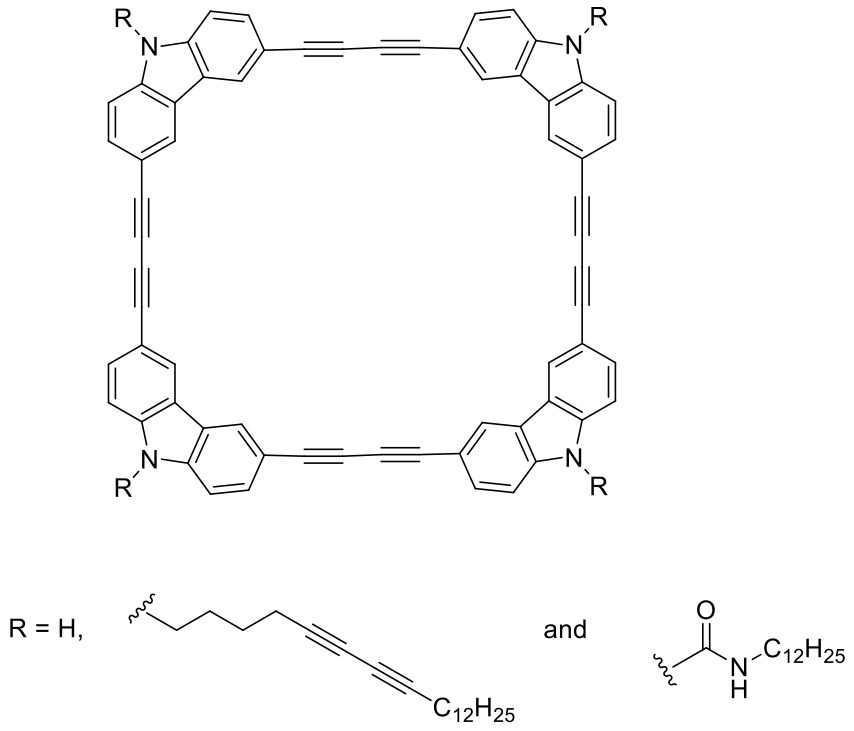

Figure 20. New tetrameric carbazole-based macrocycles with different side chains

3.2.3 Results and Discussion

Macrocycle **3.6** was prepared first. The free amine would allow for further functionalization (Scheme 25). Compound **3.3** was synthesized through two consecutive Sonogashira reactions starting from the diiodocarbazole **3.0**. The first mono-coupling used only 1.1 equiv of trimethylsilylacetylene (TMSA) to offer mono-coupled compound **3.1**. The following coupling used the more robust triisopropylsilyacetylene (TIPSA) to give compound **3.2**, which could be then selectively deprotected. However, compound **3.1** and **3.2** cannot be purified by column chromatography. Selective deprotection of the TMS group of a mixture of compounds **3.1** and **3.2** by K_2CO_3 in MeOH allowed purification of

the corresponding mono-protected bisacetylene compound **3.3** with an overall 58% yield over three steps. CuCl/$Cu(OAc)_2$ ·H_2O in pyridine promoted dimerization of **3.3** to afford half-macrocycle compound **3.4** in 86% yield. Subsequent deprotection of the TIPS group with TBAF gave the corresponding precursor **3.5** (96%). Cyclization of **3.5** by the Pd-catalyzed oxidative coupling in Et_3N and THF afforded tetramer **3.6** in 23% isolated yield.

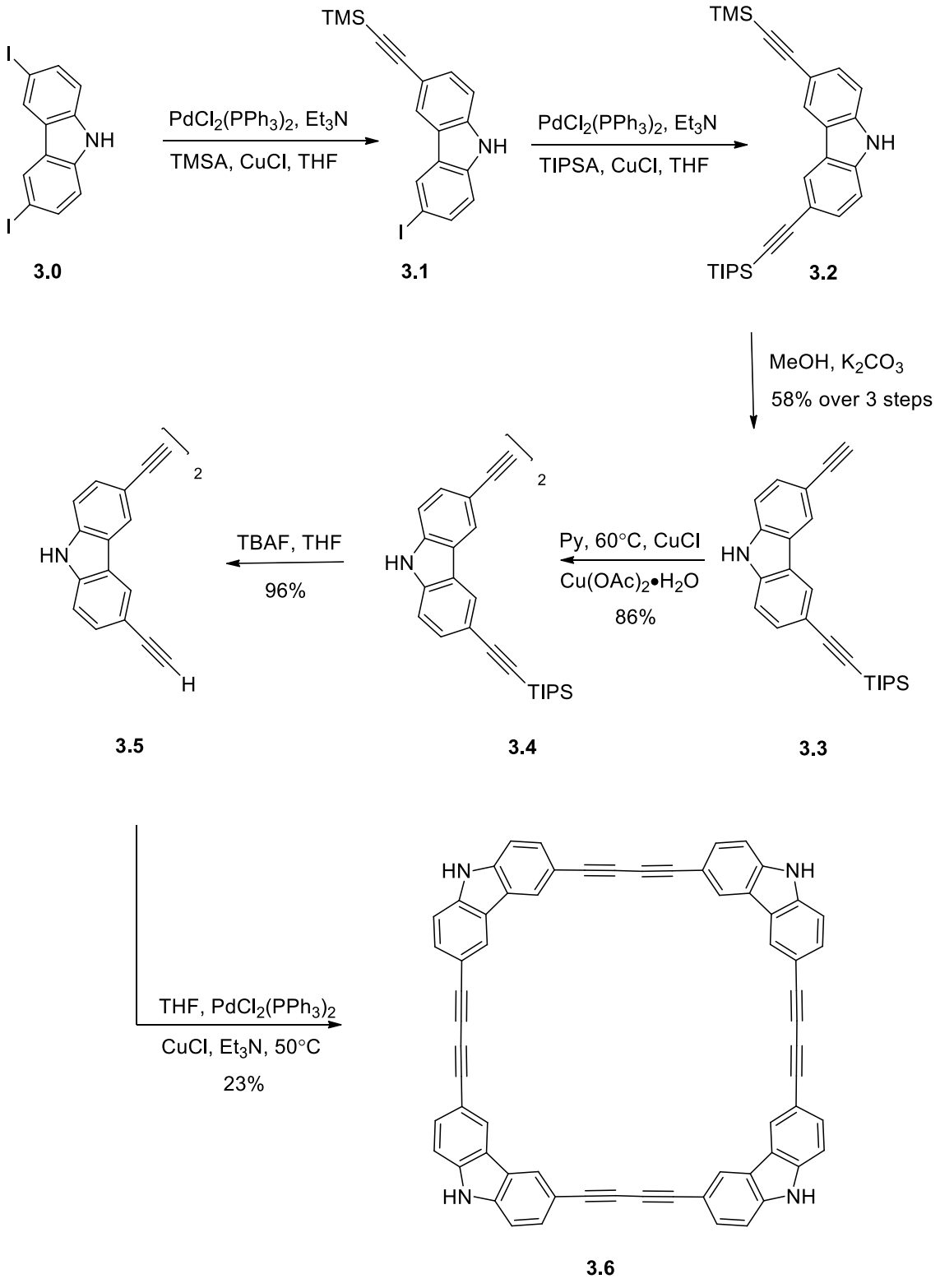

Scheme 25. Synthesis of side chain-free macrocycle **3.6**

The urea functionality-containing macrocycle was synthesized starting from the

half-macrocycle compound **3.5** (Scheme 26), which reacted with triphosgene and pyridine to afford the corresponding acid chloride and then reacted with a long chain amine to produce the desire product. Unfortunately, only the mono-substituted urea compound was isolated with a rather low yield (8%). Macrocyclization of the mono-urea compound **3.7** under high-dilution conditions was attempted although two structurally isomeric macrocycles might be obtained. However macrocyclization gave no desired product.

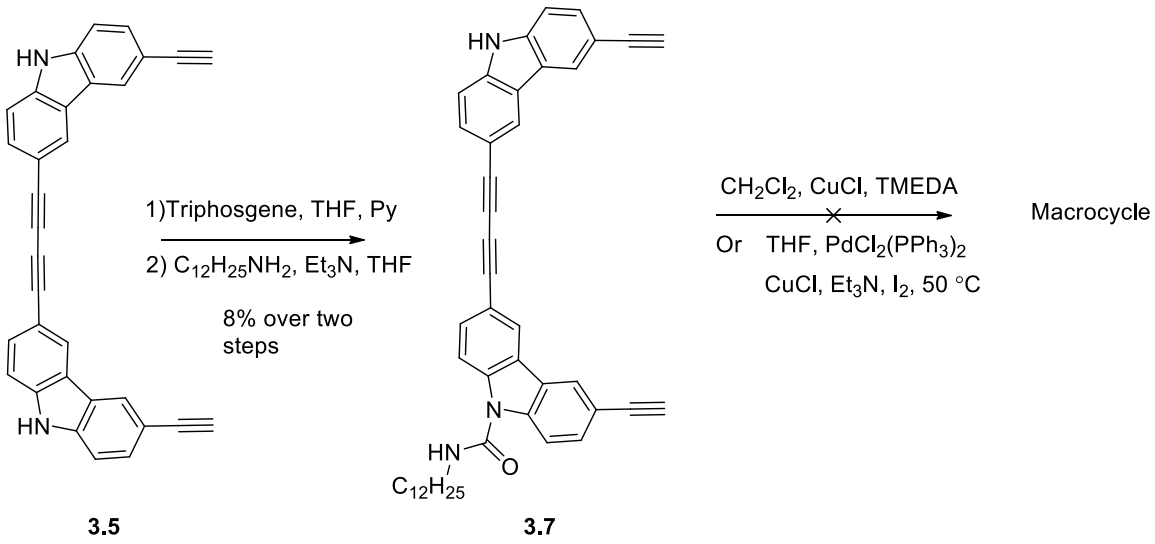

3.5 **3.7**

Scheme 26. Synthesis of urea-containing macrocycle via dimerization

Therefore, the strategy was changed so as to start with the single building block and introduced the urea side chain early in the synthesis (Scheme 27). The sequence begins by reaction of the diiodocarbazole with triphosgene in the presence of pyridine. Toluene was used as the solvent due to the need for high reaction temperature. The formed acyl intermediate was directly crystallized from the reaction mixture followed by treatment with dodecyl amine and Et_3N, which offered compound **3.9** in 96% yield. Sonogashira

reaction of **3.9** led to compound **3.10** in 97% yield. However, a problem emerged when deprotecting the TMS groups, in that using either MeOH/K_2CO_3 or TBAF led to cleavage of the urea group from the carbazole nitrogen.

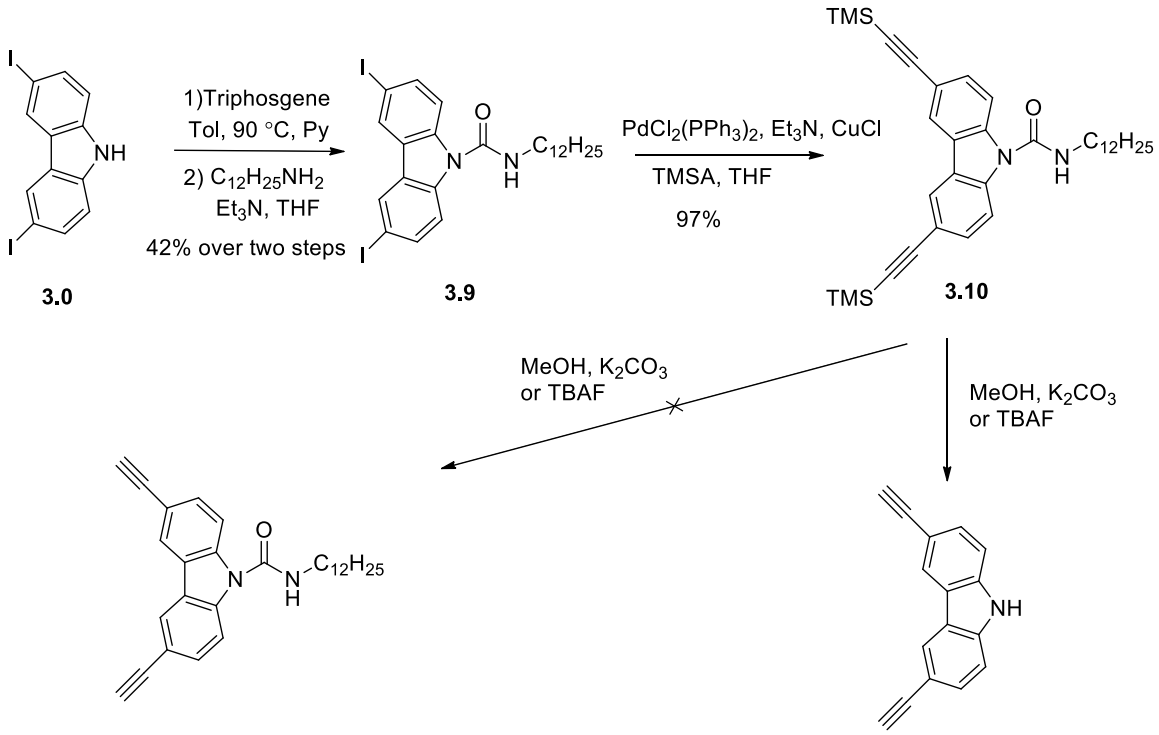

Scheme 27. Synthesis of urea-containing single unit

Therefore, the alkyne "arms" were built first via classic Sonogashira reaction followed by deprotection of the TMS group to afford compound **3.12** (Scheme 28). Then compound **3.12** reacted with triphosgene in the presence of pyridine in toluene to obtain compound **3.13**, which again crystallized from the reaction mixture directly. Further treatment of **3.13** with dodecyl amine and Et_3N produced urea compound **3.14** in 98% yield. However, macrocyclization of mono-building unit **3.14** did not give the desired macrocycle, and open-chain linear polymers without urea group were isolated as a complex mixture.

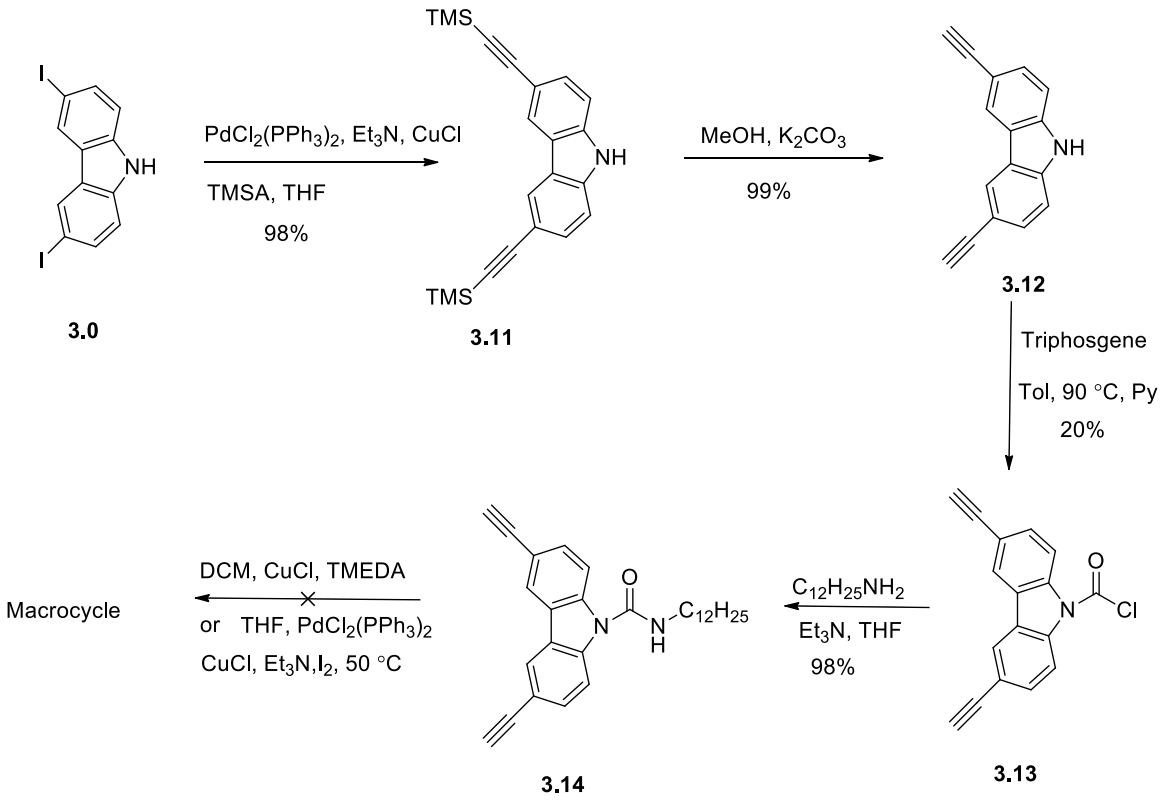

Scheme 28. Synthesis of urea-containing macrocycle via polymerization of single unit

The tosyl alkyl chain was prepared via known literature procedure.[24] Treatment of half-macrocycle **3.5** in DMF with K_2CO_3 as a base under heating (rt to 65 ℃) gave a mixture of products. When NaH was employed instead, the dialkyl compound **3.15** was formed in 40% yield. Macrocyclization via Pd-catalyzed oxidative coupling afforded **3.16** in 26% yield (Scheme 29).

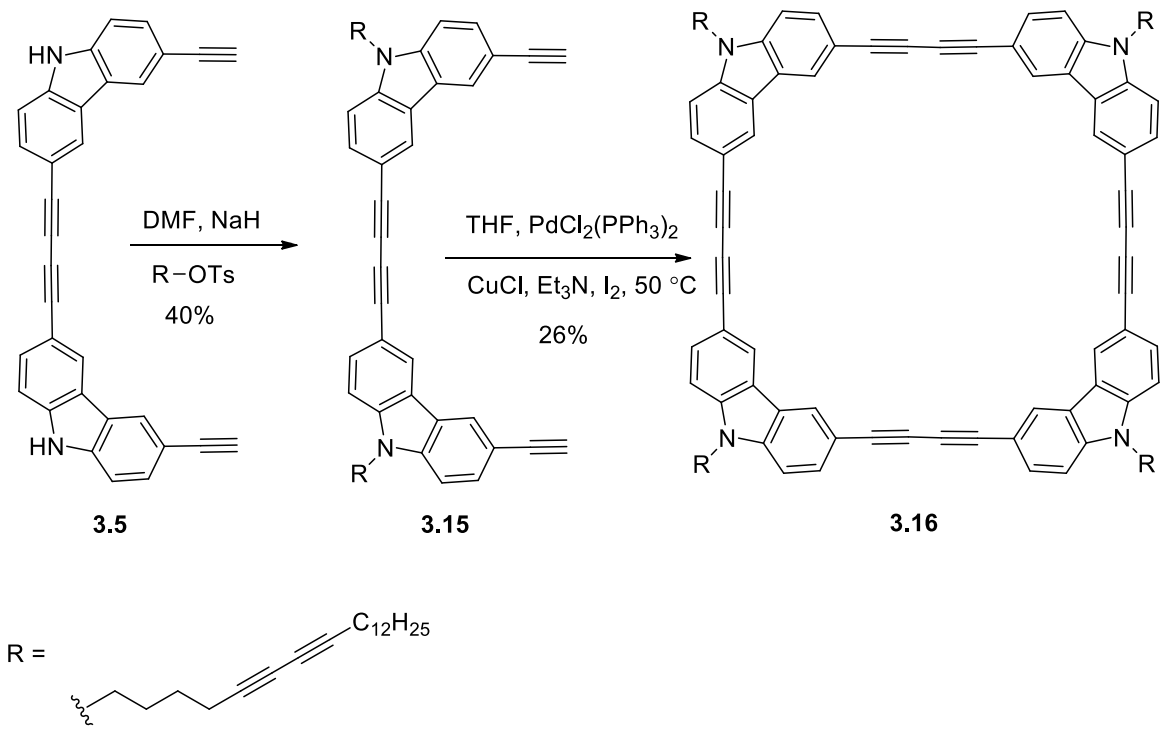

Scheme 29. Synthesis of alkylated macrocycle **3.16**

Single crystal growth for macrocycle **3.6** was carried out via vapor diffusion. A few solution systems had been tried (Table 4), EtOAc, THF, acetone and CH_2Cl_2, each in combination with hexanes. Acetone/hexanes offered only powder while other systems gave low quality crystals. The ones from EtOAc and THF were needle-like crystals while those from CH_2Cl_2 were snowflake shaped crystals. Unfortunately, all of the crystals were too small and possessed low quality for X-ray. Gelation for macrocycle **3.16** by different concentrations (1 w/v %, 2 w/v % and 10 w/v %) from common solvents was not successful.

Table 4. Vapor diffusion for macrocycle **3.6**

	EtOAc	acetone	CH_2Cl_2	THF
Hexane	C	P	C	C

P= powder, C= crystal

3.2.4 Summary

Carbazole-based tetramer building block macrocycles **3.6** (side chain free) and **3.16** (alkylated) have been successfully prepared and characterized. Both macrocycles were obtained as solids; however, no good quality single crystals have been obtained. Gelation for macrocycle **3.16** has not been successful to date, likely due to the absence of H-bonding between the units.

3.3 Experimental

General Reactions

All reactions were carried out under a dry nitrogen atmosphere except the macrocyclization, which was open to the air. All the glassware and stir bars were oven- or flame-dried. All the glassware, stir bars and needles used were washed with aqueous 1 M HCl and rinsed with deionized water then acetone. Dry THF was distilled over Na. Dry CH_2Cl_2 and DMF were distilled over CaH_2. Dry toluene was collected from a commercial solvent purification system. TMEDA was distilled over CaH_2 into a Schlenk flask and stored under N_2. Et_3N and pyridine were distilled over CaH_2 into a sealed flask under N_2. NaH was washed by pentanes under a nitrogen atmosphere before use to remove mineral

oil and further dried under nitrogen. CuCl was recrystallized by a known procedure[26] and stored in a glove box under a nitrogen atmosphere in the dark in a flask covered with foil.

Reactions were monitored by commercial thin-layer chromatography (TLC) plates. Developed TLC plates were examined under a UV lamp (254 nm) or exposed to iodine stain. Flash chromatography was performed using 230-400 mesh silica gel.

Characterization

^{1}H and ^{13}C NMR spectra were obtained in $CDCl_3$ and d_6-DMSO at 300 MHz and 75 MHz respectively. Chemical shifts are reported in parts per million (ppm, δ). $^{1}HNMR$ spectra were calibrated to residual chloroform and the d_5-DMSO peak at 7.24 ppm and 2.49 ppm respectively and carbon spectra were calibrated to $CDCl_3$ and d_6-DMSO at 77.0 ppm 39.5 ppm. DEPT 90/135 experiments were carried out to determine CH, CH_2 and CH_3 signals. Melting points were measured with a Melt-Temp apparatus and were not corrected.

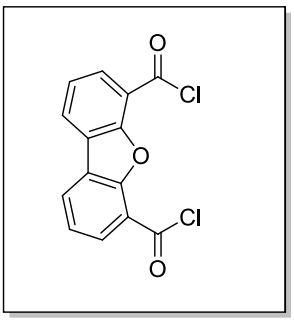

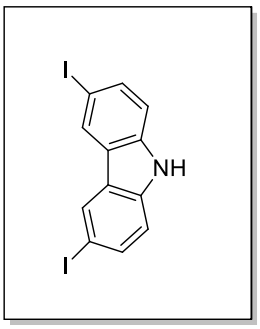

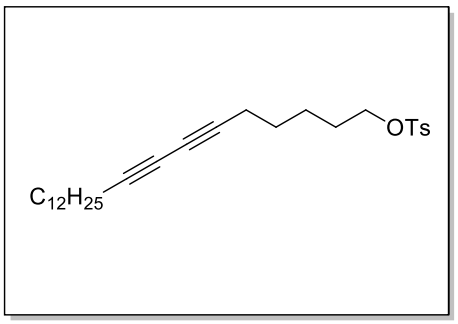

Dibenzofuran-4,6-dicarbonyl chloride, 3,6-diiodo-9*H*-carbazole and icosa-5,7-diynyl tosylate was prepared via known procedure. [24, 35, 42]

N,*N*-Di(prop-2-yn-1-yl)dibenzo[b,d]furan-4,6-dicarboxamide (3.1a)

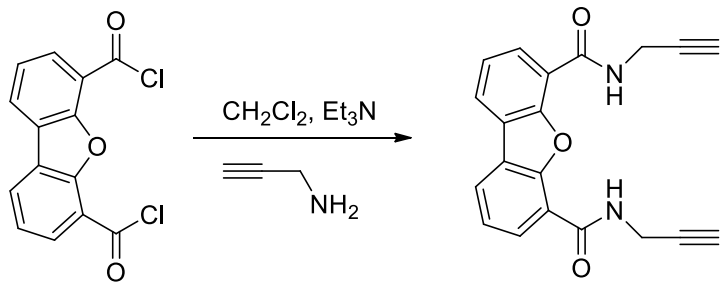

3.1a

A 50 mL round-bottom flask equipped with a stir bar, was charged with dibenzofuran-4,6-dicarbonyl chloride (360 mg, 1.0 equiv), CH_2Cl_2 (2.5 mL, 0.5 M) and Et_3N (0.41 mL, 2.4 equiv) at 0 ℃ under N_2 atmosphere. Propargyl amine (0.17 mL, 2.2 equiv) was added to the mixture dropwise over 30 min at 0 ℃. Then the reaction mixture was warmed to rt and stirred for 12 h. The reaction was quenched slowly by the addition of 1 M HCl and extracted with EtOAc (3 × 20 mL). The combined organic layers were washed with sat. $NaHCO_3$ and brine, dried over $MgSO_4$, filtered and concentrated. The residue was purified by flash chromatography on silica gel (4:1 hexane-ethyl acetate and then 2:1 hexane-ethyl acetate) to give product **3.1a** (0.24 g) as a white solid in 60% yield. mp = 248-250 ℃; ^{1}H NMR ($(CD_3)_2SO$, 300 MHz) 8.92 (t, *J* = 5.2 Hz, 2H), 8.39 (d, *J* = 7.6 Hz, 2H), 7.93 (d, *J* = 7.6 Hz, 2H), 7.56 (t, *J* = 7.6 Hz, 2H), 4.23 (d, *J* = 5.2 Hz, 4H), 3.22 (s, 2H); ^{13}C NMR ($(CD_3)_2SO$, 75 MHz) 163.1, 151.9, 128.4 (CH), 124.5 (CH), 123.9, 123.8 (CH), 119.2, 81.1, 73.2 (CH), 28.8 (CH_2)

3,3′-(9-Methyl-9*H*-carbazole-3,6-diyl)bis(prop-2-yn-1-ol) (3.2a)

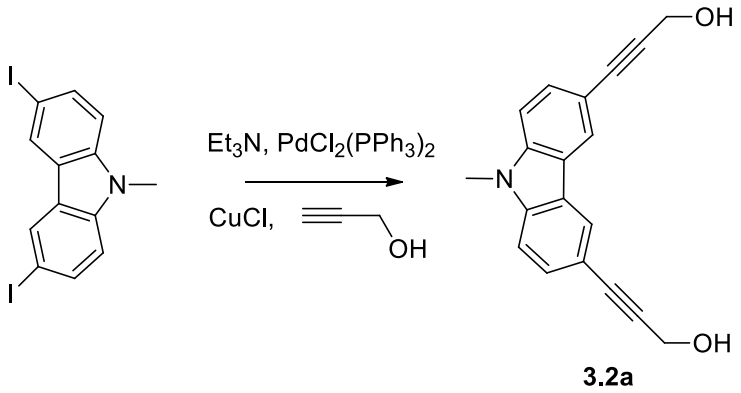

3.2a

A 50 mL round-bottom flask equipped with a stir bar was charged with 3,6-diiodo-9-methyl-9*H*-carbazole (340 mg, 1.0 equiv), $PdCl_2(PPh_3)_2$ (61 mg, 11 mol %) and CuCl (2.5 mg, 3.2 mol %). Et_3N (6.1 mL, 0.13 M) was added dropwise using a syringe followed by propargyl alcohol (0.31 mL, 6.84 equiv). The reaction was stirred for 8 h at room temperature under N_2 atmosphere. The solvent was removed in vacuo using a rotavapor. The residue was dissolved in EtOAc (20 mL) and washed with 1M HCl (20 mL), sat. $NaHCO_3$ and brine, dried over $MgSO_4$, filtered and concentrated. The residue was purified by flash chromatography on silica gel (5:1 hexane-ethyl acetate and then 1:1 hexane-ethyl acetate) to give product **3.2a** (0.1 g) as a yellow gel in 47% yield. ^{1}H NMR (CD_3OD, 300 MHz) 8.13 (s, 2H), 7.52 (d, *J* = 8.6 Hz, 2H), 7.44 (d, *J* = 8.5 Hz, 2H), 4.43 (s, 4H), 3.84 (s, 3H); ^{13}C NMR (($CD_3)_2SO$, 75 MHz) 140.5, 129.5 (CH), 123.9 (CH), 121.6, 112.9, 109.8 (CH), 87.9, 84.8, 49.5 (CH_2), 29.2 (CH_3)

9-Methyl-3,6-bis(3-(prop-2-yn-1-yloxy)prop-1-yn-1-yl)-9*H*-carbazole (3.3a)

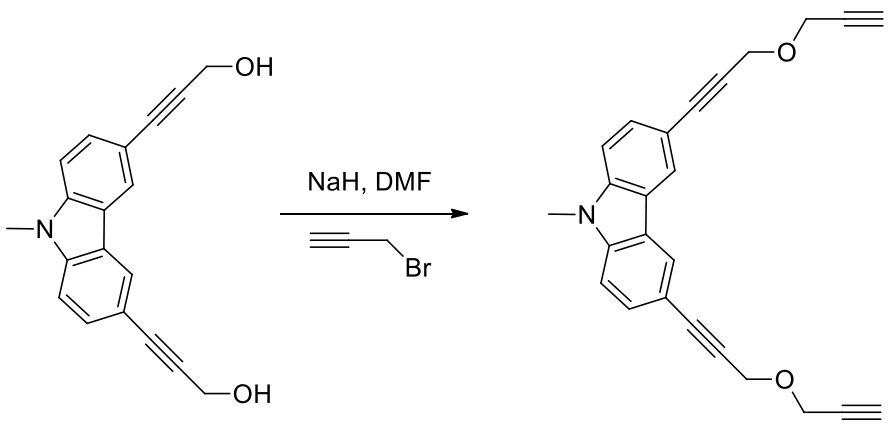

3.2a **3.3a**

A 10 mL round-bottom flask was charged with compound **3.2a** (0.18 g, 1.0 equiv) and DMF (1 mL). A 50 mL flask was charged with NaH (250 mg, 9.66 equiv washed with pentane) and 1.5 mL of DMF, cooled to 0 ℃ and equipped with a stir bar. The solution of diol **3.2a** was transferred via canula to the NaH suspension dropwise. The reaction was kept at 0 ℃ and stirred for 30 min, then propargyl bromide was added (0.3 mL, 6.0 equiv) dropwise over 30 min at 0 ℃. Then the reaction mixture was warmed to rt and stirred for 8 h. The reaction was quenched slowly by the addition of cold water and extracted with EtOAc (3 × 20 mL) .The combined organic layers were washed with sat. $NaHCO_3$ and brine, dried over $MgSO_4$, filtered and concentrated. The residue was purified by flash chromatography on silica gel (4:1 hexane-ethyl acetate and then 2:1 hexane-ethyl acetate) to give product **3.3a** (0.165 g) as a yellow gel in 73% yield. ^{1}H NMR ($CDCl_3$, 300 MHz) 8.09 (s, 2H), 7.53 (d, *J* = 8.5 Hz, 2H), 7.24 (d, *J* = 8.5 Hz, 2H), 4.54 (s, 4H), 4.37(d, *J* = 2.4 Hz, 4H), 3.73 (s, 3H), 2.49 (t, *J* = 2.3 Hz, 2H); ^{13}C NMR ($CDCl_3$, 75 MHz) 140.9,

129.9 (CH), 124.2 (CH), 122.1, 112.9, 108.6 (CH), 87.8, 82.3, 79.1, 74.9, 57.5 (CH_2), 56.4 (CH_2), 29.2 (CH_3)

3-Ethynyl-6-((triisopropylsilyl)ethynyl)-9*H*-carbazole (3.3)

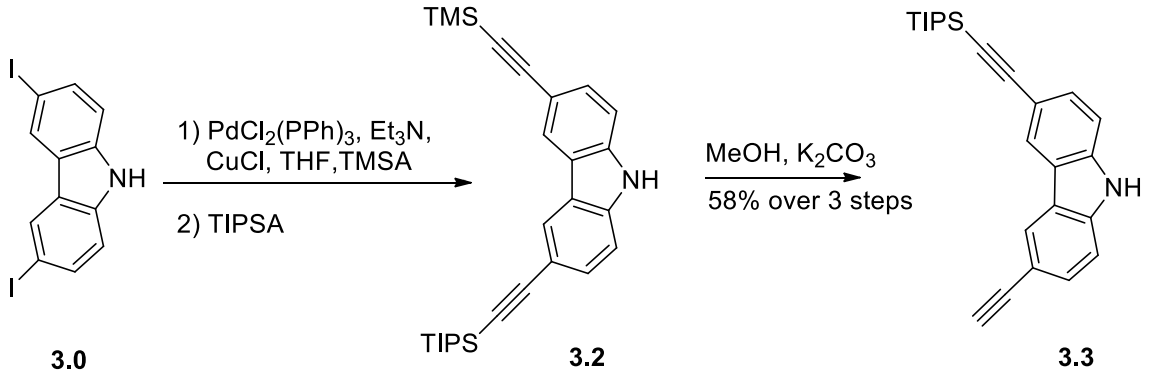

3.0 **3.2** **3.3**

A 250 mL round-bottom flask equipped with a stir bar was charged with compound **3.0** (3.0 g, 1.0 equiv), $PdCl_2(PPh_3)_2$ (0.157 g, 5 mol %) and CuCl (40 mg, 3.2 mol %). Et_3N (10 mL) was added dropwise with a syringe followed by TMSA (0.64 mL, 1.1 equiv). The reaction was stirred for 8 h at room temperature under an N_2 atmosphere. An excess of TIPSA (2.5ml) was further added and the reaction was stirred for an additional 3 h. Solvent was removed in vacuo using rotavapor. The residue was dissolved in EtOAc (100 mL) and washed with 1M HCl (100 mL), sat. $NaHCO_3$ and brine, dried over $MgSO_4$, filtered and concentrated.

The crude compound was dissolved in MeOH (200 mL), followed by the addition of K_2CO_3 (2 g). The suspension was stirred at rt for 3 h. Solvent was removed in vacuo using rotavapor. The residue was dissolved in EtOAc (100 mL) and washed with 1M HCl (100 mL), sat. $NaHCO_3$ and brine, dried over $MgSO_4$, filtered and concentrated. The residue was purified by flash chromatography on silica gel (19:1 hexane-ethyl acetate and then 9:1 hexane-ethyl acetate) to give product **3.3** (1.54 g) as a yellow gel in 58% yield

over three steps. ^{1}H NMR ($CDCl_3$, 300 MHz) 8.20 (s, 1H), 8.17 (s, 1H), 8.10 (bs, 1H), 7.54 (dt, *J* = 8.4 Hz, 1.7 Hz, 2H), 7.29-7.25(m, 2H), 3.06 (s, 1H), 1.17 (s, 21H); ^{13}C NMR ($CDCl_3$, 75 MHz) 139.6, 139.3, 130.4 (CH), 130.2 (CH), 124.8 (CH), 124.5 (CH), 122.8, 122.6, 115.0, 113.3, 110.7 (CH), 110.6 (CH), 108.1, 88.4, 84.6, 75.5, 18.8 (CH_3), 11.4 (CH)

1,4-Bis(6-((triisopropylsilyl)ethynyl)-9H-carbazol-3-yl) buta-1,3-diyne (3.4)

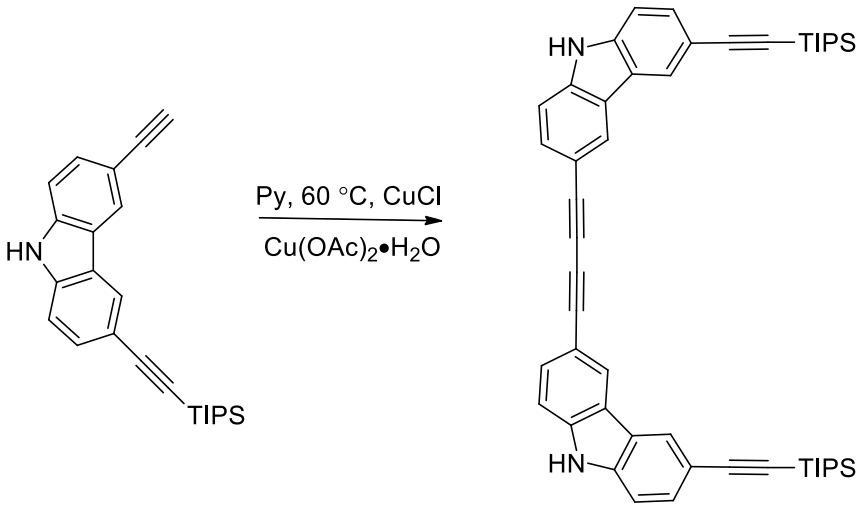

3.3 **3.4**

A solution of **3.3** (2.1 g, 1.0 equiv) in pyridine (25 mL) was added to a suspension of CuCl (5.6 g, 10 equiv) and $Cu(OAc)_2 \cdot H_2O$ (11.3 g, 10 equiv) in pyridine (10 mL). The mixture was stirred at 60 ℃ for 12 h and then filtered. After removal of the solvent, the residue was dissolved in EtOAc (100 mL) and 1 M HCl (100 mL). The phases were separated, and the organic layer was washed sat. $NaHCO_3$ then with approximately of 500 mL H_2O, until the blue color of the aqueous layer disappeared, then dried over $MgSO_4$, filtered and concentrated. The residue was purified by flash chromatography on silica gel (9:1 hexane-ethyl acetate and then 4:1 hexane-ethyl acetate) to give product **3.4** (1.8 g) as

a yellow oil in 86% yield. ^{1}H NMR ($CDCl_3$, 300 MHz) 8.30 (bs, 2H), 8.24 (s, 2H), 8.16 (s, 2H), 7.54 (d, *J* = 8.8 Hz, 4H), 7.27 (d, *J* = 8.8 Hz, 4H), 1.18 (s, 42H); ^{13}C NMR ($CDCl_3$, 75 MHz) 139.7, 139.3, 130.5 (CH), 130.4 (CH), 125.1 (CH), 124.5 (CH), 122.8, 122.5, 115.0, 113.0, 110.9 (CH), 110.6 (CH), 108.0, 88.5, 82.2, 72.9, 18.6 (CH_3), 11.4 (CH)

1,4-Bis(6-ethynyl-9H-carbazol-3-yl)buta-1,3-diyne (3.5)

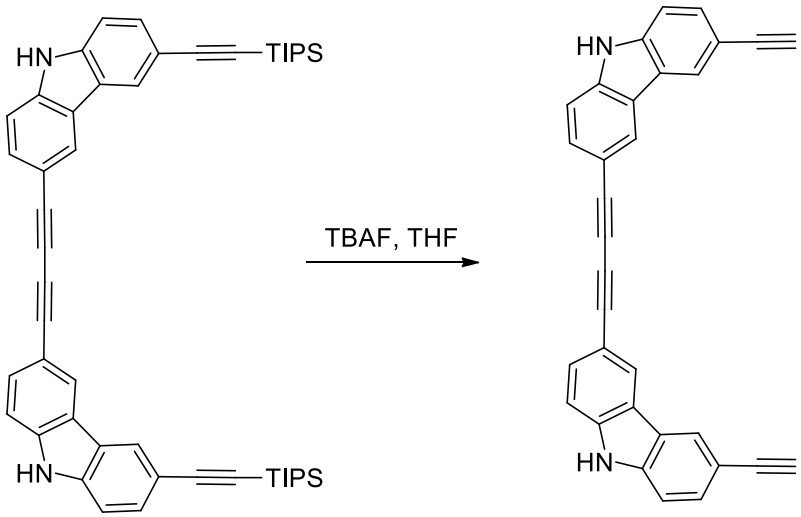

3.4 **3.5**

A 50 mL round-bottom flask equipped with a stir bar was charged with compound **3.4** (800 mg, 1.0 equiv) and THF (21 mL). TBAF (2.37 mL, 2.2 equiv) was added dropwise via syringe. The reaction was stirred for 2 h under N_2 atmosphere at room temperature. Solvent was removed in vacuo using a rotavapor. The residue was dissolved in EtOAc (50 mL) and washed with 1M HCl (50 mL). The organic layer was washed with sat. $NaHCO_3$ and brine, dried over $MgSO_4$, filtered and concentrated. The residue was purified by flash chromatography on silica gel (4:1 hexane-ethyl acetate and then 1:1 hexane-ethyl acetate) to give product **3.5** (444 mg) as a yellow solid in 96% yield. mp > 400 ℃; ^{1}H NMR ($(CD_3)_2SO$, 300 MHz) 11.82 (s, 2H), 8.50(s, 2H), 8.38 (s, 2H), 7.63 (d, *J* = 8.3 Hz, 4H), 7.53 (d, J = 8.4 Hz, 4H), 4.06 (s, 2H); ^{13}C NMR ($(CD_3)_2SO$, 75 MHz)

143.8, 143.4, 133.5 (CH), 133.2 (CH), 128.8 (CH), 127.9 (CH), 125.5, 125.2, 115.7 (CH), 115.2 (CH), 115.0, 114.2, 88.1, 86.3, 75.8, 17.3 (CH)

Synthesis side chain-free macrocycle 3.6

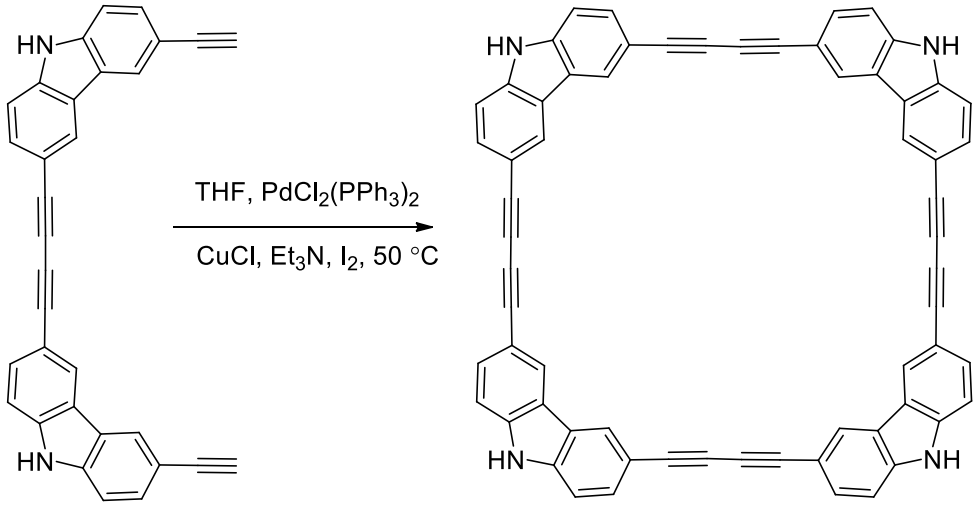

3.5 **3.6**

A solution of **3.5** (86 mg 1.0 equiv) in THF (20 mL) was added slowly to a suspension of $PdCl_2(PPh_3)_2$ (14 mg, 5 mol %), CuCl (3 mg, 3.2 mol %), and I_2 (25 mg, 0.5 equiv) in Et_3N (50 mL) and THF (400 mL) at 50 ℃. Upon completion of the slow addition (24 h), the reaction mixture was stirred for an additional 2 days. After removal of the solvent, the residue was dissolved in EtOAc (250 mL) and washed with 1M HCl, sat. $NaHCO_3$ and brine, dried over $MgSO_4$, filtered and concentrated. The residue was recrystallized from acetone to afford **3.6** (20 mg) as a light yellow solid in 23% yield. mp > 400 ℃; ^{1}H NMR ($(CD_3)_2SO$, 300 MHz) 11.94 (s, 4H), 8.54 (s, 8H), 7.64 (d, *J* = 8.9 Hz, 8H), 7.56 (d, *J* = 8.4 Hz, 8H); ^{13}C NMR ($(CD_3)_2SO$, 75 MHz) 140.4, 130.0 (CH), 125.6 (CH), 122.1, 112.0 (CH), 111.2, 82.8, 72.6

N-Dodecyl-3,6-diiodo-9*H*-carbazole-9-carboxamide (3.9)

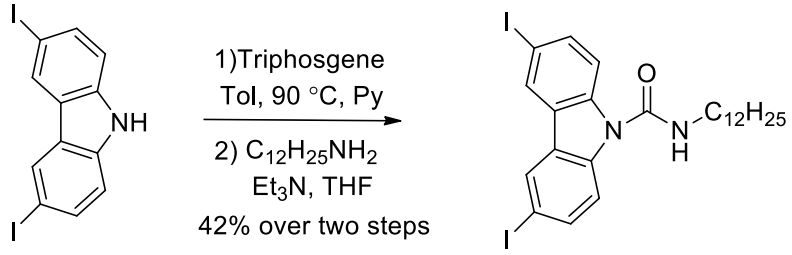

3.0 **3.9**

Compound **3.0** (7.5 g, 1.0 equiv) was dissolved in a mixture of toluene (50 mL) and pyridine (2.6 mL) and heated to 90 ℃ under stirring. Triphosgene (3.2 g, 0.35 equiv) was dissolved in toluene (5 mL) and added dropwise via syringe. After 30 min, the possible excess of phosgene was removed by a stream of nitrogen. The precipitated pyridine hydrochloride salt was removed by filtration when the mixture was hot. Solvent was removed and the crude material was used for the next step without purification.

The crude material was dissolved in THF (200 mL) followed by addition of dodecylamine (3.65 g 1.1 equiv). Et_3N (3.65 mL 1.1 equiv) was introduced afterwards dropwise via syringe over 10 min. The reaction was stirred for 2 h at room temperature. The solvent was removed in vacuo using rotavapor. The residue was dissolved in EtOAc (200 mL) and washed with 1M HCl (200 mL), sat. $NaHCO_3$ and brine, dried over $MgSO_4$, filtered and concentrated. The residue was purified by flash chromatography on silica gel (19:1 hexane-ethyl acetate and then 9:1 hexane-ethyl acetate) to give product **3.9** (4.74 g) as a white solid in 42% yield. mp = 200 ℃; ^{1}H NMR ($CDCl_3$, 300 MHz) 8.26 (s, 2H), 7.73 (s, 4H), 5.57 (bs, 1H), 3.52 (q, *J* = 6.7 Hz, 2H), 1.69 (quin, *J* = 6.7 Hz, 2H), 1.42-1.37 (m, 4H), 1.25 (s, 14H), 0.86 (t, *J* = 6.1 Hz, 3H); ^{13}C NMR ($CDCl_3$, 75 MHz) 152.0, 137.7, 136.0 (CH), 129.3 (CH), 126.0, 115.4 (CH), 85.6, 41.3 (CH_2), 31.9 (CH_2),

29.7 (CH_2), 29.6 (CH_2), 29.57 (CH_2), 29.53 (CH_2), 29.3 (CH_2), 29.2 (CH_2), 27.1 (CH_2), 22.7 (CH_2), 14.1 (CH_3)

N-Dodecyl-3,6-bis((trimethylsilyl)ethynyl)-9*H*-carbazole-9-carboxamide (3.10)

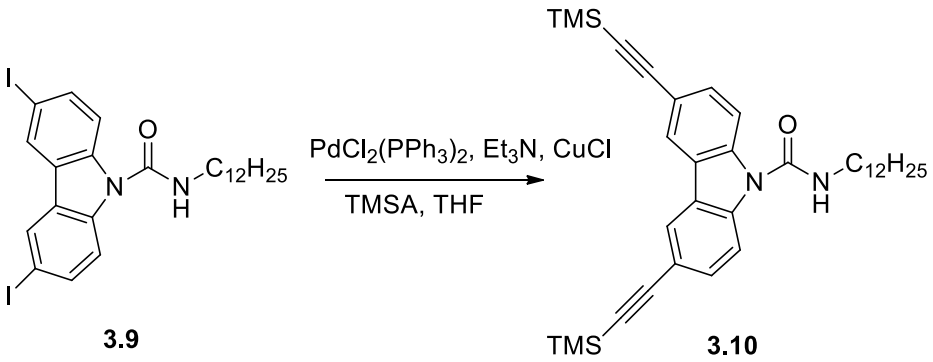

3.9 **3.10**

A 250 mL round-bottom flask was equipped with a stir bar, then charged with compound **3.9** (1.5 g, 1.0 equiv), $PdCl_2(PPh_3)_2$ (0.09 g, 5 mol %) and CuCl (0.009 g, 3.2 mol %). Et_3N (10 mL) was added dropwise by syringe followed by TMSA (0.9 mL, 2.6 equiv). The reaction was stirred for 8 h at room temperature under N_2 atmosphere. Solvent was removed in vacuo using rotavapor. The residue was dissolved in EtOAc (50 mL) and washed with 1M HCl (50 mL), sat. $NaHCO_3$ and brine, dried over $MgSO_4$, filtered and concentrated. The residue was purified by flash chromatography on silica gel (9:1 hexane-ethyl acetate and then 4:1 hexane-ethyl acetate) to give product **3.10** (1.32 g) as a yellow gel in 97% yield. ^{1}H NMR ($CDCl_3$, 300 MHz) 7.96 (s, 2H), 7.74 (d, *J* = 8.6 Hz, 2H), 7.48 (d, *J* = 8.6 Hz, 2H), 5.81 (t, *J* = 5.4 Hz, 1H), 3.45 (q, *J* = 6.7 Hz, 2H), 1.67 (quin, *J* = 6.6 Hz, 2H), 1.34-1.36 (m, 4H), 1.25 (s, 14H), 0.87 (t, *J* = 6.2 Hz, 2H), 0.29 (s, 18H); ^{13}C NMR ($CDCl_3$, 75 MHz) 152.0, 138.0, 130.8 (CH), 124.0 (CH), 116.9, 113.1 (CH), 105.3, 93.3, 41.1 (CH_2), 31.9 (CH_2), 29.6 (CH_2), 29.5 (CH_2), 29.3 (CH_2), 29.2 (CH_2), 27.0 (CH_2), 22.7 (CH_2), 14.1 (CH_3), 0.1 (CH_3)

N-Dodecyl-3,6-diethynyl-9*H*-carbazole-9-carboxamide (3.14)

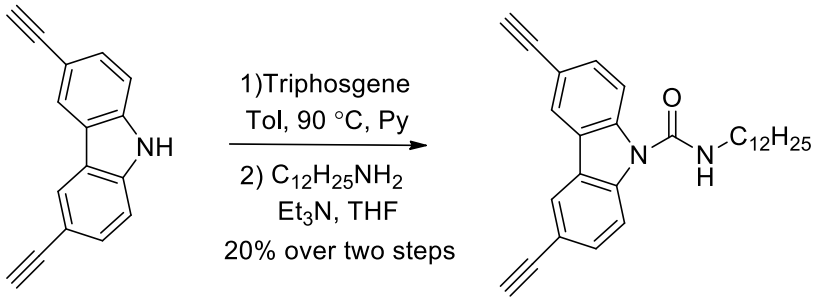

3.14

3,6-Diethynyl-9*H*-carbazole (1.9 g, 1.0 equiv) was dissolved in a mixture of toluene (24 mL) and pyridine (1.3 mL) and heated to 90 ℃ under stirring. In a second flask triphosgene (1.6 g, 0.6 equiv) was dissolved in toluene (2 mL) and added dropwise via syringe. After 30 min the possible excess of phosgene was removed by a stream of nitrogen. The precipitated pyridine hydrochloride salt was removed by filtration when the mixture was hot. Solvent was removed and the crude material was used in the next step without purification.

The crude material was dissolved in THF (24 mL) followed by the addition of dodecylamine (1.85 g 1.1 equiv). Et_3N (1.85 mL 1.1 equiv) was introduced afterwards dropwise via syringe over 10 min. The reaction was stirred for 2 h at room temperature. Solvent was removed in vacuo using a rotavapor. The residue was dissolved in EtOAc (50 mL) and washed with 1M HCl (50 mL), sat. $NaHCO_3$ and brine, dried over $MgSO_4$, filtered and concentrated. The residue was purified by flash chromatography on silica gel (19:1 hexane-ethyl acetate and then 9:1 hexane-ethyl acetate) to give product **3.9** (0.75 g) as a yellow solid in 20% yield. mp = 120-122 ℃; ^{1}H NMR ($CDCl_3$, 300 MHz) 7.92 (s, 2H), 7.70 (d, *J* = 8.6 Hz, 2H), 7.48 (d, *J* = 8.6 Hz, 2H), 5.86 (t, *J* = 5.4 Hz, 1H), 3.44 (q,

J = 6.8 Hz, 2H), 3.09 (s, 2H), 1.67 (quin, *J* = 7 Hz, 2H), 1.36-1.25 (m, 4H), 1.20 (s, 14H), 0.86 (t, *J* = 6.3 Hz); ^{13}C NMR ($CDCl_3$, 75 MHz) 151.9, 138.2, 130.9 (CH), 124.1 (CH), 123.9, 115.9, 113.1 (CH), 83.7, 76.5, 41.1 (CH_2), 31.9 (CH_2), 29.6 (CH_2), 29.56 (CH_2), 29.53 (CH_2), 29.3 (CH_2), 29.2 (CH_2), 27.0 (CH_2), 22.7 (CH_2), 14.1 (CH_3)

1,4-Bis(6-ethynyl-9-(icosa-5,7-diyn-1-yl)-9*H*-carbazol-3-yl)buta-1,3-diyne (3.15)

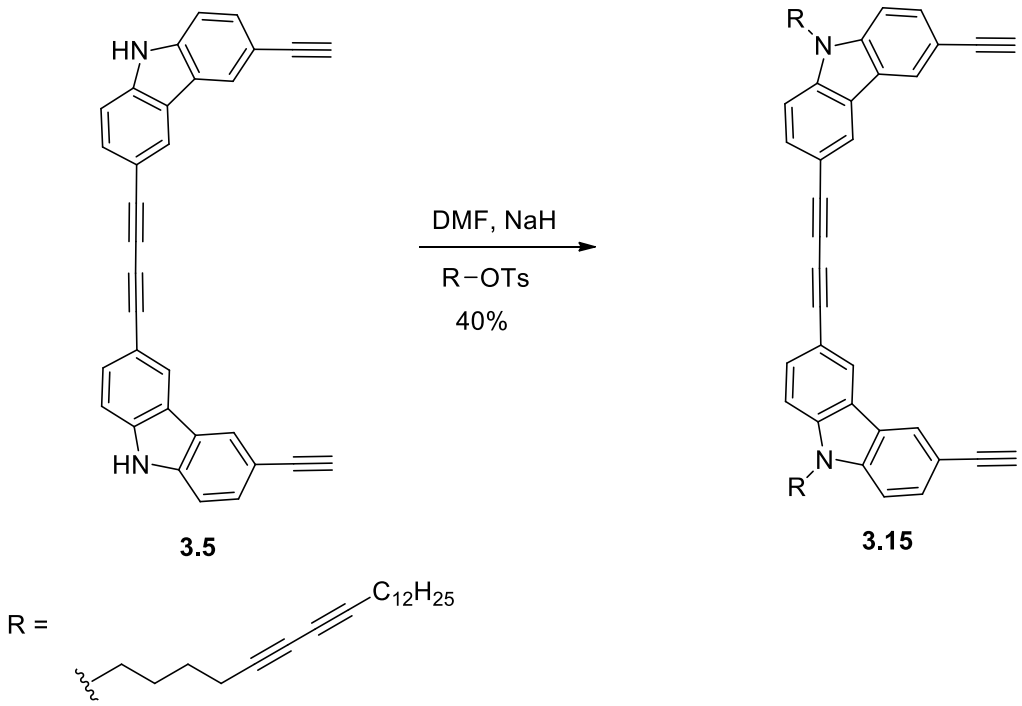

A 50 mL round-bottom flask was charged with compound **3.5** (0.1 g, 1.0 equiv) and 1 mL DMF. A second 50 mL flask was charged with NaH (60 mg, 9.66 equiv washed with pentane) and 1.5 mL of DMF, cooled to 0 ℃ and equipped with a stirring bar. The solution of **3.5** was transferred via canula to the NaH suspension dropwise. The reaction was kept at 0 ℃ and stirred for 30 min, then icosa-5,7-diynyltosylate in DMF (0.5 mL) was added dropwise over 10 min at 0 ℃. Then the reaction mixture was warmed to rt.

and stirred for 8 h. The reaction was quenched slowly by the addition of cold water and extracted with EtOAc (3 × 50 mL). The combined organic layers were washed with a large amount of water (500 mL), dried over $MgSO_4$, filtered and concentrated. The residue was purified by flash chromatography on silica gel (9:1 hexane-ethyl acetate and then 4:1 hexane-ethyl acetate) to give product **3.15** (91 mg) as a yellow liquid in 40% yield. ^{1}H NMR ($CDCl_3$, 300 MHz) 8.21 (d, *J* = 12.4 Hz, 4H), 7.65-7.58 (m, 4H), 7.35 (m, 4H), 4.28 (t, *J* = 7.0 Hz, 4H), 3.07 (s, 2H), 2.26 (quin, *J* = 7 Hz, 8H), 1.98 (quin, *J* = 7.3 Hz), 1.6-1.46 (m, 8 Hz), 1.23 (s, 36H), 0.86 (t, *J* = 6.2 Hz) ^{13}C NMR ($CDCl_3$, 75 MHz) 140.6, 140.5, 130.6 (CH), 130.3 (CH), 125.2 (CH), 124.8 (CH), 122.4, 122.2, 112.9, 112.7, 109.1 (CH), 108.9 (CH), 84.6, 82.3, 78.3, 75.6, 72.9, 66.3, 64.9, 42.8 (CH_2), 31.9 (CH_2), 29.6 (CH_2), 29.5 (CH_2), 29.3 (CH_2), 29.1 (CH_2), 28.9 (CH_2), 28.3 (CH_2), 27.9 (CH_2), 27.5 (CH_2), 25.6 (CH_2), 22.7 (CH_2), 19.2 (CH_2), 18.9 (CH_2), 14.1 (CH_3)

Synthesis alkyne substituted macrocycle 3.16

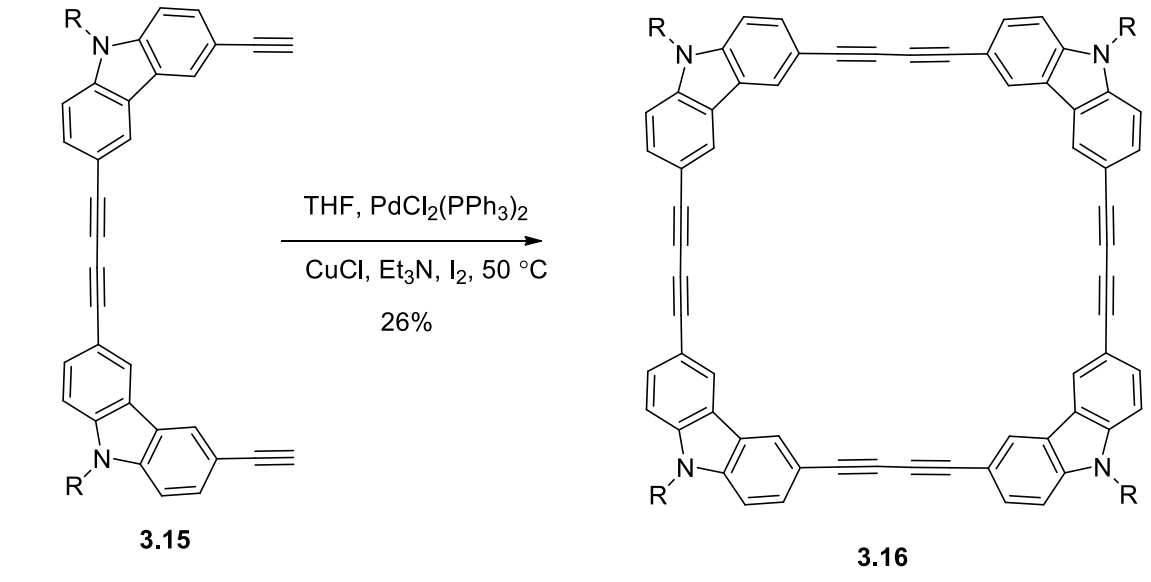

A solution of **3.15** (56 mg, 1.0 equiv) in THF (10 mL) was added slowly to a suspension of $PdCl_2(PPh_3)_2$ (10 mg, 5 mol %), CuCl (2 mg, 3.2 mol %), and I_2 (2.5 mg, 0.5 equiv) in Et_3N (25 mL) and THF (120 mL) at 50 ℃. Upon completion of the slow addition (24 h), the reaction mixture was stirred for an additional 2 days. After removal of the solvent, the residue was dissolved in EtOAc (100 mL) and washed with 1M HCl, sat. $NaHCO_3$ and brine, dried over $MgSO_4$, filtered and concentrated. The residue was purified by flash chromatography on silica gel (9:1 hexane-ethyl acetate and then 3:1 hexane-ethyl acetate) to give product **3.16** (14 mg) as a yellow amorphous powder in 26% yield. mp = 220-230 ℃; ^{1}H NMR ($CDCl_3$, 300 MHz) 8.28 (s, 8H), 7.63 (d, *J* = 8.6 Hz, 8H), 7.33 (d, *J* = 8.5 Hz, 8H), 4.29 (t, *J* = 7.0 Hz, 8H), 2.31-2.22 (m, 16H), 1.99 (quin, *J* = 6.6 Hz, 8H), 1.60-1.48 (m, 16H), 1.23 (s, 72H), 0.85 (t, *J* = 6.8 Hz, 12H). ^{13}C NMR ($CDCl_3$, 75 MHz) 140.6, 130.3 (CH), 125.4, 122.5 (CH), 112.9, 109.1 (CH), 82.2, 73.1, 66.3, 64.9, 31.9 (CH_2), 29.6 (CH_2), 29.5 (CH_2), 29.3 (CH_2), 29.1 (CH_2), 28.8 (CH_2), 28.3 (CH_2), 27.9 (CH_2), 25.6 (CH_2), 22.7 (CH_2), 19.2 (CH_2), 18.9 (CH_2), 14.1 (CH_3)

References

[1] (a) Tang, C. W. *Appl. Phys. Lett.* **1986**, *48*, 183–185; (b) Sariciftci, N. S.; Smilowitz, L.; Heeger, A. J.; Wudl, F. *Science* **1992**, *258*, 1474–1476; (c) Hoppe, H.; Sariciftci, N. S. *J. Mater. Chem.* **2004**, *19*, 1924–1926; (d) Swager, T. M. *Acc. Chem. Res.* **1998**, *31*, 201–207; (e) Yang, J. S.; Swager, T. M. *J. Am. Chem. Soc.* **1998**, *120*, 5321–5322; (f) Yang, J. S.; Swager, T. M. *J. Am. Chem. Soc.* **1998**, *120*, 11864–11873; (g) Smith, R. C. *Macromol. Rapid Commun.* **2009**, *30*, 2067–2078.

[2] (a) Balakrishnan, K.; Datar, A.; Zhang, W.; Yang, X.; Naddo, T.; Huang, J.; Zuo, J.; Yen, M.; Moore, J. S.; Zang, L. *J. Am. Chem. Soc.* **2006**, *128*, 6576–6577; (b) Tian, L.; Wang, C.; Dawn, S.; Smith, M. D.; Krause, J. A.; Shimizu, L. S. *J. Am. Chem. Soc.* **2009**, *131*, 17620–17629; (c) Yang, J.; Dewal, M. B.;Sobransingh, D.; Smith, M. D.; Xu, Y.; Shimizu, L. S. *J. Org. Chem.* **2009**, *74*, 102–110; (d) Xu, Y.; Smith, M. D.; Geer, M. F.; Pellechia, P. J.; Brown, J. C.; Wibowo, A. C.; Shimizu, L. S. *J. Am. Chem. Soc.* **2010**, *132*, 5334–5335; (e) Zang, L.; Che, Y.; Moore, J. S. *Acc. Chem. Res.* **2008**, *41*, 596–1608.

[3] Kilpin, K. J.; Gower, M. L.; Telfer, S. G.; Jameson, G. B.; Crowley, J. D. *Inorg. Chem.* **2011**, *50*, 1123–1134.

[4] Cantin, K.; Lafleur-Lambert, A.; Dufour, P.; Morin, J. F. *Eur. J. Org. Chem.* **2012**, 5335–5349.

[5] (a) Riemann, H.; Luedge, A. *Advances in Materials Research* **2009**, *14*, 41–53; (b) Binnewies, M.; Glaum, R.; Schmidt, M.; Schmidt, P. *Zeitschrift für anorganische und*

Allgemeine Chemie **2013**, *639*, 219–229.

[6] Lauher, J. W.; Fowler, F. W.; Goroff, N. S. *Acc. Chem. Res.* **2008**, *41*, 1215–1229.

[7] Njus, J. M.; Sandman, D. J. *Solid State Nucl. Mag.* **2006**, *29*, 251–257.

[8] Baughman, R. H. *J. of Polym. Sci., Polym. Phys.* **1974**, *12*, 1511–1535.

[9] Wegner, G. *Pure & Appl. Chem.* **1977**, *49*, 443–454.

[10] Pasini, D.; Ricci, M. *Curr. Org. Syn.* **2007**, *4*, 59–80.

[11] Baughman, R. H.; Yee, K. C. *J. of Polym. Sci., Polym. Phys.* **1974**, *12*, 2467–2475.

[12] Enkelmann, V.; Graf, H. J. *Acta Cryst.* **1978**, *34*, 3715–3719.

[13] Zhou, Q.; Carroll, P. J.; Swager, T. M. *J. Org. Chem.* **1994**, *59*, 1294–1301.

[14] Baldwin, K. P.; Matzger, A. J.; Scheiman, D. A.; Tessier, C. A.; Vollhardt, K. P. C.; Youngs, W. J. *Synlett* **1995**, *12*, 1215–1218.

[15] Nagasawa, J.; Yoshida, M.; Tamaoki, N. *Eur. J. Org. Chem.* **2011**, 2247–2255.

[16] Hsu T. J.; Fowler, F. W.; Lauher, J. W. *J. Am. Chem. Soc.* **2012**, *134*, 142–145.

[17] Coluccini, C.; Dondi, D.; Caricato, M.; Taglietti, A.; Boiocchic, M.; Pasini, D. *Org. Biomol. Chem.* **2010**, *8*, 1640–1649.

[18] Caricato, M.; Leza, N. J.; Gargiulli, C.; Gattuso, G.; Dondi. D.; Pasini, D. *Beilstein J. Org. Chem.* **2012**, *8*, 967–976.

[19] (a) Kodama, H.; Ito, J.; Hori, K.; Ohta, T.; Furukawa, I. *J. Organomet. Chem.* **2000**, *603*, 6–12; (b) Tsang, W. C. P.; Schrock, R. R.; Hoveyda, A. H. *Organometallics* **2001**, *20*, 5658–5669; (c) Kamei, T.; Shibaguchi, H.; Sako, M.; Toribatake, K.; Shimada, T. *Tetrahedron Lett.* **2012**, *53*, 3894–3896; (d) Takizawa, S.; Katayama, T.; Somei, H.; Asano, Y.; Yoshida, T.; Kameyama, C.; Rajesh, D.; Onitsuka, K.; Suzuki, T.; Mikami,

M.; Yamatakay, H.; Jayaprakash, D.; Sasai, H. *Tetrahedron* **2008**, *64*, 3361–3371.

[20] Tsang, W. C. P.; Schrock, R. R.; Hoveyda, A. H. *Organometallics* **2001**, *20*, 5658–5669

[21] Ghadiri, M. R.; Granja, J. R.; Milligan, R. A.; McRee, D. E.; Khazanovich, N. *Nature* **1993**, *366*, 324–327.

[22] Xu, Y.; Smith, M. D.; Geer, M. F.; Pellechia, P. J.; Brown, J. C.; Wibowo, A. C.; Shimizu, L. S. *J. Am. Chem. Soc.* **2010**, *132*, 5334–5335.

[23] Katy, C.; Simon, R. G.; Jules, R. N.; Maxime, D.; Morin, J. F. *Org. Biomol. Chem.* **2011**, *9*, 4440–4443.

[24] Simon, R. G.; Jules, R. N.; Maude, D.; Jérémie, L.; Josée, B.; Morin, J. F. *J. Am. Chem. Soc.*, **2013**, *135*, 110–113.

[25] Jeffrey, G. A. *An Introduction to Hydrogen Bonding*, *Oxford University Press*, **1997**.

[26] Perrin, D. D.; Armarego, W. L. F. *Purification of Laboratory Chemicals 3rd Edition, Pergamon Press*, Toronto, 1988, p322.

[27] Lin, P. *Chem. Rev.* **1998**, *98*, 2405–2494.

[28] (a) Kamat, P. V. *J. Phys. Chem.* **2007**, *111*, 2834–2860; (b) Umeyama, T.; Imahori, H. *Energy Environ. Sci.* **2008**, *1*, 120–133; (c) Hasobe, T. *Phys. Chem. Chem. Phys.* **2010**, *12*, 44–57; (d) Subbaiyan, N. K.; Wijesinghe, C. A.; D'Souza, F. *J. Am. Chem. Soc.* **2009**, *131*, 14646–14647; (e) Imahori, H.; Umeyama, T.; Kei, K.; Yuta, T. *Chem. Commun.* **2012**, *48*, 4032–4045; (f) Kamat, P. V.; Schatz, G. C. *J. Phys. Chem.* **2009**, *113*, 15473–15475; (g) Dang, X.; Hupp, J. T. *J. Photochem. Photobiol.A: Chem.* **2001**, *143*, 251–256.

[29] (a) Osteritz, E. M.; Baeuerle, P. *Adv. Mater.* **2006**, *18*, 447–451; (b) Pan, G. B.; Cheng, X. H.; Hoger, S.; Freyland, W. *J. Am. Chem. Soc.* **2006**, *128*, 4218–4219; (c) Katsonis, N.; Minoia, A.; Kudernac, T.; Mutai, T.; Xu, H.; Uji-I, H.; Lazzaroni, R.; Feyter, S.; Feringa, B. L. *J. Am. Chem. Soc.* **2008**, *130*, 386–387; (d) Yoshimoto, S.; Honda, Y.; Itaya O. K. *J. Am. Chem. Soc.* **2008**, *130*, 1085–1092; (e) Lu, J.; Lei, S. B.; Zeng, Q. D.; Kang, S. Z.; Wang, C.; Wan, L. J.; Bai, C. L. *J. Phys. Chem. B* **2004**, *108*, 5161–5165; (f) Xiao, W.; Passerone, D.; Ruffieux, P.; Ait-Mansour, K.; Groning, O.; Tosatti, E.; Siegel, J. S.; Fasel, R. *J. Am. Chem. Soc.* **2008**, *130*, 4767–4771; (g) Hofkens, J.; Latterini, L.; Vanoppen, P.; Faes, H.; Jeuris, K.; Feyter, S.; Kerimo, J.; Barbara, P. F.; De Schryver, F. C.; Rowan, A. E.; Nolte, R. J. M. *J. Phys. Chem. B* **1997**, *101*, 10588–10598.

[30] Wu, J. S.; Baumgarten, M.; Debije, M. G.; Warman, J. M.; Mullen, K. *Angew. Chem.* **2004**, *116*, 5445–5449; *Angew. Chem. Int. Ed.* **2004**, 43, 5331–5335;

[31] Garg, N. K.; Sarpong, R.; Stoltz, B. M. *J. Am. Chem. Soc.* **2002**, *124*, 13179–13184.

[32] Schmaltz, B.; Rouhanipour, A.; Joachim, H. R.; Pisula, W.; Mullen, K. *Angew. Chem. Int. Ed.* **2009**, *48*, 720–724.

[33] Li, F.; Carvalho, S.; Delgado, R.; Michael, G. B. D.; F ́elix, V. *R. Soc. Chem.* **2010**, 39, 9579–9587.

[34] Tomohito, I.; Sho, S.; Daisuke, T.; Kohtaro, O.; Shigeru, M. *J. Org. Chem.* **2012**, *77*, 4837–4841.

[35] Iserloh, U.; Oderaotoshi, Y.; Kanemasa, S.; Curran, D. P. *Organic Syntheses,* **2003**, *80*, 46–56.

[36] Zhao, T.; Liu, Z.; Song, Y.; Xu, W.; Zhang, D.; Zhu, D. *J. Org. Chem.* **2006**, *71*, 7422–

7432.

[37] Shanmugaraju, S.; Bar, A. K.; Chi, K. W.; Mukherjee, P. S. *Organometallics* **2010**, *29*, 2971–2980.

[38] Zang, L.; Che, Y.; Moore, J. S. *Acc. Chem. Res.* **2008**, *41*, 1596–1608.

[39] Shimizu, L. S.; Smith, M. D.; Hughes, A. D.; Shimizu, K. D. *Chem. Commun.* **2001**, 1592–1593.

[40] Shimizu, L. S.; Hughes, A. D.; Smith, M. D.; Davis, M. J.; Zhang B. P.; Loye, H. C.; Shimizu, K. D. *J. Am. Chem. Soc.* **2003**, *125*, 14972–14973.

[41] Semetey, V.; Didierjean, C.; Briand, J. P.; Aubry, A.; Guichard, G. *Angew. Chem. Int. Ed.* **2002**, *41*, 1895–1898.

[42] Wu, Y.; Guo, H.; James, T. D.; Zhao, J. *J. Org. Chem.* **2011**, *76*, 5685–5695.

Appendix

Crystallographic data for macrocycle 2.9b

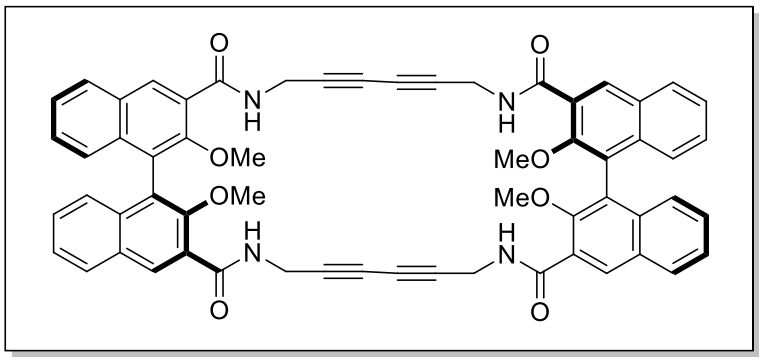

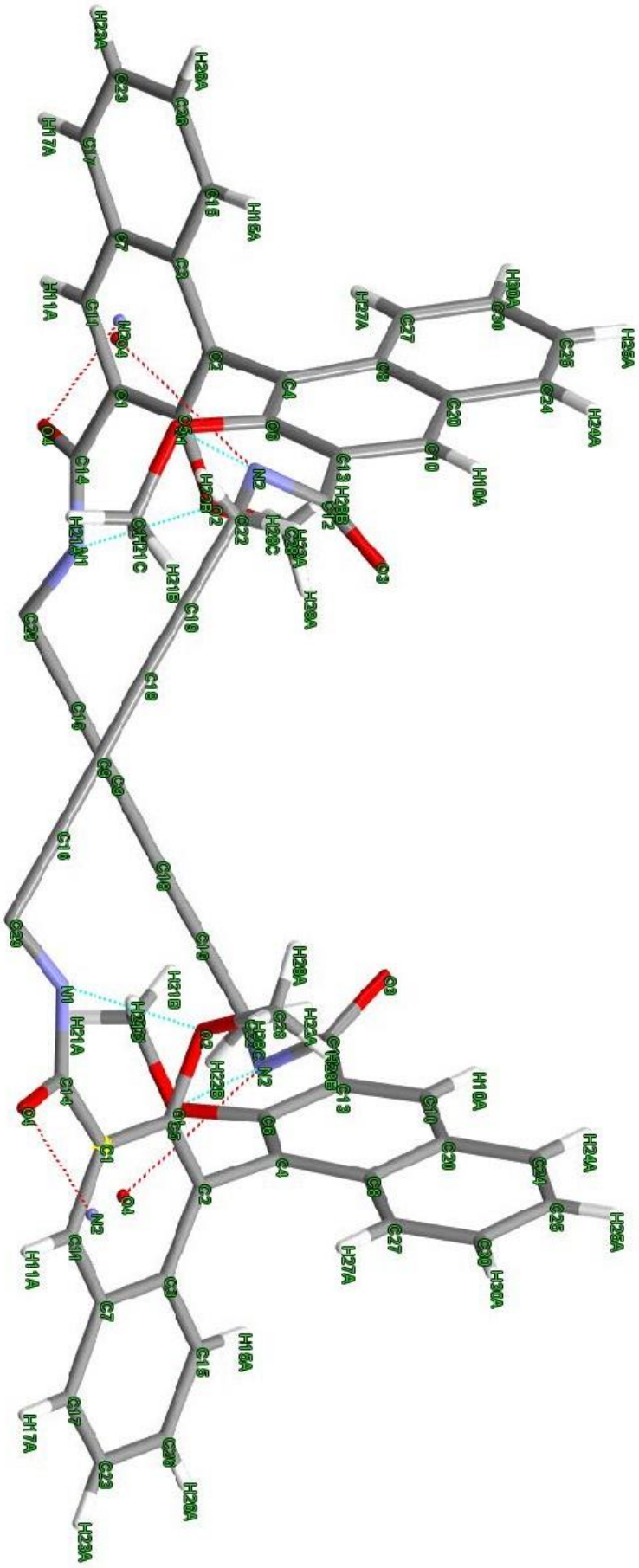

Table 5. Crystal data and structure refinement for $C_{60}H_{40}N_4O_8$.x solvent

Empirical formula	$C_{60}H_{40}N_4O_8$.x solvent
Temperature	296(2) K
Wavelength	0.71073 Å
Crystal system, space group	Tetragonal, $\boldsymbol{P4_12_12}$
Unit cell dimensions	a = 12.3236(3) Å,
	b = 12.3236(3) Å,
	c = 43.6999(13) Å
Volume	6636.8(3) $Å^3$
Z, Calculated density	4, 1.110 g/cm^3
Absorption coefficient	0.074 mm^{-1}
F(000)	2297
Crystal size	0.19 x 0.18 x 0.04 mm
Theta range for data collection	1.72 to 26.00 º
Limiting indices	-15<=h<=11, -12<=k<=15, -52<=l<=42
Reflections collected / unique	40231 / 6490 [R(int) = 0.0791]
Completeness to theta = 26.00	99.4 %
Max. and min. transmission	0.9970 and 0.9860
Refinement method	Full-matrix least-squares on F^2
Data / restraints / parameters	6490 / 6 / 386
Goodness-of-fit on F^2	2.154
Final R indices [I>2σ(I)]	R1 = 0.0902, wR2 = 0.2216
R indices (all data)	R1 = 0.1537, wR2 = 0.2421
Absolute structure parameter	0(3)
Extinction coefficient	0.0117(9)
Largest diff. peak and hole	0.623 and -0.393 e. $Å^{-3}$

Table 6. Atomic coordinates ($\times 10^4$) and equivalent isotropic displacement parameters ($Å^2 \times 10^3$) for $C_{60}H_{40}N_4O_8$.x solvent

	x	y	z	U(eq)
O(1)	805(3)	3116(3)	1068(1)	52(1)
O(2)	2581(3)	819(4)	896(1)	55(1)
O(3)	-1979(4)	2444(4)	581(1)	72(2)
O(4)	5725(4)	554(4)	1233(1)	72(2)
N(1)	4776(4)	905(5)	804(1)	62(2)
N(2)	-1275(4)	3810(5)	868(1)	55(1)
C(1)	3900(5)	1131(5)	1300(2)	49(2)
C(2)	1964(5)	1448(5)	1379(1)	45(2)
C(3)	2186(5)	1787(5)	1683(1)	48(2)
C(4)	826(5)	1340(5)	1266(1)	47(2)
C(5)	2799(5)	1127(5)	1195(1)	46(2)
C(6)	294(5)	2126(5)	1102(1)	44(2)
C(7)	3260(6)	1781(5)	1790(1)	53(2)
C(8)	262(5)	347(5)	1333(1)	52(2)
C(9)	-220(6)	5290(6)	-94(2)	57(2)
C(10)	-1263(5)	979(6)	1020(2)	56(2)
C(11)	4100(5)	1448(5)	1591(2)	54(2)
C(12)	-1375(5)	2749(6)	787(2)	53(2)
C(13)	-756(5)	1956(5)	976(1)	49(2)
C(14)	4876(6)	820(5)	1110(2)	56(2)
C(15)	1338(6)	2103(5)	1888(2)	58(2)
C(16)	229(6)	5487(5)	-327(2)	62(2)
C(17)	3475(6)	2095(6)	2097(2)	67(2)
C(18)	-758(6)	5066(5)	179(2)	55(2)
C(19)	-1275(6)	4891(6)	407(2)	56(2)
C(20)	-789(5)	179(6)	1197(2)	56(2)
C(21)	1325(6)	3277(6)	777(2)	70(2)
C(22)	-1857(6)	4645(6)	684(2)	60(2)
C(23)	2652(7)	2378(6)	2287(2)	70(2)
C(24)	-1326(6)	-836(6)	1255(2)	73(2)
C(25)	-866(7)	-1603(7)	1433(2)	84(3)
C(26)	1586(7)	2396(6)	2181(2)	70(2)
C(27)	707(6)	-479(6)	1517(2)	67(2)
C(28)	2506(6)	-351(6)	857(2)	78(2)
C(29)	5759(6)	749(7)	613(2)	88(3)
C(30)	153(7)	-1422(6)	1568(2)	85(2)
C(31A)	-3245(13)	7039(13)	287(4)	111(6)

C(31B)	-2590(20)	7520(20)	83(9)	111(6)
C(32)	-3094(14)	7517(13)	685(5)	203(7)
C(33)	-2180(30)	7920(40)	520(7)	231(19)
O(34)	4440(20)	6420(30)	2580(8)	300(30)
C(35)	5080(40)	4590(40)	2671(8)	510(40)
C(36)	4070(20)	5260(20)	2722(7)	169(19)
C(37)	1510(40)	-2290(30)	2316(8)	420(30)
O(38)	550(70)	-550(70)	2500	250(70)
C(39)	530(30)	-1650(40)	2478(7)	310(30)
H(10A)	-1935	853	930	67
H(11A)	4811	1445	1663	65
H(15A)	621	2109	1822	70
H(17A)	4186	2107	2168	81
H(21A)	1652	3984	772	106
H(21B)	796	3221	617	106
H(21C)	1874	2734	749	106
H(22A)	-2576	4382	633	72
H(22B)	-1938	5301	805	72
H(23A)	2799	2560	2490	85
H(24A)	-2001	-967	1167	88
H(25A)	-1226	-2254	1468	101
H(26A)	1033	2612	2312	85
H(27A)	1387	-382	1605	80
H(28A)	2350	-515	647	117
H(28B)	1935	-630	984	117
H(28C)	3182	-681	914	117
H(29A)	6091	1448	572	132
H(29B)	6280	307	723	132
H(30A)	454	-1952	1693	102

U(eq) is defined as one third of the trace of the orthogonalized Uij tensor.

Table 7. Bond lengths [Å] and angles [¶ for $C_{60}H_{40}N_4O_8$.x solvent

O(1)-C(6)	1.382(7)
O(1)-C(21)	1.435(7)
O(2)-C(5)	1.385(7)
O(2)-C(28)	1.456(8)
O(3)-C(12)	1.229(7)
O(4)-C(14)	1.220(7)
N(1)-C(14)	1.348(8)
N(1)-C(29)	1.485(9)
N(2)-C(12)	1.359(8)
N(2)-C(22)	1.488(8)
C(1)-C(11)	1.354(8)
C(1)-C(5)	1.432(8)
C(1)-C(14)	1.511(9)
C(2)-C(5)	1.366(8)
C(2)-C(3)	1.418(8)
C(2)-C(4)	1.493(8)
C(3)-C(7)	1.404(8)
C(3)-C(15)	1.431(8)
C(4)-C(6)	1.372(8)
C(4)-C(8)	1.437(9)
C(6)-C(13)	1.420(8)
C(7)-C(11)	1.412(9)
C(7)-C(17)	1.422(8)
C(8)-C(27)	1.409(9)
C(8)-C(20)	1.439(9)
C(9)-C(16)	1.183(9)
C(9)-C(18)	1.396(10)
C(10)-C(13)	1.370(9)
C(10)-C(20)	1.383(9)
C(12)-C(13)	1.490(9)
C(15)-C(26)	1.366(9)
C(16)-C(29)#1	1.441(10)
C(17)-C(23)	1.357(9)
C(18)-C(19)	1.202(9)
C(19)-C(22)	1.440(9)
C(20)-C(24)	1.438(9)
C(23)-C(26)	1.393(10)
C(24)-C(25)	1.350(10)
C(25)-C(30)	1.404(11)
C(27)-C(30)	1.365(10)

C(29)-C(16)#1	1.441(10)
C(31A)-C(31B)	1.34(3)
C(31A)-C(32)	1.84(2)
C(31A)-C(31B)#2	1.93(4)
C(31A)-C(33)	1.98(4)
C(31B)-C(31B)#2	0.75(8)
C(31B)-C(31A)#2	1.93(4)
C(31B)-C(33)	2.03(5)
C(32)-C(33)	1.42(3)
O(34)-C(36)#3	1.50(3)
O(34)-C(36)	1.63(4)
O(34)-O(34)#3	1.66(6)
C(35)-C(36)	1.51(4)
C(35)-C(35)#3	1.60(7)
C(36)-O(34)#3	1.50(3)
C(37)-C(39)	1.61(4)
O(38)-C(39)#4	1.35(6)
O(38)-C(39)	1.35(6)
C(39)-C(39)#4	1.96(9)

C(6)-O(1)-C(21)	114.9(5)
C(5)-O(2)-C(28)	113.3(5)
C(14)-N(1)-C(29)	118.3(6)
C(12)-N(2)-C(22)	118.8(6)
C(11)-C(1)-C(5)	118.4(6)
C(11)-C(1)-C(14)	116.4(6)
C(5)-C(1)-C(14)	125.2(6)
C(5)-C(2)-C(3)	119.4(6)
C(5)-C(2)-C(4)	119.2(5)
C(3)-C(2)-C(4)	121.2(5)
C(7)-C(3)-C(2)	119.5(6)
C(7)-C(3)-C(15)	118.8(6)
C(2)-C(3)-C(15)	121.7(6)
C(6)-C(4)-C(8)	118.5(6)
C(6)-C(4)-C(2)	123.9(6)
C(8)-C(4)-C(2)	117.6(6)
C(2)-C(5)-O(2)	119.2(5)
C(2)-C(5)-C(1)	121.6(6)
O(2)-C(5)-C(1)	119.2(5)
C(4)-C(6)-O(1)	117.5(6)
C(4)-C(6)-C(13)	122.2(6)
O(1)-C(6)-C(13)	120.3(6)
C(3)-C(7)-C(11)	119.2(6)
C(3)-C(7)-C(17)	119.3(6)

C(11)-C(7)-C(17)	121.5(6)
C(27)-C(8)-C(4)	122.9(6)
C(27)-C(8)-C(20)	118.8(6)
C(4)-C(8)-C(20)	118.2(6)
C(16)-C(9)-C(18)	179.4(9)
C(13)-C(10)-C(20)	120.8(6)
C(1)-C(11)-C(7)	121.9(6)
O(3)-C(12)-N(2)	122.6(6)
O(3)-C(12)-C(13)	121.1(7)
N(2)-C(12)-C(13)	116.2(6)
C(10)-C(13)-C(6)	119.4(6)
C(10)-C(13)-C(12)	114.8(6)
C(6)-C(13)-C(12)	125.7(6)
O(4)-C(14)-N(1)	122.4(7)
O(4)-C(14)-C(1)	120.6(6)
N(1)-C(14)-C(1)	116.9(6)
C(26)-C(15)-C(3)	119.8(7)
C(9)-C(16)-C(29)#1	177.9(8)
C(23)-C(17)-C(7)	120.6(7)
C(19)-C(18)-C(9)	176.3(8)
C(18)-C(19)-C(22)	177.3(8)
C(10)-C(20)-C(24)	121.6(7)
C(10)-C(20)-C(8)	120.6(6)
C(24)-C(20)-C(8)	117.9(7)
C(19)-C(22)-N(2)	111.0(5)
C(17)-C(23)-C(26)	120.3(7)
C(25)-C(24)-C(20)	121.1(7)
C(24)-C(25)-C(30)	120.4(8)
C(15)-C(26)-C(23)	121.3(7)
C(30)-C(27)-C(8)	120.8(8)
C(16)#1-C(29)-N(1)	110.8(6)
C(27)-C(30)-C(25)	121.0(8)
C(31B)-C(31A)-C(32)	115.2(18)
C(31B)-C(31A)-C(31B)#2	16.6(17)
C(32)-C(31A)-C(31B)#2	131.8(12)
C(31B)-C(31A)-C(33)	72.8(18)
C(32)-C(31A)-C(33)	43.5(9)
C(31B)#2-C(31A)-C(33)	88.8(14)
C(31B)#2-C(31B)-C(31A)	132.4(15)
C(31B)#2-C(31B)-C(31A)#2	30.9(11)
C(31A)-C(31B)-C(31A)#2	101.6(19)
C(31B)#2-C(31B)-C(33)	156(4)
C(31A)-C(31B)-C(33)	68(2)
C(31A)#2-C(31B)-C(33)	165(2)

C(33)-C(32)-C(31A)	73(2)
C(32)-C(33)-C(31A)	63(2)
C(32)-C(33)-C(31B)	101(3)
C(31A)-C(33)-C(31B)	39.0(10)
C(36)#3-O(34)-C(36)	92(3)
C(36)#3-O(34)-O(34)#3	62(2)
C(36)-O(34)-O(34)#3	54.3(18)
C(36)-C(35)-C(35)#3	102(2)
O(34)#3-C(36)-C(35)	110(3)
O(34)#3-C(36)-O(34)	64(3)
C(35)-C(36)-O(34)	101(3)
C(39)#4-O(38)-C(39)	93(9)
O(38)-C(39)-C(37)	120(6)
O(38)-C(39)-C(39)#4	44(4)
C(37)-C(39)-C(39)#4	82(2)

Symmetry transformations used to generate equivalent atoms:

#1 y,x,-z #2 y-1,x+1,-z #3 -y+1,-x+1,-z+1/2

#4 -y,-x,-z+1/2